

**UCLA**

**UCLA Electronic Theses and Dissertations**

**Title**

Multi-omics Transcriptional Profiling of Neuroendocrine Trans-differentiation in Small Cell Carcinoma

**Permalink**

<https://escholarship.org/uc/item/6901038g>

**Author**

Chen, Chia-Chun

**Publication Date**

2024

Peer reviewed|Thesis/dissertation

UNIVERSITY OF CALIFORNIA

Los Angeles

Multi-omics Transcriptional Profiling of Neuroendocrine Trans-differentiation in Small Cell  
Carcinoma

A dissertation submitted in partial satisfaction of the requirements for the degree Doctor of  
Philosophy in Molecular and Medical Pharmacology

by

Chia-Chun Chen

2024

© Copyright by

Chia-Chun Chen

2024

## ABSTRACT OF THE DISSERTATION

Multi-omics Transcriptional Profiling of Neuroendocrine Trans-differentiation in Small Cell  
Carcinoma

by

Chia-Chun Chen

Doctor of Philosophy in Molecular and Medical Pharmacology

University of California, Los Angeles, 2024

Professor Owen N. Witte, Co-Chair

Professor Thomas G. Graeber, Co-Chair

Cellular differentiation is a fundamental process in growth and multicellular development. Trans-differentiation from adenocarcinoma to small cell neuroendocrine carcinoma in lung and prostate cancers can occur *de novo* or induced by targeted therapies. To understand the evolving process of the trans-differentiation, a temporal multi-omics study on a forward transformation *in vitro/in vivo* model of small cell neuroendocrine prostate cancer was performed. By analyzing samples taken from various time points including human basal cells, *in vitro* transformed organoids, early, transitional, and late xenograft tumors, an arc-like transformation trajectory with bifurcated endpoints defined by ASCL1 and ASCL2 is identified. Concurrently, the transcriptional programs shift from stress-response to cellular reprogramming, to neuroendocrine differentiation. With further experimental testing, additional transcription factors such as TFAP4 exhibit dynamic control between ASCL1 and ASCL2 expression. This study provides comprehensive epigenetic landscape of trans-differentiation and potential therapeutic targets for advanced prostate cancer.

The dissertation of Chia-Chun Chen is approved.

Brigitte N. Gomperts

Caius G. Radu

Thomas G. Graeber, Committee Co-Chair

Owen N. Witte, Committee Co-Chair

University of California, Los Angeles

2024

## DEDICATION

This dissertation is dedicated to my angel grandfathers and my parents, for their life-long devotion to the family and unconditional love and support for me. This work would not be possible without them.

## TABLE OF CONTENTS

### PRELIMINARY SECTIONS

Abstract of Dissertation	ii
Committee Page	iii
Dedication	iv
Table of Contents	v
Acknowledgments	vi
Curriculum Vitae	x

### CHAPTER 1: INTRODUCTION

1.1: Cellular Differentiation and Lineage Plasticity – From One to Infinite Possibilities	
1.2: Trans-differentiation – Part I: From Adenocarcinoma to Small Cell Carcinoma	
1.3: Trans-differentiation – Part II: From Epigenetics to Key Transcription Factors	
1.4: Bioinformatic Deconvolution of Differentiation – From Bulk to Single Cell Resolution	
References	

### CHAPTER 2: TEMPORAL EVOLUTION REVEALS BIFURCATED LINEAGES IN AGGRESSIVE NEUROENDOCRINE SMALL CELL PROSTATE CANCER TRANS-DIFFERENTIATION

Summary	
Introduction	
Results	
Discussion	
Materials and Methods	
Figures	
References	

### CHAPTER 3: DISCUSSION AND CLOSING REMARKS

## ACKNOWLEDGEMENT

I would like to thank my PhD mentors, Dr. Owen Witte and Dr. Thomas Graeber. I am very grateful to have them as my co-mentors during this years-long journey at UCLA. They have taught me not only the scientific principles in research, but also emotional intelligence in life. Owen and Tom have completely different personalities and mentoring styles. They are the Yin and Yang to my scientific practice. I frequently describe our relationship to other people as I am a chef who is making a feast (dissertation) with an air fryer (Owen) and a slow cooker (Tom). The hardest part of this culinary experience has been learning how to incorporate both at the right time with the right intention and attitude.

Owen has a firecracker personality with sharp instincts and right-to-the-point advice. The air conditioner in his office is blowing so strong, yet you are constantly sweating through the conversation with him because you know you are getting the most practical and critical opinions about yourself and your work. There is no filter in front of him. I very much admire his way of approaching life and scientific questions-logically, but with a lot of curiosity. I am very thankful for his patience for the time when I was doubting myself, his honesty when I wasn't improving myself, and his encouragement when I started to feel my feet on the ground. He is a one-of-a-kind mentor with a strict father mentality.

While the air fryer provides a bombing deliciousness without grease, the slow cooker offers a tender and long-lasting tastiness. I would like to thank Tom for his continuous and warm-hearted support during my PhD training and personal growth. He has taught me that the strength of humility carries a long way in one's career and in one's life. His attention to detail and his calmness has guided me to overcome my own recklessness and obstinacy. He is always encouraging about almost everything inside and outside of the lab, and I am grateful for having the freedom and trust when it comes to what I want to do for my PhD. Having two great mentors from different fields could mean an excellent training opportunity, but it also comes with double the amount of work



and expectation. I am thankful for this special co-mentorship. It is not easy, but we have put up a great feast together.

I would like to thank Dr. Murat Maga, who is the first PI I ever worked with in UW, for seeing my potential in doing independent undergraduate research. That experience marked the start of my journey of *in vivo* mouse work, which has helped accelerate my dissertation work. I would like to thank Dr. Valeri Vasioukhin, for giving me the opportunity to do full time research at Fred Hutch. He taught me the tissue culture work himself, which is almost unheard of as a tenured professor, and has trusted me in performing a lot of difficult procedures such as *in vivo* survival surgery and micro-injection as a fresh college graduate. Three years of research technician training from him equipped me with skills and attitude that I needed to succeed in pursuing a PhD.

I would like to thank all the members in Witte and Graeber labs, as well as my program cohort. My PhD life would be dull without them. They are the reason why I look forward going to the lab every day, besides my barely successful experiments. Most of the trainees trauma-bond together, but I have made friendships that could last a life long. First and foremost, thank you Squid Squad. Thank you, Lisa, for being the real squid in the lab, bringing the laughter and big sister energy to the group. Thank you, Gmao, for being the most knowledgeable walking Google in the lab and sharing the best Asian food and bubble tea places with me. Thank you, Josh, for being the nicest person to others but me, so I can bicker with you like you are my big brother. Thank you, Miyako, for always being there physically in the lab, making the most instant and relevant memes to make us laugh during tough times. Thank you, Wendy, for being the coolest sister that anyone could ever ask for, teaching us GenZ language while running terabytes-worth of data for my dissertation. Thanks to Tyler and Matthew, who have made my dissertation possible by doing top-notch scientific work. Thank you to what we called adults in Witte lab, Greg, Evan, Donny, Donghui, Batoul, Melissa, and Jami, for helping me grow as a scientist and letting me be part of your daily life for years. I would like to thank Song, Katherine, and Nick in the Graeber lab for showing me

the ropes when I started out with zero bioinformatic background. Thank you to other members that helped and provided me with valuable feedback every week at the lab meeting. I would like to thank my program cohort, who are the first few friends I made at UCLA and have continued to support me throughout. I am very lucky to have worked with so many smart and kind people that inspire me to be better every day.

I am thankful for my family. Without them, I won't be here and be who I am today. I left Taiwan alone at the age of 18 with a fearless heart. Both of my parents work hard to provide financial support, so I can focus on studying and chasing my American dream. Little did I know that letting go of your kid, even to a foreign country, is the hardest part of parenting. I appreciate their trust and I hope I have made them proud today. I would like to thank my grandparents, for their constant worries that I might not have enough food to eat in America and their most sincere greetings from the bottom of their hearts. I am grateful for my family in Taiwan, my forever home and shelter.

I am thankful for my friends for always being there for me. Almost none of them understand what I do in my PhD, but each of them still listens to my complaints, or take me out to have drinks and good food. It can be a lonely road down the PhD path, but their presence is my sunshine when it gets dark. They are fun and caring. I feel inspired by each one of them for being who they are, doing what they do, and that's the energy to keep me going.

Lastly, I would like to thank my husband, Dathan, and the best in-laws I can ever ask for. Though this PhD is mine, it is as much his because he has been by my side since day one. His love is truly unconditional because I'm not able to provide much financially and mentally as a graduate student. He listens to me even though he understands nothing about biology, and always comforts me even though he has a whole company to run on his own. More importantly, he takes care of our dog, Remy, so I can focus on working in the lab. Special thanks to Remy for being my best listener and cuddler. He is the goofiest and the cutest furry ball. My little family is my motivation and I wake up every day smiling.

# Chia-Chun Olga Chen

## EDUCATION

---

Ph.D. Candidate, Medical and Molecular Pharmacology   UCLA	2018-2024
M.S., Regulatory Science   Johns Hopkins University	2016-2018
B.S., Biochemistry   University of Washington	2011-2015

## EXPERIENCE

---

### Clinical Development Intern | ERASCA Inc 2023

- Performed statistical analyses for SAE observed in the clinical study and led presentation at the Lead Team meeting with Chief Medical Officer and Director of Clinical Development.
- Successfully reached target number of enrolled patients by reviewing eligible packages, analyzing patient data including tumor assessment for clinical trial phase I study.
- Conducted literature review for building TPP and performed retrospective historical clinical data analysis.
- Maintained partnerships with cross-functional teams including Regulatory Affairs, Clinical Operation, CMC on the management of early phase clinical study.

### Graduate Researcher | Pharmacology, UCLA 2018-2024

*Dr. Owen Witte and Dr. Thomas Graeber's Labs*

- Identified key transcription factors implicated in advanced prostate cancer leading to a first authored publication at *Cancer Cell* and inspired multiple institutional collaborations (Fred Hutch, Duke and more).
- Familiar with multi-omics profiling using Next Generation Sequencing, including Single Cell RNA-seq (10x Genomics), RNA-seq (NovaSeq), ATAC-seq, and ChIP-seq from library preparation to data analyses.
- Proficient in multi-disciplinary research in cancer biology and bioinformatic interpretation that led to consulting 4 different collaborative projects on experimental design and bioinformatic analyses.
- Communicated science to diverse audiences by presenting at 5 national and international meetings including posters at AACR conference and invited talks at NCI Small Cell Lung Cancer Consortium, Prostate Cancer Foundation and SPORE (Specialized Program of Research Excellence).

### Teaching Assistant | Molecular Cell Developmental Biology, UCLA 2022

- Taught and led discussion sessions of advanced molecular biology class composed of total ~100 students on cell biology and experimental techniques.
- Created large scale of question bank for weekly quizzes, two midterms and one final exam.
- Designed discussion sessions and office hours that tailor to the students' needs by collecting feedback and providing 1 on 1 guidance.

### Senior Research Technician/Lab Manager | Fred Hutchinson Cancer Research Center 2015-2018

*Dr. Valeri Vasioukhin's Lab*

- Assisted in two R01 sponsored research studies investigating the cell polarity and cell adhesion in cancers which led to a co-authored publication.

- Led an independent research project in investigating the transcriptional program by YAP in skin squamous carcinoma and represented the lab to participate in the departmental meetings.
- Trained 3 research technicians and 1 undergraduate on molecular techniques and in charge of data storage, personnel, and project management.

**Undergraduate Researcher | Seattle Children’s Research Institute**

**2013-2015**

*Dr. Murat A. Maga Lab*

- Assisted and carried out experiments, including acquisition of 3D images using MicroCT and digital manual landmarking to annotate the craniofacial changes. The work led to a later publication in 2016.
- Showcased 2 research posters at the Undergraduate Research Symposium at the University of Washington.

**PEER REVIEWED PUBLICATIONS**

- **Chen, C.-C.**, Song, K..., Witte, O. and Graeber, T. *Temporal evolution reveals bifurcated lineages in aggressive neuroendocrine small cell prostate cancer trans-differentiation.* Cancer Cell 41, 2066-2082 e2069. 10.1016/j.ccell.2023.10.009, 2023
- Mao, Z., Nesterenko, P., ..., **Chen, C.-C.**, Seet, C., Crooks, G., Phillips, J., Heath, J., Strong, R., Lee, J., Wohlschlegal, J., Witte, O. *Physical and in silico immunopeptidomic profiling of a cancer antigen prostatic acid phosphatase reveals targets enabling TCR isolation.* Proc Natl Acad Sci U S A. 2022 Aug 2;119(31): e2203410119. doi: 10.1073/pnas.2203410119. 2022.
- Liang, J., ..., **Chen, C.-C.**, Varuzhanyan, G., Damoiseaux, R., Seidlits, S. K. *Hydrogel Arrays Enable Increased Throughput for Screening Effects of Matrix Components and Therapeutics in 3D Tumor Models.* J. Vis. Exp. (184), e63791, doi:10.3791/63791, 2022.
- Kwan, J., ..., **Chen, C.-C.**, Ratkovic, S., Klezovitch, O., Attisano, L., McNeill, H., Emili, A., Vasioukhin, V. *DLG5 connects cell polarity and Hippo signaling protein networks by linking PAR-1 with MST1/2.* Genes & Development, 30(24), 2696–2709, 2016.

**AWARDS**

<b>Dissertation Year Fellowship</b> , UCLA	2023-2024
<b>BSCRC Special Stipend</b> , Broad Stem Cell Research Center, UCLA	2023-2024
<b>UCLA BSCRC Pre-doctoral Fellowship</b> , Broad Stem Cell Research Center, UCLA	2021-2022

**LEADERSHIP AND ACTIVITIES**

<b>Departmental Student Representative</b>   Graduate Student Association, UCLA	2020-2021
<b>Invited Panelist Speaker</b>   Collaboration in Undergraduate Research Enrichment, UCLA	2021
<b>Member</b>   Women in Bio, Seattle	2017-2018
<b>Health Safety Committee Member</b>   Fred Hutchinson Cancer Research Center, Seattle	2016
<b>Event Planning Committee Member</b>   American Diabetes Association, Seattle	2016

## **Chapter 1 Introduction**

## **Chapter 1: Introduction**

Treatment resistance remains a serious hurdle in modern medicine. One of the mechanisms adopted by cancer cells to escape from targeted therapies is to take advantage of cellular “plasticity” – an intrinsic potential to change and modify the cell identity in response to outside stimulus and environmental cues. Both genetics (DNA sequence) and epigenetics (how a cell controls gene expression without changing the DNA sequence) contribute to how a cancer cell adapts and responds to the changes. This thesis focuses on the epigenetic regulation in the process of trans-differentiation and highlights the pan tissue parallels between prostate and lung cancers.

The first part of this chapter (1.1, 1.2 and 1.3) takes a deep dive into the basic theories and pivotal experiments of cellular differentiation from developmental and stem cell biology. A pathological example in cancer, trans-differentiation, is an adverse consequence in adenocarcinoma evolving into more aggressive small cell neuroendocrine (SCN) carcinoma. The second part of this chapter (1.3 and 1.4) examines in detail specific transcription factors and chromatin modifiers in SCN trans-differentiation, where the discoveries were made using Next Generation Sequencing with single cell resolution and bioinformatic algorithms.

### **1.1: Cellular differentiation and lineage plasticity - From One to Infinite Possibilities**

#### 1.1.1 Introduction of cellular differentiation

Cellular differentiation is broadly defined as the process of a cell becoming specialized and maturing during development<sup>1,2</sup>. In adults, different types of stem cells (undifferentiated) give rise to various types of specialty cells (differentiated) in the body. For example, hematopoietic stem cells become white and red blood cells, and neural cells give rise to astrocytes and oligodendrocytes in the brain<sup>3</sup>. The concept of cellular differentiation can be dated back to as far

as 1893 in the book, *The germ-plasm: A theory of heredity* by August Weismann<sup>4</sup>, invoking a one-way evolution in the multicellular organism by two cell types: one that passes down genetic material to the next generation (germline cells), and another produces other cell types in the body (somatic cells). This instigated the idea that each somatic cell is destined with an irreversible path in the development of certain cell type<sup>5</sup>.

However, the concept was challenged by decades of research in stem cell biology and tissue regeneration, in which new tissue is generated from the pre-existing tissue or terminally differentiated cells<sup>5</sup>. In the early twentieth century, Spemann-Mangold experiment showed that a secondary body axis at the gastrula of an amphibian embryo can be generated by grafting a series of cells taken from the left dorsal lip<sup>6</sup>. This pivotal finding demonstrated that the fate of embryonic cells is not irreversible, and more than one differentiation path is possible.

The concept of “competence” - the ability of cells to react to inducing signals, was first introduced in 1940 by Conrad Waddington<sup>7</sup>. Subsequently, he introduced “epigenetic landscape” in 1953, one of the most popular metaphors for non-singular cellular differentiation pathways<sup>8</sup>. The landscape was demonstrated as a multi-dimensional surface with a marble rolling down various permitted valleys/pathways (“chreodes”). Each valley signifies a differentiated state. Besides the conceptualization of cellular differentiation, the “Waddington landscape” emphasized how epigenetic (modification to epigenome), rather than the alteration in DNA sequence, affects the plasticity of a cell in lineage differentiation.

### 1.1.2 Trans-differentiation, dedifferentiation and reprogramming

Trans-differentiation refers to a cell that goes from one cell type to another without going through de-differentiation (or back to stem cell)<sup>9,10</sup>, also known as direct reprogramming<sup>11</sup>. The concept of trans-differentiation was first introduced as a statement describing the transformation from the cuticle-producing cells to salt-secreting cells in silk moths by Selman and Kafatos in 1975<sup>12</sup>. This

was subsequently adopted by Okada and Euchi to describe the lens cells generated from pigmented epithelial cells in newt<sup>13,14</sup>. In 1987, the first experimental evidence of rewriting the cell identity was demonstrated by overexpressing MyoD, a mammalian transcription factor expressed in skeletal muscle that directly converts mouse embryonic fibroblasts to myoblasts<sup>15</sup>. This pioneering work opened a new era of discovering critical transcription factors that can induce specific cell fates through reprogramming.

In parallel, reprogramming cellular differentiation from a differentiated to an undifferentiated state *in vitro* was demonstrated by a revolutionary discovery: Yamanaka factors<sup>16,17</sup>. Yamanaka factors are composed of four transcription factors (proteins that control the transcription and expression of certain genes), Sox2, Oct4, Klf4, and c-Myc. When ectopically expressed, they can reprogram adult somatic cells to induced-pluripotent stem cells (iPSC) *in vitro*<sup>16,17</sup>. At the same time, Yu et al also published a different set of transcription factors that can reprogram human somatic cells to iPSC exhibiting embryonic stem cell characteristics<sup>18</sup>. Since then, decades of research in the regeneration field have showcased successful reprogramming both *in vitro* and *in vivo*, as well as their therapeutic application<sup>19-25</sup>.

These breakthrough discoveries convey several critical messages. That 1) cellular differentiation is a dynamic process, and 2) master regulators in epigenetics are capable to sufficiently reprogram a cell fate and control lineage differentiation.

## **1.2: Trans-differentiation: Part I - From Adenocarcinoma to Small Cell Carcinoma**

### **1.2.1 Cancer differentiation**

Cancer cells, often described as resulting from an error during the normal cellular development, exploit cellular stress response to differentiate or de-differentiate under various condition and stress<sup>26-28</sup>. For example, hypoxia and metastasis, in which cancer cells promote undifferentiation



or undergo epithelial-mesenchymal transition to disseminate to a new site during the tumor progression<sup>29-31</sup>. Moreover, as a resistance mechanism to targeted therapy or response to different stress conditions, cancer cells can also trans-differentiate or de-differentiate to a different cellular state<sup>32-34</sup>, such as the transition from an adenocarcinoma state to a stem-like small cell neuroendocrine state<sup>35,36</sup>. In cancers, the differentiation stage of tumor cells is central for the histopathological classification<sup>27</sup>. Well differentiated tumors tend to be less aggressive and grow slower than their less differentiated counterparts<sup>27</sup>. A poorly differentiated tumor such as small cell neuroendocrine tumor exhibits more aggressive characteristics including uncontrolled cell proliferation and visceral metastasis<sup>37</sup>.

### 1.2.2 Neuroendocrine differentiation and small cell carcinoma of prostate and lung

Small cell carcinoma is a histopathological classification that often occurs with neuroendocrine characteristics. The histological characteristics include small and rounded cells with scant cytoplasm, as well as positive immunohistochemical staining of clinical markers such as SYP, CHGA, NCAM1 and NSE<sup>38-40</sup>. Despite its rarity, small cell carcinoma occurs in multiple cancers including but not limited to prostate, lung, pancreatic, head and neck, and ovarian cancers<sup>37,41-43</sup>. In this thesis, emphasis is placed on small cell lung cancer and neuroendocrine prostate cancer, as they share high degrees of overlap in molecular features and epigenetics<sup>44</sup>.

Early-stage prostate cancer including localized disease has mostly an adenocarcinoma phenotype, which is often treatable with surgery (radical prostatectomy) and radiotherapy (i.e. brachytherapy)<sup>45,46</sup>. Androgen deprivation therapy (ADT) is a hormonal therapy that targets advanced prostate cancer systematically through various regime. For instance, surgical castration (orchiectomy), luteinizing hormone-releasing hormone agonists (i.e. leuprolide), and next generation androgen signaling inhibitors (i.e. enzalutamide and abiraterone acetate) that inhibits androgen receptor<sup>47-49</sup>. However, castration resistant prostate cancer (CRPC or CRPC-Adeno) tumors no longer respond to ADT therapy<sup>50</sup>. When treatment resistance persists, CRPC trans-

differentiates into an aggressive variant, small cell neuroendocrine prostate cancer (SCNPC or NEPC) or CRPC-NE, a variant of CRPC with neuroendocrine features and mixture of adenocarcinoma<sup>35,51-56</sup>. *De novo* SCNPC is very rare and stemmed from a small population of neuroendocrine cells<sup>39,57</sup>, whereas trans-differentiation cases of SCNPC accounts for 15-20% of CRPC and become an increasing challenge in the clinic<sup>40</sup>.

In parallel, trans-differentiation from adenocarcinoma to small cell carcinoma is a salient problem in lung cancer. Lung cancer is broadly divided into non-small cell lung cancer (NSCLC) and small cell lung cancer (SCLC)<sup>58</sup>. NSCLC includes lung adenocarcinoma (LUAD), large-cell carcinoma and squamous carcinoma based on histopathological classification<sup>58</sup>. SCLC is a malignant variant that is highly associated with tobacco carcinogen and accounts for about 15% of all lung cases<sup>41,42,59</sup>. Besides arising *de novo* from neuroendocrine cells, SCLC has a rising number in clinical cases reported as transformed SCLC from LUAD patients treated with tyrosine kinase inhibitors (TKI). TKI targets epidermal growth factor receptors (EGFR), such as afatinib, erlotinib, gefitinib, dacomitinib and osimertinib<sup>60-63</sup>. LUAD with EGFR mutation and transformation to SCLC are the major resistance mechanisms to the first and second lines of EGFR-TKIs<sup>64</sup>. LUAD with wild-type EGFR also experiences transformation, however at a much lower rate<sup>65</sup>.

Small cell neuroendocrine trans-differentiation poses a major setback in the clinic due to the lack of options in the current treatment regime<sup>66</sup>. Both SCNPC and SCLC have poor prognosis with a median survival of 7 months and 2-4 months if left untreated, respectively<sup>57,67,68</sup>. There's no effective standardized treatment for small cell carcinoma. Platinum-based chemotherapy such as cisplatin and etoposide are only effective for a short amount of time until the cancer progresses<sup>69,70</sup>. To develop better therapeutics against small cell neuroendocrine cancers, a systematic molecular profiling study is crucial to understand the underlying biology and vulnerability of this challenging malignancy<sup>35,66,70</sup>.

### 1.2.3 Pre-clinical SCNPC models

To study neuroendocrine trans-differentiation in prostate cancer, there are different *in vitro* and *in vivo* models available, with various degrees of advantages and disadvantages<sup>71</sup>. The Genetically Modified Mouse Model (GEMM) is one of the most common models that may be beneficial for the complex studies of the tumor environment, trans-differentiation, and therapy resistance. Examples include the usage of PBCre4, Nk3.1CreERT or Tmpress2CreERT2 with the combination of double floxed alleles of *Pten*, *Rb1* and/or *Trp53*<sup>72-75</sup>. Overexpression of MYCN has also shown promising in modeling neuroendocrine progression such as the PRN model driven by T2-Cre and *Pten* loss<sup>76,77</sup>. In addition, co-expression of constitutively active AKT and MYC in basal cells lead to the neuroendocrine transformation *in vivo*<sup>78,79</sup>.

Patient Derived Xenograft (PDX) is a useful model to study tumoral heterogeneity and genetic assessment of SCNPC. For example, the LuCAP series encompasses a collection of genomic and phenotypic features in prostate cancer patients<sup>80</sup>. Another group has also established LTL series (Living tumor Laboratory) with comprehensive histopathology and gene expression profiling of donor tumors, with LTL331R being the most widely used model with an induced neuroendocrine phenotype<sup>81</sup>. The MDA PCa series has provided valuable information of SCNPC<sup>82</sup>. In parallel, the patient derived organoid model has gained popularity over the years. Beltran's group developed patient-derived organoids from metastatic biopsies from SCNPC patients<sup>83</sup>. These types of patient-derived organoids present a useful tool for drug screening and testing<sup>83,84</sup>.

Despite these models, there is a very limited number of SCNPC cell lines available: NCI-H660 and LASCPC-01<sup>78</sup>. Other groups have utilized a LNCAP cell line, which is derived from a patient with metastatic prostate carcinoma<sup>85</sup>, to study trans-differentiation from adenocarcinoma to SCNPC<sup>86-88</sup>.

### **1.3: Trans-differentiation – Part II: From Epigenetics to Key Transcription Factors**

#### **1.3.1 Transcriptional convergence of small cell carcinoma**

Besides the resemblance of small cell histology and the neuroendocrine marker expression, prostate, bladder, and lung cancers with small cell neuroendocrine phenotypes share similar transcriptomic and gene expression pattern<sup>44,79,89</sup>. In SCNPC and SCLC, the majority of clinical cases have inactivating mutations of P53 and RB1<sup>90-92</sup>. Experimental evidence has also shown that the loss of P53 and RB1 is essential for the advanced transformation and lineage plasticity in various small cell neuroendocrine cancer model in addition to the amplification of oncogenes, such as MYC and AKT<sup>72,73,78,79,93-96</sup>. These factors together contribute to the overall epigenetic landscape, promote neuroendocrine trans-differentiation, treatment resistance and malignant transformation in small cell carcinoma.

#### **1.3.2 Epigenetic reprogramming in small cell carcinoma**

Trans-differentiation from adenocarcinoma to small cell carcinoma entails epigenetic reprogramming<sup>35,96</sup>. Epigenetic reprogramming includes chromatin remodeling, histone modification and DNA methylation that downstream changes gene expression, driving cancer cells towards plasticity and neuroendocrine differentiation<sup>95,97-99</sup>. There is growing interest in identifying clinically targetable epigenetic regulator in advanced prostate cancer, such as the polycomb group gene family and DNA methyltransferases (DNMT) family<sup>95,98,100-102</sup>. For example, EZH2, a histone methyltransferase and a catalytic subunit of the polycomb repressive complex 2 (PRC2), is responsible for the oncogenic activation in advanced prostate cancer.<sup>77,103,104</sup> EZH2 is also tightly coupled with DNMTs through recruitment<sup>105</sup>. DNMT1 is also found to be significantly enriched in SCNPC and SCLC compared to non-small cell carcinoma. Ablation of DNMTs in pre-clinical advanced prostate cancer has proven effective attenuation in tumor growth<sup>106</sup>. Other epigenetic modifiers such as SIRT1, a histone deacetylase (HDAC), induces neuroendocrine

differentiation through activation of the AKT pathway<sup>107</sup>. Together, these epigenetic modulators regulate a unique transcriptomic landscape of small cell carcinoma, facilitating a higher level of gene regulation towards neuroendocrine trans-differentiation.

### 1.3.3 Pioneer factors instigate neuroendocrine differentiation in prostate cancer

Besides epigenetic editing, pioneer transcription factors play an important role in instigating activation of the neuroendocrine transcriptional program in prostate cancer<sup>108,109</sup>. Pioneer factors are capable of binding to closed chromatin and inducing DNA accessibility that leads to cell fate reprogramming<sup>110,111</sup>. Forkhead box protein family genes such as FOXA1 are one of the most studied pioneer factors in prostate cancer<sup>108</sup>. High expression of FOXA1 in prostate cancer is associated with poor prognosis, potentially contributed by its role in activating AR transcriptional program through recruitment and direct interaction with AR<sup>112-114</sup>. Particularly, 25% of SCNPC have FOXA1 mutations that alter the lineage plasticity, including the blockage of luminal differentiation and activation of the neuroendocrine program<sup>115-117</sup>. In parallel, FOXA2 is not only a sensitive marker with specificity in SCNPC, but also responsible for KIT signaling pathway activation and driving the neuroendocrine trans-differentiation<sup>75,118</sup>. Nonetheless, ASCL1, a classical pioneer factor in neuronal and glioblastoma development<sup>119-122</sup>, activates neuronal and stem-like programs through chromatin remodeling in SCNPC<sup>123</sup>.

### 1.3.4 Subtypes of small cell carcinoma defined by transcription factors

Small cell carcinoma is a heterogeneous malignancy. SCLC can be divided into two categories: neuroendocrine (NE) and non-neuroendocrine (non-NE). Each category contains two subtypes that are molecularly defined as SCLC-A (ASCL1) and SCLC-N (NEUROD1), as well as SCLC-P (POU2F3) and SCLC-Y (YAP), respectively<sup>124-126</sup>. These four transcription factors represent the subtypes of SCLC based on not only the individual expression pattern, but also comprehensive transcriptomic and histopathological profiling on various tumor tissues and models<sup>124,127</sup>. Distinct

clinical characteristics presented by these four subtypes also implicate therapeutic treatments and outcomes<sup>128,129</sup>. Similarly, there are two clinical subtypes of SCNPC defined by ASCL1 and NEUROD1 through transcriptomic analysis on cell lines, patient-derived xenografts, and clinical samples<sup>130</sup>.

Functionally, ASCL1 is a class II basic-helix-loop-helix (bHLH) transcription factor that heterodimerizes with other class I bHLH proteins to activate specific transcriptional programs. It is involved in neurogenesis, neural stem cells, and glioblastoma through various signaling pathways such as Wnt and Notch pathways<sup>119,122,131-136</sup>. Combinatorial expression of ASCL1, BRN2 and MTY1L are sufficient to reprogram fibroblasts into neurons<sup>135,137</sup>. In small cell carcinoma, around 70% of SCLC clinical cases expresses ASCL1 by immunochemical analysis<sup>127,138,139</sup>. ASCL1 is required for pulmonary neuroendocrine differentiation and tumorigenesis, presenting a potential therapeutic target for SCLC<sup>140-144</sup>. In prostate cancer, ASCL1 is further demonstrated to drive and support neural and plastic lineage, as well as contribute to the ferroptosis resistance<sup>123,145,146</sup>.

Another neuroendocrine subtype of SCLC and SCNPC is defined by NEUROD1. NEUROD1 is a bHLH factor involved in the development of enteroendocrine cells in the gastrointestinal tract and plays an important role in the central nervous system and neurogenesis<sup>147-149</sup>. NEUROD1 is highly expressed in aggressive SCLC and promotes tumor cell survival and migration, via regulation of the receptor tyrosine kinase tropomyosin-related kinase B (TrkB)<sup>150,151</sup>. The molecular profiling of SCNPC identified that this NEUROD1 subtype, despite sharing similar chromatin accessibility of neuroendocrine transcription factors with the ASCL1 subtype, contains a distinct transcriptional landscape enriched in EBF and LHX transcription factor motifs<sup>130</sup>.

In the non-neuroendocrine class of small cell carcinoma, the POU2F3 subtype is identified with higher frequency in SCLC than SCNPC<sup>76,152</sup>. POU2F3, also known as OCT11, is a transcription factor that is important for specification of a rare chemosensory cell type, tuft cells, found in

gastrointestinal and respiratory tracts<sup>153,154</sup>. It is also found to be essential for the tuft cell-like variant of SCLC through binding to OCA-T complex<sup>155,156</sup>. In addition, ASCL2 is identified as one of the unique dependencies in the POU2F3 subtype in SCLC<sup>155</sup>, and is co-expressed with POU2F3 in subpopulations of SCNPC tumor cells<sup>76</sup>.

The YAP1 subtype is considered the rarest subtype of SCLC due to low expression and lack of exclusivity in clinical cases<sup>127</sup>. Silencing YAP1 by RB1 mutation is found to be important for SCLC cells to metastasize<sup>157</sup>. However, the YAP1 subtype exhibits the worst clinical outcome comparing to other SCLC subtypes and acquires a distinct inflammatory phenotype including high interferon- $\gamma$  response genes, PD-L1 and T-cell functional impairment<sup>158,159</sup>. YAP1 is known to be a transcription co-regulator downstream of the canonical Hippo pathway in controlling organ size and development<sup>160</sup>. Its involvement in tissue regeneration and cancer is extensive<sup>161,162</sup>. Interestingly, YAP1 activity defines pan-cancer into binary classes (YAP on/YAP off) with distinct adhesion phenotypes and vulnerability<sup>163</sup>. The YAP off solid cancer group has neuroendocrine features and loss of RB1, including retinoblastoma, SCLC and SCNPC<sup>163</sup>. YAP1 is also found to drive chemoresistance and change cell fate from neuroendocrine to non-neuroendocrine by induction of REST expression<sup>164</sup>.

These four subtypes of small cell carcinoma in prostate and lung defined by these transcription factors are the current foundation in the field to classify clinical cases and identify unique molecular vulnerabilities for targeted therapies. However, with more single cell resolution-based studies, a mixture of these four transcription factors defined cell population have been identified within the same tumor, suggesting a high intra-tumoral heterogeneity as an emerging challenge in targeting small cell carcinoma<sup>130</sup>.

### 1.3.5 Critical transcription factors in SCNPC

Neuroendocrine trans-differentiation requires a rewrite of the transcriptional landscape coordinated by various transcription factors<sup>165</sup>. Several transcription factors have been shown to be responsible for the neuroendocrine trans-differentiation and the survival of small cell cancer cells. For example, BRN2 (also known as POU3F2), is an AR-dependent transcriptional driver for neuroendocrine differentiation in CRPC<sup>86</sup>. Continuous investigation of BRN2 led to a first-in-field orally available inhibitor through the disruption between BRN2 and DNA in SCNPC<sup>166</sup>. Moreover, BRN4 is found to be actively released in prostate cancer extracellular vesicles with BRN2, promoting CRPC to SCNPC transition<sup>167</sup>. In SCLC, ablation of BRN2 significantly decreases neuroendocrine genes such as NCAM1, ASCL1 and CHGA, and vice versa. TTF1 is subsequently identified as a lineage-specific transcription factor through co-expression with BRN2 in SCLC<sup>168</sup>.

One of the transcription factors that is BRN2-dependent is SOX2<sup>86</sup>. SOX2 belongs to SRY homolog box protein family. It is well known as one of the reprogramming factors in stem cell biology and has a pivotal role from embryogenesis to adult homeostasis<sup>16,169,170</sup>. In cancers, SOX2 amplification is found in about 27% of the SCLC clinical samples<sup>171,172</sup>. It is identified as an oncogenic driver for neuroendocrine transformation and required for cancer cell proliferation in SCLC<sup>171,173</sup>, exhibiting higher sensitivity upon inhibition in the ASCL1 subtype than in the YAP1 subtype<sup>174</sup>. In addition, SOX2 is found to be indispensable for activating lineage plasticity and antiandrogen resistance in P53-RB1 negative prostate cancer<sup>73</sup> alongside the previous report that SOX2 is required for tumor initiation in the RB1 loss retinoblastoma<sup>175</sup>. Despite direct targeting of SOX2 being a challenge in small cell carcinoma, research has shown that the exportin 1 inhibitor, Selinexor, prevents neuroendocrine differentiation through down regulation of SOX2 in SCLC<sup>176</sup>.

ONECUT2, also known as OC-2, is associated with a wide range of biological processes including cell proliferation and differentiation in both normal and cancer development<sup>177,178</sup>. In SCNPC, ONECUT2 is identified as a targetable master regulator of the AR signaling network<sup>179,180</sup>. The underlying molecular mechanism is the activation of SMAD3 dependent regulation of hypoxia



signaling in SCNPC, leading to the possibility of targeting hypoxic metastatic CRPC with a hypoxia-activated prodrug such as evofosfamide (TH-302)<sup>180</sup>.

## **1.4: Bioinformatic Deconvolution of Differentiation – From Bulk to Single Cell Resolution**

### **1.4.1 Transcriptional network and chromatin accessibility in small cell carcinoma**

With multiple transcription factors identified in regulating neuroendocrine trans-differentiation, more systematic and data-driven approaches have been applied to deconvolute the overall transcriptional network, to investigate the relationship between these transcription factors and associated phenotypes. For example, simulation analysis by Boolean modeling identifies a “hybrid” phenotype that explains the tumoral heterogeneity in SCLC, by using attractor states that are defined by neuroendocrine or mesenchymal signatures<sup>181</sup>. Similarly, the other research group adopts an archetype approach to further characterize the transition of the cellular states and suggests that cell plasticity may be driven by the response to the microenvironmental perturbations and treatments in SCLC<sup>182</sup>. Other analyses rely on more of a structural graph theory concept that recognizes the critical components in a complex network, termed “hubs”, which helps generate more leads for functional testing of the targeted pathways in SCLC<sup>183</sup>.

Gene expression data from bulk RNA sequencing is crucial for studying the above-mentioned transcriptional network. However, to determination of which and how transcription factors regulate the transcriptional program will rely on chromatin accessibility analysis by the use of Assay of Transposase Accessible Chromatin (ATAC) sequencing. ATAC-sequencing utilizes the hyperactivity of Tn5 transposase with a simple protocol to allow epigenetic profiling at the open chromatin regions<sup>184</sup>. The application of ATAC-sequencing is extensive across fields and downstream analyses such as motif enrichment, nucleosome positioning and transcription factor footprinting are useful tools for studying transcriptional control and epigenetic regulation<sup>185</sup>.

#### 1.4.2 Single cell RNA based technology in studying lineage differentiation

Next generation sequencing revolutionized genomic research by providing higher efficiency and throughput capabilities than Sanger sequencing<sup>186</sup>. In cancer studies, bulk RNA sequencing contributes to the most widely available datasets such as TCGA, Cancer Cell Line Encyclopedia, and DepMap<sup>187,188</sup>, for its predominant usages in studying general trends, tumor classification, and gene expression patterns in cancers<sup>189</sup>. With the advanced developments in sequencing technologies, single cell-based sequencing offers higher resolution than bulk sequencing, in terms of studying cellular heterogeneity, differentiation status, cell types and the transcriptional landscape of individual cells<sup>188,190,191</sup>.

One of the most common applications of single cell-based technology in studying cellular differentiation is single cell RNA sequencing. It offers a powerful approach in reconstructing differentiation trajectories within a single cell by different algorithm and methods, including inference-based lineage tracing and prediction of differentiation states<sup>192,193</sup>. This type of prediction algorithm, though does not necessarily reflect genetic relationship, overcomes the challenge in experimentally labeling a cell with a heritable mark and tracking its progeny<sup>194</sup>. To name a few, CytoTRACE is a framework that is based on one simple observation: total number of genes expressed in a cell decreases during differentiation. Validation of the platform has been shown in identifying less-differentiated cell population with target genes that contribute to treatment resistance within the luminal progenitor epithelium in breast cancer<sup>195</sup>. RNA velocity, which utilizes the dynamic relationship between unspliced and spliced RNA to predict the differentiation status of a given cell<sup>196</sup>. The extensive application of RNA velocity unravels the transcriptional kinetics of embryonic brain development, pancreatic endocrinogenesis and identification of transient cellular states<sup>196-198</sup>. Another bioinformatic tool such as Monocle2 is based on reverse graph embedding, a type of machine learning, to predict the differentiation state with no requirement of priori genes in the biological process<sup>199</sup>.

The other wide application of single cell RNA based technology is *in situ* hybridization (ISH). With the advancement from traditional radiolabel based fluorescence ISH to non-radioisotopic technology, the technique has evolved to allow multiplex detection and spatial arrangement of single cells on tissue sections<sup>200</sup>. One of the popular platforms for researchers is RNAscope. RNAscope utilizes a proprietary double-Z branched DNA probe design strategy to eliminate non-specific hybridization<sup>201</sup>. It allows detection of lower expressed genes and multiple genes in one setting, both of which are the limitation for traditional ISH technique, and has been used to support multiple clinical biomarker discoveries and transcriptional basic science studies since its invention in 2012<sup>201,202</sup>.

#### 1.4.3 Studying small cell carcinoma using a multi-omics approach

Small cell carcinoma is a heterogeneous malignancy and challenging to study due to limited models and clinical materials. Efforts have been put into maximizing the usage of the samples and conducting more comprehensive transcriptomic profiling, such as single cell RNA sequencing on needle biopsy samples and small pieces of resected tumors. By comparing over 50,000 single cell transcriptomes of SCLC to lung adenocarcinoma from patient biospecimens, Chan et al identifies a PLCG2-high subpopulation that is responsible for the pro-metastatic phenotype in SCLC<sup>203</sup>. In SCNPC, Dong et al profiles over 20,000 single cell transcriptomes from needle biopsy samples of 6 CRPC patients and determines that neuroendocrine trans-differentiation arises from a luminal-like rather than basal cell compartment<sup>204</sup>. These studies provide valuable insights into tumor heterogeneity and the clinical relevance in studying the pathogenesis of small cell carcinoma.

A multi-omics approach includes usage of a combination of different sequencing and profiling methods to deconvolute a complex biological system<sup>205</sup>. It is a powerful integrative approach to characterize samples and allow more in-depth analysis from various perspectives. In studying neuroendocrine trans-differentiation, Tang et al uses ATAC-sequencing, RNA-sequencing, and

DNA sequencing to profile CRPC organoids, patient-derived xenografts, and tumor derived cell lines. The study identified four subtypes including AR dependent, neuroendocrine, Wnt-dependent and stem cell-like that guide therapeutic decisions<sup>206</sup>. With single cell resolution, Han et al combined both single cell RNA and ATAC-sequencing in a pre-clinical *in vivo* study to investigate the FOXA2-driven lineage plasticity<sup>75</sup>. In SCLC, integration of genomics, transcriptomics, proteomics, and phospho-proteomics of 112 paired tumor and adjacent lung tissues from SCLC patients yields subtype-specific therapeutic strategy<sup>207</sup>.

With the advancement of sequencing technology and immense studies on the epigenetic regulation in small cell cancers, we set forth to understand the chronological order of transcriptional changes and to pinpoint each above-mentioned transcription factors during the neuroendocrine trans-differentiation. We performed a comprehensive transcriptomic profiling on an established small cell carcinoma model (termed PARCB)<sup>79</sup> using multi-omics sequencing<sup>208</sup>. The study reveals distinct transcriptional patterns of gene expression and chromatin accessibility at each stage of the SCNPC development, along with single cell based sequencing and histopathological analysis.

## Reference

1. Betts, J.G., Young, K.A., and Wise, J.A. (2021). *Anatomy and Physiology 2e*, 2e Edition (OpenStax).
2. Cooper, G.M. (2000). *The cell : a molecular approach* / Geoffrey M. Cooper, 2nd Edition (ASM Press).
3. Zakrzewski, W., Dobrzynski, M., Szymonowicz, M., and Rybak, Z. (2019). Stem cells: past, present, and future. *Stem Cell Res Ther* 10, 68. 10.1186/s13287-019-1165-5.
4. Weismann, A., Parker, W.N., and Rönnefeldt, H. (1893). *The germ-plasm : a theory of heredity* / by August Weismann, tr. by W. Newton Parker and Harriet Rönnefeldt (W. Scott).
5. Sanchez Alvarado, A., and Yamanaka, S. (2014). Rethinking differentiation: stem cells, regeneration, and plasticity. *Cell* 157, 110-119. 10.1016/j.cell.2014.02.041.
6. Spemann, H. (1938). *Embryonic development and induction* / by Hans Spemann (Yale University press; London, H. Milford, Oxford University Press).
7. Waddington, C.H. (1940). *Organisers & genes* / by C.H. Waddington (University Press).
8. Waddington, C.H. (1957). *The strategy of the genes; a discussion of some aspects of theoretical biology.* / With an appendix by H. Kacser (Macmillan).
9. Küntziger, T., and Collas, P. (2004). Transdifferentiation. *Handbook of stem cells* /, 147-151. 10.1016/B978-012436643-5/50103-6.
10. Shen, C.N., Burke, Z.D., and Tosh, D. (2004). Transdifferentiation, metaplasia and tissue regeneration. *Organogenesis* 1, 36-44. 10.4161/org.1.2.1409.
11. Wang, H., Yang, Y., Liu, J., and Qian, L. (2021). Direct cell reprogramming: approaches, mechanisms and progress. *Nat Rev Mol Cell Biol* 22, 410-424. 10.1038/s41580-021-00335-z.

12. Selman, K., and Kafatos, F.C. (1974). Transdifferentiation in the labial gland of silk moths: is DNA required for cellular metamorphosis? *Cell Differ* 3, 81-94. 10.1016/0045-6039(74)90030-x.
13. Eguchi, G., and Okada, T.S. (1973). Differentiation of lens tissue from the progeny of chick retinal pigment cells cultured in vitro: a demonstration of a switch of cell types in clonal cell culture. *Proc Natl Acad Sci U S A* 70, 1495-1499. 10.1073/pnas.70.5.1495.
14. Eguchi, G., and Kodama, R. (1993). Transdifferentiation. *Curr Opin Cell Biol* 5, 1023-1028. 10.1016/0955-0674(93)90087-7.
15. Davis, R.L., Weintraub, H., and Lassar, A.B. (1987). Expression of a single transfected cDNA converts fibroblasts to myoblasts. *Cell* 51, 987-1000. 10.1016/0092-8674(87)90585-x.
16. Takahashi, K., and Yamanaka, S. (2006). Induction of pluripotent stem cells from mouse embryonic and adult fibroblast cultures by defined factors. *Cell* 126, 663-676. 10.1016/j.cell.2006.07.024.
17. Takahashi, K., Tanabe, K., Ohnuki, M., Narita, M., Ichisaka, T., Tomoda, K., and Yamanaka, S. (2007). Induction of pluripotent stem cells from adult human fibroblasts by defined factors. *Cell* 131, 861-872. 10.1016/j.cell.2007.11.019.
18. Yu, J., Vodyanik, M.A., Smuga-Otto, K., Antosiewicz-Bourget, J., Frane, J.L., Tian, S., Nie, J., Jonsdottir, G.A., Ruotti, V., Stewart, R., et al. (2007). Induced pluripotent stem cell lines derived from human somatic cells. *Science* 318, 1917-1920. 10.1126/science.1151526.
19. Yamanaka, S. (2012). Induced pluripotent stem cells: past, present, and future. *Cell Stem Cell* 10, 678-684. 10.1016/j.stem.2012.05.005.
20. Wernig, M., Meissner, A., Foreman, R., Brambrink, T., Ku, M., Hochedlinger, K., Bernstein, B.E., and Jaenisch, R. (2007). In vitro reprogramming of fibroblasts into a pluripotent ES-cell-like state. *Nature* 448, 318-324. 10.1038/nature05944.

21. Lowry, W.E., Richter, L., Yachechko, R., Pyle, A.D., Tchieu, J., Sridharan, R., Clark, A.T., and Plath, K. (2008). Generation of human induced pluripotent stem cells from dermal fibroblasts. *Proc Natl Acad Sci U S A* 105, 2883-2888. 10.1073/pnas.0711983105.
22. Park, I.H., Zhao, R., West, J.A., Yabuuchi, A., Huo, H., Ince, T.A., Lerou, P.H., Lensch, M.W., and Daley, G.Q. (2008). Reprogramming of human somatic cells to pluripotency with defined factors. *Nature* 451, 141-146. 10.1038/nature06534.
23. Hanna, J., Wernig, M., Markoulaki, S., Sun, C.W., Meissner, A., Cassady, J.P., Beard, C., Brambrink, T., Wu, L.C., Townes, T.M., and Jaenisch, R. (2007). Treatment of sickle cell anemia mouse model with iPS cells generated from autologous skin. *Science* 318, 1920-1923. 10.1126/science.1152092.
24. Kriks, S., Shim, J.W., Piao, J., Ganat, Y.M., Wakeman, D.R., Xie, Z., Carrillo-Reid, L., Auyeung, G., Antonacci, C., Buch, A., et al. (2011). Dopamine neurons derived from human ES cells efficiently engraft in animal models of Parkinson's disease. *Nature* 480, 547-551. 10.1038/nature10648.
25. Nori, S., Okada, Y., Yasuda, A., Tsuji, O., Takahashi, Y., Kobayashi, Y., Fujiyoshi, K., Koike, M., Uchiyama, Y., Ikeda, E., et al. (2011). Grafted human-induced pluripotent stem-cell-derived neurospheres promote motor functional recovery after spinal cord injury in mice. *Proc Natl Acad Sci U S A* 108, 16825-16830. 10.1073/pnas.1108077108.
26. Brabletz, T. (2012). To differentiate or not--routes towards metastasis. *Nat Rev Cancer* 12, 425-436. 10.1038/nrc3265.
27. Jogi, A., Vaapil, M., Johansson, M., and Pahlman, S. (2012). Cancer cell differentiation heterogeneity and aggressive behavior in solid tumors. *Ups J Med Sci* 117, 217-224. 10.3109/03009734.2012.659294.
28. Barry Pierce, G., and Johnson, L.D. (1971). Differentiation and cancer. *In Vitro* 7, 140-145. 10.1007/bf02617957.

29. Heerboth, S., Housman, G., Leary, M., Longacre, M., Byler, S., Lapinska, K., Willbanks, A., and Sarkar, S. (2015). EMT and tumor metastasis. *Clin Transl Med* 4, 6. 10.1186/s40169-015-0048-3.
30. Senft, D., and Ronai, Z.A. (2016). Adaptive Stress Responses During Tumor Metastasis and Dormancy. *Trends Cancer* 2, 429-442. 10.1016/j.trecan.2016.06.004.
31. Kim, Y., Lin, Q., Glazer, P.M., and Yun, Z. (2009). Hypoxic tumor microenvironment and cancer cell differentiation. *Curr Mol Med* 9, 425-434. 10.2174/156652409788167113.
32. Oh, H., Hwang, I., Jang, J.Y., Wu, L., Cao, D., Yao, J., Ying, H., Li, J.Y., Yao, Y., Hu, B., et al. (2021). Therapy-Induced Transdifferentiation Promotes Glioma Growth Independent of EGFR Signaling. *Cancer Res* 81, 1528-1539. 10.1158/0008-5472.CAN-20-1810.
33. Han, X., Li, F., Fang, Z., Gao, Y., Li, F., Fang, R., Yao, S., Sun, Y., Li, L., Zhang, W., et al. (2014). Transdifferentiation of lung adenocarcinoma in mice with *Lkb1* deficiency to squamous cell carcinoma. *Nat Commun* 5, 3261. 10.1038/ncomms4261.
34. Quintanal-Villalonga, A., Taniguchi, H., Zhan, Y.A., Hasan, M.M., Chavan, S.S., Meng, F., Uddin, F., Allaj, V., Manoj, P., Shah, N.S., et al. (2021). Comprehensive molecular characterization of lung tumors implicates AKT and MYC signaling in adenocarcinoma to squamous cell transdifferentiation. *J Hematol Oncol* 14, 170. 10.1186/s13045-021-01186-z.
35. Beltran, H., Hruszkewycz, A., Scher, H.I., Hildesheim, J., Isaacs, J., Yu, E.Y., Kelly, K., Lin, D., Dicker, A., Arnold, J., et al. (2019). The Role of Lineage Plasticity in Prostate Cancer Therapy Resistance. *Clin Cancer Res* 25, 6916-6924. 10.1158/1078-0432.CCR-19-1423.
36. Yuan, T.C., Veeramani, S., and Lin, M.F. (2007). Neuroendocrine-like prostate cancer cells: neuroendocrine transdifferentiation of prostate adenocarcinoma cells. *Endocr Relat Cancer* 14, 531-547. 10.1677/ERC-07-0061.



37. Nadal, R., Schweizer, M., Kryvenko, O.N., Epstein, J.I., and Eisenberger, M.A. (2014). Small cell carcinoma of the prostate. *Nat Rev Urol* 11, 213-219. 10.1038/nrurol.2014.21.
38. Travis, W.D. (2012). Update on small cell carcinoma and its differentiation from squamous cell carcinoma and other non-small cell carcinomas. *Mod Pathol* 25 *Suppl* 1, S18-30. 10.1038/modpathol.2011.150.
39. Wang, W., and Epstein, J.I. (2008). Small cell carcinoma of the prostate. A morphologic and immunohistochemical study of 95 cases. *Am J Surg Pathol* 32, 65-71. 10.1097/PAS.0b013e318058a96b.
40. Aggarwal, R., Huang, J., Alumkal, J.J., Zhang, L., Feng, F.Y., Thomas, G.V., Weinstein, A.S., Friedl, V., Zhang, C., Witte, O.N., et al. (2018). Clinical and Genomic Characterization of Treatment-Emergent Small-Cell Neuroendocrine Prostate Cancer: A Multi-institutional Prospective Study. *J Clin Oncol* 36, 2492-2503. 10.1200/JCO.2017.77.6880.
41. Rudin, C.M., Brambilla, E., Faivre-Finn, C., and Sage, J. (2021). Small-cell lung cancer. *Nat Rev Dis Primers* 7, 3. 10.1038/s41572-020-00235-0.
42. Megyesfalvi, Z., Gay, C.M., Popper, H., Pirker, R., Ostoros, G., Heeke, S., Lang, C., Hoetzenecker, K., Schwendenwein, A., Boettiger, K., et al. (2023). Clinical insights into small cell lung cancer: Tumor heterogeneity, diagnosis, therapy, and future directions. *CA: A Cancer Journal for Clinicians* 73, 620-652. <https://doi.org/10.3322/caac.21785>.
43. Pointer, K.B., Ko, H.C., Brower, J.V., Witek, M.E., Kimple, R.J., Lloyd, R.V., Harari, P.M., and Baschnagel, A.M. (2017). Small cell carcinoma of the head and neck: An analysis of the National Cancer Database. *Oral Oncol* 69, 92-98. 10.1016/j.oraloncology.2017.04.009.
44. Balanis, N.G., Sheu, K.M., Esedebe, F.N., Patel, S.J., Smith, B.A., Park, J.W., Alhani, S., Gomperts, B.N., Huang, J., Witte, O.N., and Graeber, T.G. (2019). Pan-cancer Convergence to a Small-Cell Neuroendocrine Phenotype that Shares Susceptibilities

- with Hematological Malignancies. *Cancer Cell* 36, 17-34 e17.  
10.1016/j.ccell.2019.06.005.
45. Rosario, E., and Rosario, D.J. (2023). Localized Prostate Cancer. In StatPearls.
  46. Keyes, M., Crook, J., Morton, G., Vigneault, E., Usmani, N., and Morris, W.J. (2013). Treatment options for localized prostate cancer. *Can Fam Physician* 59, 1269-1274.
  47. Huggins, C., and Hodges, C.V. (2002). Studies on prostatic cancer. I. The effect of castration, of estrogen and of androgen injection on serum phosphatases in metastatic carcinoma of the prostate. 1941. *J Urol* 167, 948-951; discussion 952.
  48. Sharifi, N., Gulley, J.L., and Dahut, W.L. (2005). Androgen deprivation therapy for prostate cancer. *JAMA* 294, 238-244. 10.1001/jama.294.2.238.
  49. Schroder, F., Crawford, E.D., Axcrone, K., Payne, H., and Keane, T.E. (2012). Androgen deprivation therapy: past, present and future. *BJU Int* 109 *Suppl* 6, 1-12. 10.1111/j.1464-410X.2012.11215.x.
  50. Watson, P.A., Arora, V.K., and Sawyers, C.L. (2015). Emerging mechanisms of resistance to androgen receptor inhibitors in prostate cancer. *Nat Rev Cancer* 15, 701-711. 10.1038/nrc4016.
  51. Puca, L., Vlachostergios, P.J., and Beltran, H. (2019). Neuroendocrine Differentiation in Prostate Cancer: Emerging Biology, Models, and Therapies. *Cold Spring Harb Perspect Med* 9. 10.1101/cshperspect.a030593.
  52. Abida, W., Cyrta, J., Heller, G., Prandi, D., Armenia, J., Coleman, I., Cieslik, M., Benelli, M., Robinson, D., Van Allen, E.M., et al. (2019). Genomic correlates of clinical outcome in advanced prostate cancer. *Proc Natl Acad Sci U S A* 116, 11428-11436.  
10.1073/pnas.1902651116.
  53. Beltran, H., Prandi, D., Mosquera, J.M., Benelli, M., Puca, L., Cyrta, J., Marotz, C., Giannopoulou, E., Chakravarthi, B.V., Varambally, S., et al. (2016). Divergent clonal

- evolution of castration-resistant neuroendocrine prostate cancer. *Nat Med* 22, 298-305. 10.1038/nm.4045.
54. Zhang, Q., Han, Y., Zhang, Y., Liu, D., Ming, J., Huang, B., and Qiu, X. (2020). Treatment-Emergent Neuroendocrine Prostate Cancer: A Clinicopathological and Immunohistochemical Analysis of 94 Cases. *Front Oncol* 10, 571308. 10.3389/fonc.2020.571308.
55. Beltran, H., Romanel, A., Conteduca, V., Casiraghi, N., Sigouros, M., Franceschini, G.M., Orlando, F., Fedrizzi, T., Ku, S.Y., Dann, E., et al. (2020). Circulating tumor DNA profile recognizes transformation to castration-resistant neuroendocrine prostate cancer. *J Clin Invest* 130, 1653-1668. 10.1172/JCI131041.
56. Aggarwal, R., Zhang, T., Small, E.J., and Armstrong, A.J. (2014). Neuroendocrine prostate cancer: subtypes, biology, and clinical outcomes. *J Natl Compr Canc Netw* 12, 719-726. 10.6004/jnccn.2014.0073.
57. Yamada, Y., and Beltran, H. (2021). Clinical and Biological Features of Neuroendocrine Prostate Cancer. *Curr Oncol Rep* 23, 15. 10.1007/s11912-020-01003-9.
58. Pikor, L.A., Ramnarine, V.R., Lam, S., and Lam, W.L. (2013). Genetic alterations defining NSCLC subtypes and their therapeutic implications. *Lung Cancer* 82, 179-189. 10.1016/j.lungcan.2013.07.025.
59. Alvarado-Luna, G., and Morales-Espinosa, D. (2016). Treatment for small cell lung cancer, where are we now?-a review. *Transl Lung Cancer Res* 5, 26-38. 10.3978/j.issn.2218-6751.2016.01.13.
60. Yang, S.R., Schultheis, A.M., Yu, H., Mandelker, D., Ladanyi, M., and Buttner, R. (2022). Precision medicine in non-small cell lung cancer: Current applications and future directions. *Semin Cancer Biol* 84, 184-198. 10.1016/j.semcancer.2020.07.009.

61. Yin, X., Li, Y., Wang, H., Jia, T., Wang, E., Luo, Y., Wei, Y., Qin, Z., and Ma, X. (2022). Small cell lung cancer transformation: From pathogenesis to treatment. *Semin Cancer Biol* 86, 595-606. 10.1016/j.semcancer.2022.03.006.
62. Zakowski, M.F., Ladanyi, M., and Kris, M.G. (2006). EGFR Mutations in Small-Cell Lung Cancers in Patients Who Have Never Smoked. *New England Journal of Medicine* 355, 213-215. 10.1056/NEJMc053610.
63. Clamon, G., Zeitler, W., An, J., and Hejleh, T.A. (2020). Transformational Changes Between Non–Small Cell and Small Cell Lung Cancer—Biological and Clinical Relevance—A Review. *American Journal of Clinical Oncology* 43, 670-675. 10.1097/coc.0000000000000720.
64. Chai, X., Zhang, X., Li, W., and Chai, J. (2021). Small cell lung cancer transformation during antitumor therapies: A systematic review. *Open Med (Wars)* 16, 1160-1167. 10.1515/med-2021-0321.
65. Oser, M.G., Niederst, M.J., Sequist, L.V., and Engelman, J.A. (2015). Transformation from non-small-cell lung cancer to small-cell lung cancer: molecular drivers and cells of origin. *Lancet Oncol* 16, e165-172. 10.1016/S1470-2045(14)71180-5.
66. Caliman, E., Fancelli, S., Petroni, G., Gatta Michelet, M.R., Cosso, F., Ottanelli, C., Mazzoni, F., Voltolini, L., Pillozzi, S., and Antonuzzo, L. (2023). Challenges in the treatment of small cell lung cancer in the era of immunotherapy and molecular classification. *Lung Cancer* 175, 88-100. 10.1016/j.lungcan.2022.11.014.
67. Wang, H.T., Yao, Y.H., Li, B.G., Tang, Y., Chang, J.W., and Zhang, J. (2014). Neuroendocrine Prostate Cancer (NEPC) progressing from conventional prostatic adenocarcinoma: factors associated with time to development of NEPC and survival from NEPC diagnosis—a systematic review and pooled analysis. *J Clin Oncol* 32, 3383-3390. 10.1200/JCO.2013.54.3553.
68. Basumallik, N., and Agarwal, M. (2023). Small Cell Lung Cancer. In *StatPearls*.

69. Hara, M., Kira, S., Kamiyama, M., Ihara, T., Sato, T., and Mitsui, T. (2022). Neuroendocrine prostate cancer treated with multimodal examination and therapy: A case report. *Urol Case Rep* 44, 102158. 10.1016/j.eucr.2022.102158.
70. Farago, A.F., and Keane, F.K. (2018). Current standards for clinical management of small cell lung cancer. *Transl Lung Cancer Res* 7, 69-79. 10.21037/tlcr.2018.01.16.
71. Cacciatore, A., Albino, D., Catapano, C.V., and Carbone, G.M. (2023). Preclinical Models of Neuroendocrine Prostate Cancer. *Curr Protoc* 3, e742. 10.1002/cpz1.742.
72. Ku, S.Y., Rosario, S., Wang, Y., Mu, P., Seshadri, M., Goodrich, Z.W., Goodrich, M.M., Labbe, D.P., Gomez, E.C., Wang, J., et al. (2017). Rb1 and Trp53 cooperate to suppress prostate cancer lineage plasticity, metastasis, and antiandrogen resistance. *Science* 355, 78-83. 10.1126/science.aah4199.
73. Mu, P., Zhang, Z., Benelli, M., Karthaus, W.R., Hoover, E., Chen, C.C., Wongvipat, J., Ku, S.Y., Gao, D., Cao, Z., et al. (2017). SOX2 promotes lineage plasticity and antiandrogen resistance in TP53- and RB1-deficient prostate cancer. *Science* 355, 84-88. 10.1126/science.aah4307.
74. Zou, M., Toivanen, R., Mitrofanova, A., Floch, N., Hayati, S., Sun, Y., Le Magnen, C., Chester, D., Mostaghel, E.A., Califano, A., et al. (2017). Transdifferentiation as a Mechanism of Treatment Resistance in a Mouse Model of Castration-Resistant Prostate Cancer. *Cancer Discov* 7, 736-749. 10.1158/2159-8290.CD-16-1174.
75. Han, M., Li, F., Zhang, Y., Dai, P., He, J., Li, Y., Zhu, Y., Zheng, J., Huang, H., Bai, F., and Gao, D. (2022). FOXA2 drives lineage plasticity and KIT pathway activation in neuroendocrine prostate cancer. *Cancer Cell* 40, 1306-1323 e1308. 10.1016/j.ccell.2022.10.011.
76. Brady, N.J., Bagadion, A.M., Singh, R., Conteduca, V., Van Emmenis, L., Arceci, E., Pakula, H., Carelli, R., Khani, F., Bakht, M., et al. (2021). Temporal evolution of cellular

- heterogeneity during the progression to advanced AR-negative prostate cancer. *Nat Commun* 12, 3372. 10.1038/s41467-021-23780-y.
77. Dardenne, E., Beltran, H., Benelli, M., Gayvert, K., Berger, A., Puca, L., Cyrta, J., Sboner, A., Noorzad, Z., MacDonald, T., et al. (2016). N-Myc Induces an EZH2-Mediated Transcriptional Program Driving Neuroendocrine Prostate Cancer. *Cancer Cell* 30, 563-577. 10.1016/j.ccell.2016.09.005.
78. Lee, J.K., Phillips, J.W., Smith, B.A., Park, J.W., Stoyanova, T., McCaffrey, E.F., Baertsch, R., Sokolov, A., Meyerowitz, J.G., Mathis, C., et al. (2016). N-Myc Drives Neuroendocrine Prostate Cancer Initiated from Human Prostate Epithelial Cells. *Cancer Cell* 29, 536-547. 10.1016/j.ccell.2016.03.001.
79. Park, J.W., Lee, J.K., Sheu, K.M., Wang, L., Balanis, N.G., Nguyen, K., Smith, B.A., Cheng, C., Tsai, B.L., Cheng, D.H., et al. (2018). Reprogramming normal human epithelial tissues to a common, lethal neuroendocrine cancer lineage. *Science* 362, 91-95. 10.1126/science.aat5749.
80. Nguyen, H.M., Vessella, R.L., Morrissey, C., Brown, L.G., Coleman, I.M., Higano, C.S., Mostaghel, E.A., Zhang, X., True, L.D., Lam, H.M., et al. (2017). LuCaP Prostate Cancer Patient-Derived Xenografts Reflect the Molecular Heterogeneity of Advanced Disease and Serve as Models for Evaluating Cancer Therapeutics. *Prostate* 77, 654-671. 10.1002/pros.23313.
81. Lin, D., Wyatt, A.W., Xue, H., Wang, Y., Dong, X., Haegert, A., Wu, R., Brahmabhatt, S., Mo, F., Jong, L., et al. (2014). High fidelity patient-derived xenografts for accelerating prostate cancer discovery and drug development. *Cancer Res* 74, 1272-1283. 10.1158/0008-5472.Can-13-2921-t.
82. Tzelepi, V., Zhang, J., Lu, J.F., Kleb, B., Wu, G., Wan, X., Hoang, A., Efstathiou, E., Sircar, K., Navone, N.M., et al. (2012). Modeling a lethal prostate cancer variant with

- small-cell carcinoma features. *Clin Cancer Res* 18, 666-677. 10.1158/1078-0432.CCR-11-1867.
83. Puca, L., Bareja, R., Prandi, D., Shaw, R., Benelli, M., Karthaus, W.R., Hess, J., Sigouros, M., Donoghue, A., Kossai, M., et al. (2018). Patient derived organoids to model rare prostate cancer phenotypes. *Nat Commun* 9, 2404. 10.1038/s41467-018-04495-z.
84. Chan, J.M., Zaidi, S., Love, J.R., Zhao, J.L., Setty, M., Wadosky, K.M., Gopalan, A., Choo, Z.N., Persad, S., Choi, J., et al. (2022). Lineage plasticity in prostate cancer depends on JAK/STAT inflammatory signaling. *Science* 377, 1180-1191. 10.1126/science.abn0478.
85. Horoszewicz, J.S., Leong, S.S., Kawinski, E., Karr, J.P., Rosenthal, H., Chu, T.M., Mirand, E.A., and Murphy, G.P. (1983). LNCaP model of human prostatic carcinoma. *Cancer Res* 43, 1809-1818.
86. Bishop, J.L., Thaper, D., Vahid, S., Davies, A., Ketola, K., Kuruma, H., Jama, R., Nip, K.M., Angeles, A., Johnson, F., et al. (2017). The Master Neural Transcription Factor BRN2 Is an Androgen Receptor-Suppressed Driver of Neuroendocrine Differentiation in Prostate Cancer. *Cancer Discov* 7, 54-71. 10.1158/2159-8290.CD-15-1263.
87. Shen, R., Dorai, T., Szaboies, M., Katz, A.E., Olsson, C.A., and Buttyan, R. (1997). Transdifferentiation of cultured human prostate cancer cells to a neuroendocrine cell phenotype in a hormone-depleted medium. *Urol Oncol* 3, 67-75. 10.1016/s1078-1439(97)00039-2.
88. Li, Y., Chen, R., Bowden, M., Mo, F., Lin, Y.Y., Gleave, M., Collins, C., and Dong, X. (2017). Establishment of a neuroendocrine prostate cancer model driven by the RNA splicing factor SRRM4. *Oncotarget* 8, 66878-66888. 10.18632/oncotarget.19916.
89. Wang, L., Smith, B.A., Balanis, N.G., Tsai, B.L., Nguyen, K., Cheng, M.W., Obusan, M.B., Esedebe, F.N., Patel, S.J., Zhang, H., et al. (2020). A genetically defined disease

- model reveals that urothelial cells can initiate divergent bladder cancer phenotypes. *Proc Natl Acad Sci U S A* 117, 563-572. 10.1073/pnas.1915770117.
90. Wang, Q., Gümüş, Z.H., Colarossi, C., Memeo, L., Wang, X., Kong, C.Y., and Boffetta, P. (2023). SCLC: Epidemiology, Risk Factors, Genetic Susceptibility, Molecular Pathology, Screening, and Early Detection. *Journal of Thoracic Oncology* 18, 31-46. <https://doi.org/10.1016/j.jtho.2022.10.002>.
  91. Chen, J., Shi, M., Chuen Choi, S.Y., Wang, Y., Lin, D., Zeng, H., and Wang, Y. (2023). Genomic alterations in neuroendocrine prostate cancer: A systematic review and meta-analysis. *BJUI Compass* 4, 256-265. 10.1002/bco2.212.
  92. Nyquist, M.D., Corella, A., Coleman, I., De Sarkar, N., Kaipainen, A., Ha, G., Gulati, R., Ang, L., Chatterjee, P., Lucas, J., et al. (2020). Combined TP53 and RB1 Loss Promotes Prostate Cancer Resistance to a Spectrum of Therapeutics and Confers Vulnerability to Replication Stress. *Cell Rep* 31, 107669. 10.1016/j.celrep.2020.107669.
  93. Meuwissen, R., Linn, S.C., Linnoila, R.I., Zevenhoven, J., Mooi, W.J., and Berns, A. (2003). Induction of small cell lung cancer by somatic inactivation of both Trp53 and Rb1 in a conditional mouse model. *Cancer Cell* 4, 181-189. 10.1016/s1535-6108(03)00220-4.
  94. Ireland, A.S., Micinski, A.M., Kastner, D.W., Guo, B., Wait, S.J., Spainhower, K.B., Conley, C.C., Chen, O.S., Guthrie, M.R., Soltero, D., et al. (2020). MYC Drives Temporal Evolution of Small Cell Lung Cancer Subtypes by Reprogramming Neuroendocrine Fate. *Cancer Cell* 38, 60-78 e12. 10.1016/j.ccell.2020.05.001.
  95. Berger, A., Brady, N.J., Bareja, R., Robinson, B., Conteduca, V., Augello, M.A., Puca, L., Ahmed, A., Dardenne, E., Lu, X., et al. (2019). N-Myc-mediated epigenetic reprogramming drives lineage plasticity in advanced prostate cancer. *J Clin Invest* 129, 3924-3940. 10.1172/JCI127961.



96. Kim, D.W., Kim, K.C., Kim, K.B., Dunn, C.T., and Park, K.S. (2018). Transcriptional deregulation underlying the pathogenesis of small cell lung cancer. *Transl Lung Cancer Res* 7, 4-20. 10.21037/tlcr.2017.10.07.
97. Chakraborty, G., Gupta, K., and Kyprianou, N. (2023). Epigenetic mechanisms underlying subtype heterogeneity and tumor recurrence in prostate cancer. *Nat Commun* 14, 567. 10.1038/s41467-023-36253-1.
98. Ge, R., Wang, Z., Montironi, R., Jiang, Z., Cheng, M., Santoni, M., Huang, K., Massari, F., Lu, X., Cimadamore, A., et al. (2020). Epigenetic modulations and lineage plasticity in advanced prostate cancer. *Ann Oncol* 31, 470-479. 10.1016/j.annonc.2020.02.002.
99. Smith, B.A., Balanis, N.G., Nanjundiah, A., Sheu, K.M., Tsai, B.L., Zhang, Q., Park, J.W., Thompson, M., Huang, J., Witte, O.N., and Graeber, T.G. (2018). A Human Adult Stem Cell Signature Marks Aggressive Variants across Epithelial Cancers. *Cell Rep* 24, 3353-3366 e3355. 10.1016/j.celrep.2018.08.062.
100. Cheng, W.C., and Wang, H.J. (2021). Current advances of targeting epigenetic modifications in neuroendocrine prostate cancer. *Tzu Chi Med J* 33, 224-232. 10.4103/tcmj.tcmj\_220\_20.
101. Kinney, S.R., Moser, M.T., Pascual, M., Grealley, J.M., Foster, B.A., and Karpf, A.R. (2010). Opposing roles of Dnmt1 in early- and late-stage murine prostate cancer. *Mol Cell Biol* 30, 4159-4174. 10.1128/MCB.00235-10.
102. Storck, W.K., May, A.M., Westbrook, T.C., Duan, Z., Morrissey, C., Yates, J.A., and Alumkal, J.J. (2022). The Role of Epigenetic Change in Therapy-Induced Neuroendocrine Prostate Cancer Lineage Plasticity. *Front Endocrinol (Lausanne)* 13, 926585. 10.3389/fendo.2022.926585.
103. Xu, K., Wu, Z.J., Groner, A.C., He, H.H., Cai, C., Lis, R.T., Wu, X., Stack, E.C., Loda, M., Liu, T., et al. (2012). EZH2 oncogenic activity in castration-resistant prostate cancer cells is Polycomb-independent. *Science* 338, 1465-1469. 10.1126/science.1227604.

104. Gan, L., Yang, Y., Li, Q., Feng, Y., Liu, T., and Guo, W. (2018). Epigenetic regulation of cancer progression by EZH2: from biological insights to therapeutic potential. *Biomark Res* 6, 10. 10.1186/s40364-018-0122-2.
105. Vire, E., Brenner, C., Deplus, R., Blanchon, L., Fraga, M., Didelot, C., Morey, L., Van Eynde, A., Bernard, D., Vanderwinden, J.M., et al. (2006). The Polycomb group protein EZH2 directly controls DNA methylation. *Nature* 439, 871-874. 10.1038/nature04431.
106. Yamada, Y., Venkadakrishnan, V.B., Mizuno, K., Bakht, M., Ku, S.Y., Garcia, M.M., and Beltran, H. (2023). Targeting DNA methylation and B7-H3 in RB1-deficient and neuroendocrine prostate cancer. *Sci Transl Med* 15, eadf6732. 10.1126/scitranslmed.adf6732.
107. Ruan, L., Wang, L., Wang, X., He, M., and Yao, X. (2018). SIRT1 contributes to neuroendocrine differentiation of prostate cancer. *Oncotarget* 9, 2002-2016. 10.18632/oncotarget.23111.
108. Leach, D.A., Fernandes, R.C., and Bevan, C.L. (2022). Cellular specificity of androgen receptor, coregulators, and pioneer factors in prostate cancer. *Endocr Oncol* 2, R112-R131. 10.1530/EO-22-0065.
109. Hankey, W., Chen, Z., and Wang, Q. (2020). Shaping Chromatin States in Prostate Cancer by Pioneer Transcription Factors. *Cancer Res* 80, 2427-2436. 10.1158/0008-5472.CAN-19-3447.
110. Iwafuchi-Doi, M., and Zaret, K.S. (2016). Cell fate control by pioneer transcription factors. *Development* 143, 1833-1837. 10.1242/dev.133900.
111. Sunkel, B.D., and Stanton, B.Z. (2021). Pioneer factors in development and cancer. *iScience* 24, 103132. 10.1016/j.isci.2021.103132.
112. Lupien, M., Eeckhoute, J., Meyer, C.A., Wang, Q., Zhang, Y., Li, W., Carroll, J.S., Liu, X.S., and Brown, M. (2008). FoxA1 translates epigenetic signatures into enhancer-driven lineage-specific transcription. *Cell* 132, 958-970. 10.1016/j.cell.2008.01.018.

113. Jain, R.K., Mehta, R.J., Nakshatri, H., Idrees, M.T., and Badve, S.S. (2011). High-level expression of forkhead-box protein A1 in metastatic prostate cancer. *Histopathology* 58, 766-772. 10.1111/j.1365-2559.2011.03796.x.
114. Gao, N., Zhang, J., Rao, M.A., Case, T.C., Mirosevich, J., Wang, Y., Jin, R., Gupta, A., Rennie, P.S., and Matusik, R.J. (2003). The role of hepatocyte nuclear factor-3 alpha (Forkhead Box A1) and androgen receptor in transcriptional regulation of prostatic genes. *Mol Endocrinol* 17, 1484-1507. 10.1210/me.2003-0020.
115. Adams, E.J., Karthaus, W.R., Hoover, E., Liu, D., Gruet, A., Zhang, Z., Cho, H., DiLoreto, R., Chhangawala, S., Liu, Y., et al. (2019). FOXA1 mutations alter pioneering activity, differentiation and prostate cancer phenotypes. *Nature* 571, 408-412. 10.1038/s41586-019-1318-9.
116. Parolia, A., Cieslik, M., Chu, S.C., Xiao, L., Ouchi, T., Zhang, Y., Wang, X., Vats, P., Cao, X., Pitchiaya, S., et al. (2019). Distinct structural classes of activating FOXA1 alterations in advanced prostate cancer. *Nature* 571, 413-418. 10.1038/s41586-019-1347-4.
117. Baca, S.C., Takeda, D.Y., Seo, J.H., Hwang, J., Ku, S.Y., Arafeh, R., Arnoff, T., Agarwal, S., Bell, C., O'Connor, E., et al. (2021). Reprogramming of the FOXA1 cistrome in treatment-emergent neuroendocrine prostate cancer. *Nat Commun* 12, 1979. 10.1038/s41467-021-22139-7.
118. Park, J.W., Lee, J.K., Witte, O.N., and Huang, J. (2017). FOXA2 is a sensitive and specific marker for small cell neuroendocrine carcinoma of the prostate. *Mod Pathol* 30, 1262-1272. 10.1038/modpathol.2017.44.
119. Raposo, A., Vasconcelos, F.F., Drechsel, D., Marie, C., Johnston, C., Dolle, D., Bithell, A., Gillotin, S., van den Berg, D.L.C., Ettwiller, L., et al. (2015). Ascl1 Coordinately Regulates Gene Expression and the Chromatin Landscape during Neurogenesis. *Cell Rep* 10, 1544-1556. 10.1016/j.celrep.2015.02.025.

120. Wapinski, O.L., Lee, Q.Y., Chen, A.C., Li, R., Corces, M.R., Ang, C.E., Treutlein, B., Xiang, C., Baubet, V., Suchy, F.P., et al. (2017). Rapid Chromatin Switch in the Direct Reprogramming of Fibroblasts to Neurons. *Cell Rep* 20, 3236-3247. 10.1016/j.celrep.2017.09.011.
121. Parkinson, L.M., Gillen, S.L., Woods, L.M., Chaytor, L., Marcos, D., Ali, F.R., Carroll, J.S., and Philpott, A. (2022). The proneural transcription factor ASCL1 regulates cell proliferation and primes for differentiation in neuroblastoma. *Front Cell Dev Biol* 10, 942579. 10.3389/fcell.2022.942579.
122. Park, N.I., Guilhamon, P., Desai, K., McAdam, R.F., Langille, E., O'Connor, M., Lan, X., Whetstone, H., Coutinho, F.J., Vanner, R.J., et al. (2017). ASCL1 Reorganizes Chromatin to Direct Neuronal Fate and Suppress Tumorigenicity of Glioblastoma Stem Cells. *Cell Stem Cell* 21, 209-224 e207. 10.1016/j.stem.2017.06.004.
123. Nouruzi, S., Ganguli, D., Tabrizian, N., Kobelev, M., Sivak, O., Namekawa, T., Thaper, D., Baca, S.C., Freedman, M.L., Aguda, A., et al. (2022). ASCL1 activates neuronal stem cell-like lineage programming through remodeling of the chromatin landscape in prostate cancer. *Nat Commun* 13, 2282. 10.1038/s41467-022-29963-5.
124. Rudin, C.M., Poirier, J.T., Byers, L.A., Dive, C., Dowlati, A., George, J., Heymach, J.V., Johnson, J.E., Lehman, J.M., MacPherson, D., et al. (2019). Molecular subtypes of small cell lung cancer: a synthesis of human and mouse model data. *Nat Rev Cancer* 19, 289-297. 10.1038/s41568-019-0133-9.
125. George, J., Lim, J.S., Jang, S.J., Cun, Y., Ozretic, L., Kong, G., Leenders, F., Lu, X., Fernandez-Cuesta, L., Bosco, G., et al. (2015). Comprehensive genomic profiles of small cell lung cancer. *Nature* 524, 47-53. 10.1038/nature14664.
126. Caesar, R., Egger, J.V., Chavan, S., Socci, N.D., Jones, C.B., Kombak, F.E., Asher, M., Roehrl, M.H., Shah, N.S., Allaj, V., et al. (2022). Genomic and transcriptomic analysis of

- a library of small cell lung cancer patient-derived xenografts. *Nat Commun* 13, 2144.  
10.1038/s41467-022-29794-4.
127. Baine, M.K., Hsieh, M.S., Lai, W.V., Egger, J.V., Jungbluth, A.A., Daneshbod, Y., Beras, A., Spencer, R., Lopardo, J., Bodd, F., et al. (2020). SCLC Subtypes Defined by ASCL1, NEUROD1, POU2F3, and YAP1: A Comprehensive Immunohistochemical and Histopathologic Characterization. *J Thorac Oncol* 15, 1823-1835.  
10.1016/j.jtho.2020.09.009.
128. Schwendenwein, A., Megyesfalvi, Z., Barany, N., Valko, Z., Bugyik, E., Lang, C., Ferencz, B., Paku, S., Lantos, A., Fillinger, J., et al. (2021). Molecular profiles of small cell lung cancer subtypes: therapeutic implications. *Mol Ther Oncolytics* 20, 470-483.  
10.1016/j.omto.2021.02.004.
129. Gay, C.M., Stewart, C.A., Park, E.M., Diao, L., Groves, S.M., Heeke, S., Nabet, B.Y., Fujimoto, J., Solis, L.M., Lu, W., et al. (2021). Patterns of transcription factor programs and immune pathway activation define four major subtypes of SCLC with distinct therapeutic vulnerabilities. *Cancer Cell* 39, 346-360 e347. 10.1016/j.ccell.2020.12.014.
130. Cejas, P., Xie, Y., Font-Tello, A., Lim, K., Syamala, S., Qiu, X., Tewari, A.K., Shah, N., Nguyen, H.M., Patel, R.A., et al. (2021). Subtype heterogeneity and epigenetic convergence in neuroendocrine prostate cancer. *Nat Commun* 12, 5775.  
10.1038/s41467-021-26042-z.
131. Kageyama, R., Ohtsuka, T., Hatakeyama, J., and Ohsawa, R. (2005). Roles of bHLH genes in neural stem cell differentiation. *Exp Cell Res* 306, 343-348.  
10.1016/j.yexcr.2005.03.015.
132. Kim, E.J., Ables, J.L., Dickel, L.K., Eisch, A.J., and Johnson, J.E. (2011). Ascl1 (Mash1) defines cells with long-term neurogenic potential in subgranular and subventricular zones in adult mouse brain. *PLoS One* 6, e18472. 10.1371/journal.pone.0018472.

133. Helms, A.W., Battiste, J., Henke, R.M., Nakada, Y., Simplicio, N., Guillemot, F., and Johnson, J.E. (2005). Sequential roles for Mash1 and Ngn2 in the generation of dorsal spinal cord interneurons. *Development* 132, 2709-2719. 10.1242/dev.01859.
134. Vue, T.Y., Kollipara, R.K., Borromeo, M.D., Smith, T., Mashimo, T., Burns, D.K., Bachoo, R.M., and Johnson, J.E. (2020). ASCL1 regulates neurodevelopmental transcription factors and cell cycle genes in brain tumors of glioma mouse models. *Glia* 68, 2613-2630. 10.1002/glia.23873.
135. Vierbuchen, T., Ostermeier, A., Pang, Z.P., Kokubu, Y., Sudhof, T.C., and Wernig, M. (2010). Direct conversion of fibroblasts to functional neurons by defined factors. *Nature* 463, 1035-1041. 10.1038/nature08797.
136. Paun, O., Tan, Y.X., Patel, H., Strohbuecker, S., Ghanate, A., Cobolli-Gigli, C., Llorian Sopena, M., Gerontogianni, L., Goldstone, R., Ang, S.L., et al. (2023). Pioneer factor ASCL1 cooperates with the mSWI/SNF complex at distal regulatory elements to regulate human neural differentiation. *Genes Dev* 37, 218-242. 10.1101/gad.350269.122.
137. Pang, Z.P., Yang, N., Vierbuchen, T., Ostermeier, A., Fuentes, D.R., Yang, T.Q., Citri, A., Sebastiano, V., Marro, S., Sudhof, T.C., and Wernig, M. (2011). Induction of human neuronal cells by defined transcription factors. *Nature* 476, 220-223. 10.1038/nature10202.
138. Qu, S., Fetsch, P., Thomas, A., Pommier, Y., Schrupp, D.S., Miettinen, M.M., and Chen, H. (2022). Molecular Subtypes of Primary SCLC Tumors and Their Associations With Neuroendocrine and Therapeutic Markers. *J Thorac Oncol* 17, 141-153. 10.1016/j.jtho.2021.08.763.
139. Ding, X.L., Su, Y.G., Yu, L., Bai, Z.L., Bai, X.H., Chen, X.Z., Yang, X., Zhao, R., He, J.X., and Wang, Y.Y. (2022). Clinical characteristics and patient outcomes of molecular subtypes of small cell lung cancer (SCLC). *World J Surg Oncol* 20, 54. 10.1186/s12957-022-02528-y.

140. Jiang, T., Collins, B.J., Jin, N., Watkins, D.N., Brock, M.V., Matsui, W., Nelkin, B.D., and Ball, D.W. (2009). Achaete-scute complex homologue 1 regulates tumor-initiating capacity in human small cell lung cancer. *Cancer Res* 69, 845-854. 10.1158/0008-5472.CAN-08-2762.
141. Borges, M., Linnoila, R.I., van de Velde, H.J., Chen, H., Nelkin, B.D., Mabry, M., Baylin, S.B., and Ball, D.W. (1997). An achaete-scute homologue essential for neuroendocrine differentiation in the lung. *Nature* 386, 852-855. 10.1038/386852a0.
142. Osada, H., Tatematsu, Y., Yatabe, Y., Horio, Y., and Takahashi, T. (2005). ASH1 gene is a specific therapeutic target for lung cancers with neuroendocrine features. *Cancer Res* 65, 10680-10685. 10.1158/0008-5472.CAN-05-1404.
143. Augustyn, A., Borromeo, M., Wang, T., Fujimoto, J., Shao, C., Dospoy, P.D., Lee, V., Tan, C., Sullivan, J.P., Larsen, J.E., et al. (2014). ASCL1 is a lineage oncogene providing therapeutic targets for high-grade neuroendocrine lung cancers. *Proc Natl Acad Sci U S A* 111, 14788-14793. 10.1073/pnas.1410419111.
144. Borromeo, M.D., Savage, T.K., Kollipara, R.K., He, M., Augustyn, A., Osborne, J.K., Girard, L., Minna, J.D., Gazdar, A.F., Cobb, M.H., and Johnson, J.E. (2016). ASCL1 and NEUROD1 Reveal Heterogeneity in Pulmonary Neuroendocrine Tumors and Regulate Distinct Genetic Programs. *Cell Rep* 16, 1259-1272. 10.1016/j.celrep.2016.06.081.
145. Nie, J., Zhang, P., Liang, C., Yu, Y., and Wang, X. (2023). ASCL1-mediated ferroptosis resistance enhances the progress of castration-resistant prostate cancer to neurosecretory prostate cancer. *Free Radic Biol Med* 205, 318-331. 10.1016/j.freeradbiomed.2023.06.006.
146. Tabrizian, N., Nouruzi, S., Cui, C.J., Kobelev, M., Namekawa, T., Lodhia, I., Talal, A., Sivak, O., Ganguli, D., and Zoubeidi, A. (2023). ASCL1 is activated downstream of the ROR2/CREB signaling pathway to support lineage plasticity in prostate cancer. *Cell Reports* 42, 112937. <https://doi.org/10.1016/j.celrep.2023.112937>.

147. Boutin, C., Hardt, O., de Chevigny, A., Core, N., Goebbels, S., Seidenfaden, R., Bosio, A., and Cremer, H. (2010). NeuroD1 induces terminal neuronal differentiation in olfactory neurogenesis. *Proc Natl Acad Sci U S A* *107*, 1201-1206. 10.1073/pnas.0909015107.
148. Gao, Z., Ure, K., Ables, J.L., Lagace, D.C., Nave, K.A., Goebbels, S., Eisch, A.J., and Hsieh, J. (2009). Neurod1 is essential for the survival and maturation of adult-born neurons. *Nat Neurosci* *12*, 1090-1092. 10.1038/nn.2385.
149. Mutoh, H., Naya, F.J., Tsai, M.J., and Leiter, A.B. (1998). The basic helix-loop-helix protein BETA2 interacts with p300 to coordinate differentiation of secretin-expressing enteroendocrine cells. *Genes Dev* *12*, 820-830. 10.1101/gad.12.6.820.
150. Osborne, J.K., Larsen, J.E., Shields, M.D., Gonzales, J.X., Shames, D.S., Sato, M., Kulkarni, A., Wistuba, II, Girard, L., Minna, J.D., and Cobb, M.H. (2013). NeuroD1 regulates survival and migration of neuroendocrine lung carcinomas via signaling molecules TrkB and NCAM. *Proc Natl Acad Sci U S A* *110*, 6524-6529. 10.1073/pnas.1303932110.
151. Ikematsu, Y., Tanaka, K., Toyokawa, G., Ijichi, K., Ando, N., Yoneshima, Y., Iwama, E., Inoue, H., Tagawa, T., Nakanishi, Y., and Okamoto, I. (2020). NEUROD1 is highly expressed in extensive-disease small cell lung cancer and promotes tumor cell migration. *Lung Cancer* *146*, 97-104. 10.1016/j.lungcan.2020.05.012.
152. Baine, M.K., Febres-Aldana, C.A., Chang, J.C., Jungbluth, A.A., Sethi, S., Antonescu, C.R., Travis, W.D., Hsieh, M.S., Roh, M.S., Homer, R.J., et al. (2022). POU2F3 in SCLC: Clinicopathologic and Genomic Analysis With a Focus on Its Diagnostic Utility in Neuroendocrine-Low SCLC. *J Thorac Oncol* *17*, 1109-1121. 10.1016/j.jtho.2022.06.004.
153. Gerbe, F., Sidot, E., Smyth, D.J., Ohmoto, M., Matsumoto, I., Dardalhon, V., Cesses, P., Garnier, L., Pouzolles, M., Brulin, B., et al. (2016). Intestinal epithelial tuft cells initiate type 2 mucosal immunity to helminth parasites. *Nature* *529*, 226-230. 10.1038/nature16527.



154. Yamashita, J., Ohmoto, M., Yamaguchi, T., Matsumoto, I., and Hirota, J. (2017). Skn-1a/Pou2f3 functions as a master regulator to generate Trpm5-expressing chemosensory cells in mice. *PLoS One* 12, e0189340. 10.1371/journal.pone.0189340.
155. Huang, Y.H., Klingbeil, O., He, X.Y., Wu, X.S., Arun, G., Lu, B., Somerville, T.D.D., Milazzo, J.P., Wilkinson, J.E., Demerdash, O.E., et al. (2018). POU2F3 is a master regulator of a tuft cell-like variant of small cell lung cancer. *Genes Dev* 32, 915-928. 10.1101/gad.314815.118.
156. Wu, X.S., He, X.Y., Ipsaro, J.J., Huang, Y.H., Preall, J.B., Ng, D., Shue, Y.T., Sage, J., Egeblad, M., Joshua-Tor, L., and Vakoc, C.R. (2022). OCA-T1 and OCA-T2 are coactivators of POU2F3 in the tuft cell lineage. *Nature* 607, 169-175. 10.1038/s41586-022-04842-7.
157. Wu, Z., Su, J., Li, F.L., Chen, T., Mayner, J., Engler, A., Ma, S., Li, Q., and Guan, K.L. (2023). YAP silencing by RB1 mutation is essential for small-cell lung cancer metastasis. *Nat Commun* 14, 5916. 10.1038/s41467-023-41585-z.
158. Owonikoko, T.K., Dwivedi, B., Chen, Z., Zhang, C., Barwick, B., Ernani, V., Zhang, G., Gilbert-Ross, M., Carlisle, J., Khuri, F.R., et al. (2021). YAP1 Expression in SCLC Defines a Distinct Subtype With T-cell-Inflamed Phenotype. *J Thorac Oncol* 16, 464-476. 10.1016/j.jtho.2020.11.006.
159. Chen, P., Sun, C., Wang, H., Zhao, W., Wu, Y., Guo, H., Zhou, C., and He, Y. (2023). YAP1 expression is associated with survival and immunosuppression in small cell lung cancer. *Cell Death & Disease* 14, 636. 10.1038/s41419-023-06053-y.
160. Pan, D. (2010). The hippo signaling pathway in development and cancer. *Dev Cell* 19, 491-505. 10.1016/j.devcel.2010.09.011.
161. Piccolo, S., Panciera, T., Contessotto, P., and Cordenonsi, M. (2023). YAP/TAZ as master regulators in cancer: modulation, function and therapeutic approaches. *Nat Cancer* 4, 9-26. 10.1038/s43018-022-00473-z.

162. Moya, I.M., and Halder, G. (2019). Hippo–YAP/TAZ signalling in organ regeneration and regenerative medicine. *Nature Reviews Molecular Cell Biology* 20, 211-226.  
10.1038/s41580-018-0086-y.
163. Pearson, J.D., Huang, K., Pacal, M., McCurdy, S.R., Lu, S., Aubry, A., Yu, T., Wadosky, K.M., Zhang, L., Wang, T., et al. (2021). Binary pan-cancer classes with distinct vulnerabilities defined by pro- or anti-cancer YAP/TEAD activity. *Cancer Cell* 39, 1115-1134 e1112. 10.1016/j.ccell.2021.06.016.
164. Wu, Q., Guo, J., Liu, Y., Zheng, Q., Li, X., Wu, C., Fang, D., Chen, X., Ma, L., Xu, P., et al. (2021). YAP drives fate conversion and chemoresistance of small cell lung cancer. *Sci Adv* 7, eabg1850. 10.1126/sciadv.abg1850.
165. Davies, A., Zoubeidi, A., and Selth, L.A. (2020). The epigenetic and transcriptional landscape of neuroendocrine prostate cancer. *Endocr Relat Cancer* 27, R35-R50.  
10.1530/ERC-19-0420.
166. Thaper, D., Munuganti, R., Aguda, A., Kim, S., Ku, S., Sivak, O., Kumar, S., Vahid, S., Ganguli, D., Beltran, H., et al. (2022). Discovery and characterization of a first-in-field transcription factor BRN2 inhibitor for the treatment of neuroendocrine prostate cancer. *bioRxiv*, 2022.2005.2004.490172. 10.1101/2022.05.04.490172.
167. Bhagirath, D., Yang, T.L., Tabatabai, Z.L., Majid, S., Dahiya, R., Tanaka, Y., and Saini, S. (2019). BRN4 Is a Novel Driver of Neuroendocrine Differentiation in Castration-Resistant Prostate Cancer and Is Selectively Released in Extracellular Vesicles with BRN2. *Clin Cancer Res* 25, 6532-6545. 10.1158/1078-0432.CCR-19-0498.
168. Sakaeda, M., Sato, H., Ishii, J., Miyata, C., Kamma, H., Shishido-Hara, Y., Shimoyamada, H., Fujiwara, M., Endo, T., Tanaka, R., et al. (2013). Neural lineage-specific homeoprotein BRN2 is directly involved in TTF1 expression in small-cell lung cancer. *Lab Invest* 93, 408-421. 10.1038/labinvest.2013.2.

169. Feng, R., and Wen, J. (2015). Overview of the roles of Sox2 in stem cell and development. *Biol Chem* 396, 883-891. 10.1515/hsz-2014-0317.
170. Schaefer, T., and Lengerke, C. (2020). SOX2 protein biochemistry in stemness, reprogramming, and cancer: the PI3K/AKT/SOX2 axis and beyond. *Oncogene* 39, 278-292. 10.1038/s41388-019-0997-x.
171. Rudin, C.M., Durinck, S., Stawiski, E.W., Poirier, J.T., Modrusan, Z., Shames, D.S., Bergbower, E.A., Guan, Y., Shin, J., Guillory, J., et al. (2012). Comprehensive genomic analysis identifies SOX2 as a frequently amplified gene in small-cell lung cancer. *Nat Genet* 44, 1111-1116. 10.1038/ng.2405.
172. Karachaliou, N., Rosell, R., and Viteri, S. (2013). The role of SOX2 in small cell lung cancer, lung adenocarcinoma and squamous cell carcinoma of the lung. *Transl Lung Cancer Res* 2, 172-179. 10.3978/j.issn.2218-6751.2013.01.01.
173. Voigt, E., Wallenburg, M., Wollenzien, H., Thompson, E., Kumar, K., Feiner, J., McNally, M., Friesen, H., Mukherjee, M., Afeworki, Y., and Kareta, M.S. (2021). Sox2 Is an Oncogenic Driver of Small-Cell Lung Cancer and Promotes the Classic Neuroendocrine Subtype. *Mol Cancer Res* 19, 2015-2025. 10.1158/1541-7786.MCR-20-1006.
174. Tenjin, Y., Matsuura, K., Kudoh, S., Usuki, S., Yamada, T., Matsuo, A., Sato, Y., Saito, H., Fujino, K., Wakimoto, J., et al. (2020). Distinct transcriptional programs of SOX2 in different types of small cell lung cancers. *Lab Invest* 100, 1575-1588. 10.1038/s41374-020-00479-0.
175. Kareta, M.S., Gorges, L.L., Hafeez, S., Benayoun, B.A., Marro, S., Zmoos, A.F., Cecchini, M.J., Spacek, D., Batista, L.F., O'Brien, M., et al. (2015). Inhibition of pluripotency networks by the Rb tumor suppressor restricts reprogramming and tumorigenesis. *Cell Stem Cell* 16, 39-50. 10.1016/j.stem.2014.10.019.
176. Quintanal-Villalonga, A., Durani, V., Sabet, A., Redin, E., Kawasaki, K., Shafer, M., Karthaus, W.R., Zaidi, S., Zhan, Y.A., Manoj, P., et al. (2023). Exportin 1 inhibition

- prevents neuroendocrine transformation through SOX2 down-regulation in lung and prostate cancers. *Sci Transl Med* 15, eadf7006. 10.1126/scitranslmed.adf7006.
177. Yu, J., Li, D., and Jiang, H. (2020). Emerging role of ONECUT2 in tumors. *Oncol Lett* 20, 328. 10.3892/ol.2020.12192.
  178. Choi, W.W., Boland, J.L., and Lin, J. (2022). ONECUT2 as a key mediator of androgen receptor-independent cell growth and neuroendocrine differentiation in castration-resistant prostate cancer. *Cancer Drug Resist* 5, 165-170. 10.20517/cdr.2021.108.
  179. Rotinen, M., You, S., Yang, J., Coetzee, S.G., Reis-Sobreiro, M., Huang, W.C., Huang, F., Pan, X., Yanez, A., Hazelett, D.J., et al. (2018). ONECUT2 is a targetable master regulator of lethal prostate cancer that suppresses the androgen axis. *Nat Med* 24, 1887-1898. 10.1038/s41591-018-0241-1.
  180. Guo, H., Ci, X., Ahmed, M., Hua, J.T., Soares, F., Lin, D., Puca, L., Vosoughi, A., Xue, H., Li, E., et al. (2019). ONECUT2 is a driver of neuroendocrine prostate cancer. *Nat Commun* 10, 278. 10.1038/s41467-018-08133-6.
  181. Udyavar, A.R., Wooten, D.J., Hoeksema, M., Bansal, M., Califano, A., Estrada, L., Schnell, S., Irish, J.M., Massion, P.P., and Quaranta, V. (2017). Novel Hybrid Phenotype Revealed in Small Cell Lung Cancer by a Transcription Factor Network Model That Can Explain Tumor Heterogeneity. *Cancer Res* 77, 1063-1074. 10.1158/0008-5472.CAN-16-1467.
  182. Groves, S.M., Ildefonso, G.V., McAtee, C.O., Ozawa, P.M.M., Ireland, A.S., Stauffer, P.E., Wasdin, P.T., Huang, X., Qiao, Y., Lim, J.S., et al. (2022). Archetype tasks link intratumoral heterogeneity to plasticity and cancer hallmarks in small cell lung cancer. *Cell Syst* 13, 690-710 e617. 10.1016/j.cels.2022.07.006.
  183. Ozen, M., and Lopez, C.F. (2023). Data-driven structural analysis of small cell lung cancer transcription factor network suggests potential subtype regulators and transition pathways. *NPJ Syst Biol Appl* 9, 55. 10.1038/s41540-023-00316-2.

184. Buenrostro, J.D., Giresi, P.G., Zaba, L.C., Chang, H.Y., and Greenleaf, W.J. (2013). Transposition of native chromatin for fast and sensitive epigenomic profiling of open chromatin, DNA-binding proteins and nucleosome position. *Nat Methods* 10, 1213-1218. 10.1038/nmeth.2688.
185. Yan, F., Powell, D.R., Curtis, D.J., and Wong, N.C. (2020). From reads to insight: a hitchhiker's guide to ATAC-seq data analysis. *Genome Biol* 21, 22. 10.1186/s13059-020-1929-3.
186. Hu, T., Chitnis, N., Monos, D., and Dinh, A. (2021). Next-generation sequencing technologies: An overview. *Hum Immunol* 82, 801-811. 10.1016/j.humimm.2021.02.012.
187. Cancer Genome Atlas Research, N., Weinstein, J.N., Collisson, E.A., Mills, G.B., Shaw, K.R., Ozenberger, B.A., Ellrott, K., Shmulevich, I., Sander, C., and Stuart, J.M. (2013). The Cancer Genome Atlas Pan-Cancer analysis project. *Nat Genet* 45, 1113-1120. 10.1038/ng.2764.
188. Meyers, R.M., Bryan, J.G., McFarland, J.M., Weir, B.A., Sizemore, A.E., Xu, H., Dharia, N.V., Montgomery, P.G., Cowley, G.S., Pantel, S., et al. (2017). Computational correction of copy number effect improves specificity of CRISPR-Cas9 essentiality screens in cancer cells. *Nat Genet* 49, 1779-1784. 10.1038/ng.3984.
189. Li, X., and Wang, C.Y. (2021). From bulk, single-cell to spatial RNA sequencing. *Int J Oral Sci* 13, 36. 10.1038/s41368-021-00146-0.
190. Yu, X., Abbas-Aghababazadeh, F., Chen, Y.A., and Fridley, B.L. (2021). Statistical and Bioinformatics Analysis of Data from Bulk and Single-Cell RNA Sequencing Experiments. *Methods Mol Biol* 2194, 143-175. 10.1007/978-1-0716-0849-4\_9.
191. Grun, D., Muraro, M.J., Boisset, J.C., Wiebrands, K., Lyubimova, A., Dharmadhikari, G., van den Born, M., van Es, J., Jansen, E., Clevers, H., et al. (2016). De Novo Prediction of Stem Cell Identity using Single-Cell Transcriptome Data. *Cell Stem Cell* 19, 266-277. 10.1016/j.stem.2016.05.010.

192. Saelens, W., Cannoodt, R., Todorov, H., and Saeys, Y. (2019). A comparison of single-cell trajectory inference methods. *Nat Biotechnol* 37, 547-554. 10.1038/s41587-019-0071-9.
193. Shin, J., Berg, D.A., Zhu, Y., Shin, J.Y., Song, J., Bonaguidi, M.A., Enikolopov, G., Nauen, D.W., Christian, K.M., Ming, G.L., and Song, H. (2015). Single-Cell RNA-Seq with Waterfall Reveals Molecular Cascades underlying Adult Neurogenesis. *Cell Stem Cell* 17, 360-372. 10.1016/j.stem.2015.07.013.
194. Kester, L., and van Oudenaarden, A. (2018). Single-Cell Transcriptomics Meets Lineage Tracing. *Cell Stem Cell* 23, 166-179. 10.1016/j.stem.2018.04.014.
195. Gulati, G.S., Sikandar, S.S., Wesche, D.J., Manjunath, A., Bharadwaj, A., Berger, M.J., Ilagan, F., Kuo, Angera H., Hsieh, R.W., Cai, S., et al. (2020). Single-cell transcriptional diversity is a hallmark of developmental potential. *Science* 367, 405-411. doi:10.1126/science.aax0249.
196. La Manno, G., Soldatov, R., Zeisel, A., Braun, E., Hochgerner, H., Petukhov, V., Lidschreiber, K., Kastrioti, M.E., Lonnerberg, P., Furlan, A., et al. (2018). RNA velocity of single cells. *Nature* 560, 494-498. 10.1038/s41586-018-0414-6.
197. Bergen, V., Lange, M., Peidli, S., Wolf, F.A., and Theis, F.J. (2020). Generalizing RNA velocity to transient cell states through dynamical modeling. *Nat Biotechnol* 38, 1408-1414. 10.1038/s41587-020-0591-3.
198. Qiao, C., and Huang, Y. (2021). Representation learning of RNA velocity reveals robust cell transitions. *Proc Natl Acad Sci U S A* 118. 10.1073/pnas.2105859118.
199. Qiu, X., Mao, Q., Tang, Y., Wang, L., Chawla, R., Pliner, H.A., and Trapnell, C. (2017). Reversed graph embedding resolves complex single-cell trajectories. *Nat Methods* 14, 979-982. 10.1038/nmeth.4402.
200. Young, A.P., Jackson, D.J., and Wyeth, R.C. (2020). A technical review and guide to RNA fluorescence in situ hybridization. *PeerJ* 8, e8806. 10.7717/peerj.8806.

201. Wang, F., Flanagan, J., Su, N., Wang, L.C., Bui, S., Nielson, A., Wu, X., Vo, H.T., Ma, X.J., and Luo, Y. (2012). RNAscope: a novel in situ RNA analysis platform for formalin-fixed, paraffin-embedded tissues. *J Mol Diagn* 14, 22-29. 10.1016/j.jmoldx.2011.08.002.
202. Atout, S., Shurrab, S., and Loveridge, C. (2022). Evaluation of the Suitability of RNAscope as a Technique to Measure Gene Expression in Clinical Diagnostics: A Systematic Review. *Molecular Diagnosis & Therapy* 26, 19-37. 10.1007/s40291-021-00570-2.
203. Chan, J.M., Quintanal-Villalonga, A., Gao, V.R., Xie, Y., Allaj, V., Chaudhary, O., Masilionis, I., Egger, J., Chow, A., Walle, T., et al. (2021). Signatures of plasticity, metastasis, and immunosuppression in an atlas of human small cell lung cancer. *Cancer Cell* 39, 1479-1496 e1418. 10.1016/j.ccell.2021.09.008.
204. Dong, B., Miao, J., Wang, Y., Luo, W., Ji, Z., Lai, H., Zhang, M., Cheng, X., Wang, J., Fang, Y., et al. (2020). Single-cell analysis supports a luminal-neuroendocrine transdifferentiation in human prostate cancer. *Commun Biol* 3, 778. 10.1038/s42003-020-01476-1.
205. Hasin, Y., Seldin, M., and Lusk, A. (2017). Multi-omics approaches to disease. *Genome Biol* 18, 83. 10.1186/s13059-017-1215-1.
206. Tang, F., Xu, D., Wang, S., Wong, C.K., Martinez-Fundichely, A., Lee, C.J., Cohen, S., Park, J., Hill, C.E., Eng, K., et al. (2022). Chromatin profiles classify castration-resistant prostate cancers suggesting therapeutic targets. *Science* 376, eabe1505. 10.1126/science.abe1505.
207. Liu, Q., Zhang, J., Guo, C., Wang, M., Wang, C., Yan, Y., Sun, L., Wang, D., Zhang, L., Yu, H., et al. (2024). Proteogenomic characterization of small cell lung cancer identifies biological insights and subtype-specific therapeutic strategies. *Cell* 187, 184-203 e128. 10.1016/j.cell.2023.12.004.

208. Chen, C.C., Tran, W., Song, K., Sugimoto, T., Obusan, M.B., Wang, L., Sheu, K.M., Cheng, D., Ta, L., Varuzhanyan, G., et al. (2023). Temporal evolution reveals bifurcated lineages in aggressive neuroendocrine small cell prostate cancer trans-differentiation. *Cancer Cell* 41, 2066-2082 e2069. [10.1016/j.ccell.2023.10.009](https://doi.org/10.1016/j.ccell.2023.10.009).



**Chapter 2: Temporal evolution reveals bifurcated lineages in aggressive neuroendocrine small cell prostate cancer trans-differentiation**

This chapter is a modified version of the journal published in *Cancer Cell* on December 11<sup>th</sup>, 2023.

Title: Temporal evolution reveals bifurcated lineages in aggressive neuroendocrine small cell prostate cancer trans-differentiation

Authors: Chia-Chun Chen<sup>1</sup>, Wendy Tran<sup>2</sup>, Kai Song<sup>3</sup>, Tyler Sugimoto<sup>2</sup>, Matthew B. Obusan<sup>2</sup>, Liang Wang<sup>2</sup>, Katherine M. Sheu<sup>2</sup>, Donghui Cheng<sup>4</sup>, Lisa Ta<sup>1</sup>, Grigor Varuzhanyan<sup>2</sup>, Arthur Huang<sup>1</sup>, Runzhe Xu<sup>5</sup>, Yuanhong Zeng<sup>1</sup>, Amirreza Borujerdpur<sup>1</sup>, Nicholas A. Bayley<sup>1</sup>, Miyako Noguchi<sup>2</sup>, Zhiyuan Mao<sup>1</sup>, Colm Morrissey<sup>6</sup>, Eva Corey<sup>6</sup>, Peter S. Nelson<sup>7,8,9</sup>, Yue Zhao<sup>10, 11</sup>, Jiaoti Huang<sup>10</sup>, Jung Wook Park<sup>10</sup>, Owen N. Witte<sup>1,2,4,12,13,14\*</sup> and Thomas G. Graeber<sup>1,14,15,16,17\*†</sup>

Affiliation:

1. Department of Molecular and Medical Pharmacology, University of California Los Angeles (UCLA), Los Angeles, CA, USA
2. Department of Microbiology, Immunology, and Molecular Genetics, UCLA, Los Angeles, CA, USA
3. Department of Bioengineering, UCLA, Los Angeles, CA, USA
4. Eli and Edythe Broad Stem Cell Research Center, UCLA, Los Angeles, CA, USA
5. Department of Biological Chemistry, UCLA, Los Angeles, USA
6. Department of Urology, University of Washington School of Medicine, Seattle, WA, USA
7. Division of Human Biology, Fred Hutchinson Cancer Center, Seattle, WA, USA
8. Division of Clinical Research, Fred Hutchinson Cancer Center, Seattle, WA, USA
9. Department of Medicine, University of Washington School of Medicine, Seattle, WA, USA
10. Department of Pathology, Duke University School of Medicine, Durham, NC, USA
11. Department of Pathology, College of Basic Medical Sciences and the First Hospital, China Medical University, Shenyang, China

12. Molecular Biology Institute, UCLA, Los Angeles, CA, USA
13. Parker Institute for Cancer Immunotherapy, UCLA, Los Angeles, CA, USA
14. Jonsson Comprehensive Cancer Center, UCLA, Los Angeles, USA
15. Crump Institute for Molecular Imaging, UCLA, Los Angeles, USA
16. California NanoSystems Institute, UCLA, Los Angeles, USA
17. Metabolomics Center, UCLA, Los Angeles, USA

\* Corresponding Authors Emails:

Owen N. Witte [owenwitte@mednet.ucla.edu](mailto:owenwitte@mednet.ucla.edu)

Thomas G. Graeber [TGraeber@mednet.ucla.edu](mailto:TGraeber@mednet.ucla.edu)

†Lead Contact Email:

Thomas G. Graeber [TGraeber@mednet.ucla.edu](mailto:TGraeber@mednet.ucla.edu)

## SUMMARY

Trans-differentiation from an adenocarcinoma to a small cell neuroendocrine state is associated with therapy resistance in multiple cancer types. To gain insight into the underlying molecular events of the trans-differentiation, we perform a multi-omics time course analysis of a pan-small cell neuroendocrine cancer model (termed PARCB), a forward genetic transformation using human prostate basal cells and identify a shared developmental, arc-like, and entropy-high trajectory among all transformation model replicates. Further mapping with single cell resolution reveals two distinct lineages defined by mutually exclusive expression of ASCL1 or ASCL2. Temporal regulation by groups of transcription factors across developmental stages reveals that cellular reprogramming precedes the induction of neuronal programs. TFAP4 and ASCL1/2 feedback are identified as potential regulators of ASCL1 and ASCL2 expression. Our study provides temporal transcriptional patterns and uncovers pan-tissue parallels between prostate and lung cancers, as well as connections to normal neuroendocrine cell states.

## INTRODUCTION

Small cell neuroendocrine (SCN) cancer is an aggressive variant that arises from multiple tissues such as the lung and prostate<sup>1,2</sup>. SCN is characterized by its histologically defined small cell morphology of densely packed cells with scant cytoplasm, poor differentiation, and aggressive tumor growth, as well as expression of canonical neuroendocrine markers including SYP, CHGA and NCAM1<sup>3</sup>. In addition to their phenotypic resemblance, SCN cancers across multiple tissues show a striking transcriptional and epigenetic convergence in clinically annotated tumors<sup>4,5</sup>. This molecular signature convergence is recapitulated by our established SCN transformation model that utilizes either normal lung epithelial cells, patient-derived benign prostate epithelial or bladder urothelial cells as the cells of origin<sup>6,7</sup>.

Small cell neuroendocrine prostate cancer (SCNPC) occurs either *de novo* (<1% of untreated prostate cancer cases), or through therapy-mediated transversion of castration resistant prostate cancer (CRPC) (~20% of the resistance cases). CRPC is a resistant variant of prostate adenocarcinoma (PRAD), which often responds to androgen deprivation therapy<sup>8,9</sup>. Trans-differentiation from PRAD to the SCNPC state entails complicated epigenetic reprogramming at the chromatin level, resulting in transcriptional changes driven by a number of key master regulators<sup>10,11</sup>. For example, methylation modulated by EZH2 and activation of transcriptional programs by SOX2 are required in *TP53* and *RB1* loss-mediated neuroendocrine differentiation in mouse transgenic models of SCNPC<sup>12,13</sup>. Oncogenic mutation of *FOXA1* potentiates pioneering activity and differentiation status of prostate cancer<sup>14,15</sup>. Lastly, knockdown of transcription factors such as *ONECUT2* has been shown to inhibit SCN differentiation<sup>16,17</sup>. While the importance of these factors has been demonstrated, the chronological sequence of the associated epigenetic and transcriptional changes remains uncharacterized during the progression to SCNPC. Examination of the temporal evolution of lung cancer revealed a connection between transcription factor defined subtypes and cell plasticity<sup>18,19</sup>. In our study, we sought to answer the following

questions: 1) when do SCN-associated transcription factors emerge during SCNPC progression, 2) how do they coordinate SCN differentiation, and 3) can we identify a transition state defined by transcription factors that can be targeted?

Leveraging our previously developed human pan-small cell neuroendocrine cancer model, the PARCB forward genetics transformation model (driven by knockdown of *RB1*, alongside exogenous expression of dominant negative *TP53*, *cMYC*, *BCL2* and myristoylated *AKT1* via three lentiviral vectors)<sup>6,7</sup>, tumor samples were harvested at different time points for multi-omics analyses. The transcriptional and epigenetic status of each time point was determined using integrative bulk RNA sequencing, ATAC sequencing, and single cell RNA sequencing. This longitudinal study provides insight into the temporal evolution of the epigenetic and transcriptional landscape during trans-differentiation and small cell cancer progression. We found consistent transcriptional patterns and differentiation trajectories across samples generated from independent patient tissues, as well as a bifurcation of end-stage neuroendocrine lineages, defined by ASCL1 and ASCL2 and their associated programs.

Achates-scute complex (AS-C) proteins are basic helix-loop-helix (bHLH) transcription factors, first identified in *Drosophila Melanogaster*<sup>20</sup>. They are important in the development of peripheral nervous systems and sensory organs<sup>21</sup>. Mammalian ASCL1 is a well-known neuroendocrine transcription factor in small cell cancers<sup>22-24</sup>. Independently, ASCL2 is involved in embryonic development, colorectal stem cell biology and cancer<sup>25-30</sup>. ASCL2 is largely understudied in SCNPC, mainly shown to be co-expressed with POU2F3 in non-neuroendocrine cell populations<sup>5,31</sup>. Here, our study reveals temporal transcriptional patterns during small cell neuroendocrine differentiation in prostate cancer and associated lineage programs governed by general mutually exclusivity between ASCL1 and ASCL2. Follow-up analysis elucidated a transcriptional network circuitry between ASCL1, ASCL2, and the transcription factor TFAP4 which was implicated by the trajectory data.

## RESULTS

### **Temporal gene expression programs of the PARCB transformation model reveal SCNPC trans-differentiation pathways**

To determine the timing of SCN differentiation events during prostate cancer development, we utilized the PARCB model system<sup>6</sup>. Independent transformations were performed on basal cells extracted from benign regions of epithelial tissue from 10 prostate adenocarcinoma patients. Basal cells were transformed by the oncogenic lentiviral PARCB cocktail and subsequently cultured in an organoid system *in vitro*<sup>6</sup>. Transformed organoid-expanded cells from each patient tissue sample were subcutaneously implanted into multiple immunocompromised mice to allow for time-course collection of tumors from the matched starting material (**Figure 1A**). The tumors were collected at approximately two-week intervals until reaching 1 cm<sup>3</sup> in size or occurrence of ulceration, whichever came first. The transformed tumor cells were triply fluorescent due to the lentiviral integration<sup>6</sup>, which allowed for cancer cell purification by fluorescence-activated cell sorting (FACS) followed by multi-omics sequencing and analysis (**Figure 1A**). Each patient series (P1-P10) contains five to six time point samples ranging from basal cells (TP1) to organoids (TP2) to tumors (TP3-TP5/TP6) (**Figure 1A**). Upon histological examination of the tumor issues by pathologists, we found that the time course tumors transitioned from squamous, to adenocarcinoma, then to mixed and eventually SCN phenotypes (**Figure 1A and Figure S1A-C**). Furthermore, clinically defined neuroendocrine markers, including SYP and NCAM1, emerge during the transition to late stages of the tumor progression (**Figure 1A**). The basal cell marker p63 were only positive in early-stage tumors by immunohistochemistry (IHC) staining (**Figure S1D**).

We first performed a temporal analysis of gene expression using bulk RNA sequencing to understand the changes in the transcriptional landscape during SCNPC trans-differentiation. By projection of PARCB samples onto principal component analysis (PCA) of clinical lung and

prostate cancer tumor samples<sup>4,10,32-36</sup>, we validated that PARCB time course samples follow the transcriptionally defined convergence trajectory from adenocarcinoma to SCN states (**Figure 1B and Figure S1E**). Additional SCNPC associated factors including *ASCL1* and *NEUROD1* were also elevated during the progression (**Figure 1C**). The mRNA of androgen receptor (AR) was expressed in tumors at the early stage (**Figure 1C**), but the protein level was not detectable by immunostaining (**Figure S1D**). Taken together, the histological and omics data indicate that PARCB time course tumors recapitulate both the phenotypic and transcriptional changes observed in the clinic and provide a model system for studying the temporal evolution of SCNPC development.

To determine the transformation trajectories among the time course series generated from the 10 independent patient samples (P1-P10), we performed clustering and PCA of the transcriptomic data. To account for potential asynchronous development among each patient series and each individual tumor, we defined hierarchical clusters (HCs) of samples by their corresponding differential gene modules and found the resulting 6 clusters (HC1-6) to generally correspond with the time of collection (**Figure 1D and Table S1A**). This provides a clustering-based trans-differentiation reference frame and informs our subsequent multi-omics analyses. Unsupervised PCA demonstrates that the individual transformation paths of each series follow a generally consistent “arc-like” trajectory with a discernable bifurcation in late-stage samples (**Figure 1E, Figure S1E-F and Table S1B**). The late tumors were hence further defined as “Class I” and “Class II” tumors with correspondent HC5 and HC6 gene modules, respectively. HC2 to HC6 had elevated SCNPC signature scores compared to adenocarcinoma signature score (**Figure S1G**). This last finding supports the existence of two transcriptional programs or end points defining the terminal SCNPC tumor phenotypes.

Gene ontology enrichment analysis of the corresponding 6 differential gene modules identified biological processes enriched uniquely or shared among HCs, including Inflammatory response



(HC1 and HC3, patient derived basal cells and early tumors, respectively), cell proliferation (HC2, *in vitro* organoids), epidermis development (HC3, early tumors), cell activation (HC4, transitional tumors), stem cell differentiation (HC5, Class I late tumors) and neuro-/chemical synapse (HC5 and HC6, both classes of late tumors) (**Figure 1E and Table S1C**). The transcriptome evolution supports the idea that trans-differentiation from adenocarcinoma to the SCN state is a systematically coordinated process, that involves a transitional stage followed by bifurcated pathways enriched in neuronal/neuroendocrine gene signatures.

### **Sequential transcription regulators modulate reprogramming and neuroendocrine programs through a highly entropic and accessible chromatin state**

Temporal analyses on single transcription factor defined subtypes of small cell lung cancer (SCLC) models have delineated lineage plasticity in the development of lung neuroendocrine tumors <sup>18</sup>. We sought to define the transcriptional evolution in SCNPC through an extensive survey of over 1600 transcription factors <sup>37</sup> by chromatin accessibility analyses using ATAC sequencing <sup>38</sup>. A significant increase in overall accessible chromatin peaks across chromosomes is observed starting at the tumors at transitional stage (HC4) to late stages (HC5 and HC6) (**Figure 2A**). Unsupervised PCA using ATAC-sequencing data showed an arc-like and bifurcated trajectory consistent with the pattern observed using the RNA-sequencing data (**Figure 1D and 2B**). The Shannon entropy has been used to estimate the plasticity potential of a biological sample to change cellular state <sup>39,40</sup>. We found that transitional samples (HC4) have the highest entropy (**Figure 2B**), suggesting there exists a high potential and less well-defined transcriptional state during the trans-differentiation process.

To identify transcription factors that recognize the chromatin accessible regions at each stage of the transformation trajectory, we first looked at the overall accessibility near the transcription start

sites (TSS) (**Figure 2C**). Transitional samples (HC4) have a strong increase in the accessible peaks as estimated by Shannon entropy calculations (**Figure 2B and 2C**), consistent with the gene-expression-based entropy calculations (**Figure S2A**). Next, motif enrichment analysis was performed on the accessible peaks from each HCs in a “one versus the rest” fashion. Since transcription factors from the same family share similar motifs and are deposited into a variety of databases, we used a pipeline that applies an ensemble of existing computational tools and suites of motifs (*de novo* and known) <sup>41</sup> (**Figure 2D and Table S1D**). Motif enrichment analysis implicated that 1) representative stress-responsive factors such as NFkB, JUN, ATF and STAT proteins were active from early to transition stage (HC1-4), 2) reprogramming factors such as POU/OCT and SOX families were active in Class I (HC5) tumors, and 3) neuronal/neural factors including ASCL and NEUROD family proteins were found at the later stage in Class II (HC6) tumors (**Figure 2D**). Due to ASCL1, ASCL2 and other bHLH factors sharing the same E-box motif, and the stringent “one HC versus the rest” differential accessibility analysis, the motif suite containing ASCL1 and ASCL2 factors is highly enriched and ranked in HC6 compared to HC5 (**Figure 2D**). Nonetheless, when HC6 is left out of the analysis, HC5 does demonstrate strong enrichment for the motif suite containing ASCL1 and ASCL2 factors, compared to HC1-4. (**Figure S2B**). The enrichment of stem-like and neuroendocrine programs in HC4-5 and HC6, respectively, was further confirmed by signature scores derived from the literature <sup>33,42</sup> (**Figure S2C**). This analysis provides a view of the overall transcriptional shift of the chromatin accessibility during trans-differentiation.

To determine whether expression of the transcription factors corresponds to their inferred activity from the motif enrichment analysis, we summarized the top ranked transcription factors (based on PC1, PC2 and PC3 loadings) across the transformation stages (HC1-HC6) (**Figure 2E and Figure S2D, Table S1E**) from the perspective of the PCA-based transformation trajectory (**Figure 1E and Figure S1F**). Overall, we observed that 1) *AR* mRNA expression is lost during progression

towards late-stage tumors, 2) *FOXA1*, a known transcription factor of SCNPC<sup>14,15</sup>, is shown to emerge at the early-transition stage, and 3) well-known neuroendocrine transcription factors such as *ASCL1*, *NEUROD1*, *ONECUT2*, *SOX2*, *INSM1* and *FOXA2* were increased towards the late stage (**Figure 2E and Figure S2D**)<sup>43-45</sup>. This analysis also revealed additional candidate stage-specific transcription factors that are largely understudied in SCNPC, such as *LTF*, *ESR1*, *ZIC2* and *TBX10* (**Figure 2E**). *ASCL1* and *ASCL2* expression were elevated in the late tumor stages (**Figure 1C and Figure 2E-F**). Notably, their expression was enriched in separate tumor endpoints (HC5: *ASCL2*+ and HC6: *ASCL1*+), supporting their probable contribution to the bifurcated trajectories (**Figure 2E-F and Figure S2D**).

### **Transcription factor-defined cell populations contribute to lineage divergence and tumor heterogeneity**

To determine the degree of heterogeneity within the time course tumors, we performed single cell RNA sequencing on four time-defined serial tumor sets: P2, P5, P7 and P8 (TP3-TP6) (**Figure 3A**). Dimension reduction analysis (Uniform Manifold Approximation and Projection, UMAP) was used to visualize the overall distribution of cell populations at each time point of SCNPC development (**Figure 3A-B and Figure S3A**). Overall, a lineage differentiation from basal (*KRT5*+) to luminal (*KRT18*+) was observed from early to late tumors (**Figure 3B-C**). *YAP1*, whose expression defines a non-neuroendocrine SCLC subtype<sup>46</sup> and whose high expression is frequently seen in CRPC-PRAD but not SCNPC<sup>47</sup>, is enriched in the early tumor cell populations (**Figure 3B-C**).

To understand the association of known SCN transcription factors in contributing to intra-tumoral heterogeneity, we first assigned a SCNPC score<sup>33</sup> to each cell (**Figure S3B**). Despite the high SCNPC scores across populations of single cells, the number of *NEUROD1* and/or *ONECUT2*

positive cells is very low, while deeper single cell sequencing depth would be required to fully investigate this result (**Figure 3C and Figure S3B**). Other well-known neuroendocrine transcription factors such as *ASCL1*, *INSM1* and *FOXA2* are enriched in the same cell cluster with high SCNPC score (**Figure 3C and Figure S3B**). However, in another cell cluster, *ASCL2*, *POU2F3* and *SOX9* were co-expressed with a medium level of SCNPC score (**Figure 3C and Figure S3B**). The general mutual exclusivity of *ASCL1* and *ASCL2* in single cells further supports *ASCL1* and *ASCL2* contributing to the bifurcated endpoint trajectories observed in the bulk tumors (**Figure 3C and Figure S3C-D**).

Single cell datasets available as reference from longitudinal clinical samples in advanced prostate cancer are rare, thus a cell type inference analysis using reference pure cell types was applied to infer the identity of individual cells in PARCB tumors<sup>48</sup>. Five out of a total of 36 reference cell types from the Human Primary Cell Database were highly enriched in the PARCB time course tumor samples (**Figure 3D**). All tumor cells share a similar transcriptome as epithelial cells (**Figure 3D**). Particularly, a majority of tumor cells (other than early-stage cells) exhibit stem-like gene expression patterns reflective of embryonic stem cells and induced pluripotent stem cells, indicative of a de-differentiation shift during SCNPC development and trans-differentiation (**Figure 3D**). Additionally, later-stage cells expressing either *ASCL1* or *ASCL2* had neuronal-like gene expression profiles, confirming the emergence of SCN differentiation (**Figure 3B-D**).

Single cell analysis supports the overall gene expression and chromatin accessibility patterns observed in bulk tumors. Projection of single cells onto the PCA framework generated from bulk RNA-sequencing samples (**Figure 1E and Figure S1F**) demonstrated that tumors clustering distinctly by bulk RNA-sequencing indeed consist primarily of single cells in the corresponding different transcriptional states, with some degree of heterogeneity (**Figure 3E**). Furthermore, transcription factors with high expression in tumors defined by bulk RNA-sequencing analysis (**Figure 2E**) show heterogenous patterns among single cells (**Figure S3E**). Tumors at transitional

stage (HC4) and late stage (HC5) have the highest degree of gene fluctuation, further highlighting a potential role for increased intratumoral heterogeneity during the trans-differentiation process (**Figure S3E**). Importantly, we further validated the mutually exclusive expression pattern of *ASCL1* and *ASCL2* in multiple clinical and GEMM single cell RNA-sequencing datasets<sup>31,49-51</sup>. This analysis confirmed that *ASCL2* is generally enriched in non-NE cells/adenocarcinoma and *ASCL1* is more abundant in high NE cells/SCNPC clinically (**Figure 3F**), consistent with the PARCB temporal study (**Figure S3F**). *ASCL1* and *ASCL2* double-positive cells are observed at a low frequency, primarily in SCNPC tumors, and may reflect a transitional state between adenocarcinoma and SCN phenotypes (**Figure 3F**).

### **ASCL1 and ASCL2 specify independent transcriptional programs and sub-lineages in SCNPC**

Given that *ASCL1* and *ASCL2* expression levels are mutually exclusive in single cells, we asked whether *ASCL1* and *ASCL2* represent separate cellular sub-lineages by inferred clonal tracing analyses<sup>52</sup>. With *KRT5* (basal marker) set as the beginning of the tracing, the inferred tracing results in three primary lineage branches/states (**Figure 4A**). As hypothesized, single cells expressing either *ASCL1* or *ASCL2* are enriched in different lineage branches (**Figure 4A-B**). This result is further supported by a different analytic tool (RNA velocity) that measures the temporal ratio of un-spliced to spliced mRNAs to infer lineage trajectory<sup>53</sup> (**Figure S4A**). The inferred clonal tracing results complemented the real-time-based analysis visualized as the total composition of *ASCL1*- or *ASCL2*- positive, double positive and negative populations over time (**Figure 4C**), supporting that *ASCL1* and *ASCL2* are associated with independent sub-lineages. Double-positive cells are very infrequent in the PARCB temporal tumors. The double-positive population observed in the P2-TP5 tumor may capture the cells undergoing the transitional state

(**Figure 4C**), and the overall low double-positive frequency is consistent with the clinical results above (**Figure 3F**).

To further characterize the transcriptional difference between cells expressing a high level of *ASCL1* or *ASCL2*, we analyzed their differential gene expression profiles (**Figure 4D and Table S1F**). Genes that are involved in synaptic and neuroendocrine regulation such as *DDC*, *CACNA1A* and *INSM1* are enriched in *ASCL1*+ cells. *ASCL2*+ cells express genes with stem-like characteristics such as *SOX9* and *POU2F3* (**Figure 4D**). *SOX9* is directly regulated by *ASCL2* in intestinal stem cells<sup>29</sup>, suggesting a possible contribution to stem-like properties in SCNPC trans-differentiation. Upon further investigation, we observed that genes implicated in the intestinal stem cell program such as *EPBH3* and *TNFRSF9*<sup>29</sup> are positively correlated with *ASCL2*, but not *ASCL1* (**Figure S4B**). In contrast, a well-known intestinal stem cell marker, *LGR5*<sup>54</sup>, has no correlation with either *ASCL1* or *ASCL2*, consistent with it having a more tissue specific intestinal role (**Figure S4B**).

To identify the transcriptional programs that are associated with either *ASCL1* or *ASCL2* in prostate cancer, we constructed an inferred network<sup>55</sup> using multiple bulk RNA sequencing prostate cancer and model datasets including The Cancer Genome Atlas (TCGA), additional patient tumor (Beltran), and SCNPC model (Park) datasets<sup>6,33</sup>. The analysis identified 336 and 352 genes regulated independently by *ASCL1* or *ASCL2* (**Figure 4E and Table S1G**). Strikingly, there are only 5 genes from the inference analysis that are regulated by both factors: *TMEM74*, *RGS16*, *LHFPL4*, *CDCA7L* and *SOX2* (**Figure 4E**). This result is consistent with the demonstrated role of *SOX2* in regulating neuroendocrine differentiation in null *TP53* and *RB1* backgrounds<sup>13</sup>, hence showing that *SOX2* is involved in both *ASCL1* and *ASCL2* associated neuroendocrine sub-lineages. Genes that are regulated by *ASCL1* are enriched in neuroendocrine differentiation markers and factors such as *SYP*, *CHGA*, *NCAM1*, and *NEUROD1* (**Figure 4E**). *ASCL2* is associated with genes including *PTGS1/COX1*, *POU2F3*, *ANXA1* which

are generally immune and stress responsive, and stem-like (**Figure 4D-E**). We further confirmed that PARCB tumor-derived cell lines from different tissues of origin (prostate, bladder, and lung) all have only one or the other gene expression patterns associated with either ASCL1 or ASCL2 expression (**Figure 4F and Figure S4C**). We next validated the predicted transcriptional programs of ASCL1 and ASCL2 by exogenously expressing either ASCL1 or ASCL2 in ASCL2+ or ASCL1+ cell lines, respectively. ASCL1 exogenous expression in ASCL2+ cells, increased the ASCL1 transcriptional program as indicated by increased signature score (**Figure S4D**). However, ASCL2 exogenous expression in ASCL1+ cells, did not have notable effect, suggesting that the ASCL1 endpoint state has higher stability (**Figure S4D**).

*In situ* hybridization of *ASCL1* and *ASCL2* mRNA in the transitional PARCB tumor samples further confirmed the mutually exclusive expression pattern (**Figure 4G**). The staining patterns demonstrated both *ASCL1* and *ASCL2* mixed populations (**left, Figure 4G**), as well as patch regions potentially resulting from local clonal expansion (**right, Figure 4G**) of *ASCL1*+ or *ASCL2*+ cells. Our combined results support that ASCL1 and ASCL2 define independent cellular sub-lineages and transcriptional programs with stem-like and neuroendocrine enrichment in SCNPC.

### **ASCL1 and ASCL2 as pan-cancer classifiers**

Clinical subtypes are fairly well-defined in SCLC<sup>46,56</sup>, but molecular subtyping remains an evolving challenge in SCNPC<sup>8</sup>. By performing projection analysis of our samples onto a gene expression or chromatin accessibility PCA framework defined by the Tang et al. dataset of patient metastatic CRPC phenotypes<sup>57</sup>, we found that PARCB temporal samples share similar transcriptome and epigenome signatures, including a shared stem-cell like (SCL) group and a shared NEPC group (**Figure 5A**).

Given the high degrees of similarity in transcriptional profiles of SCLC and SCNPC <sup>4</sup>, we compared our HC classification of the PARCB time course samples to the SCLC clinical subtypes: ASCL1 (A), NEUROD1 (N), POU2F3 (P) and YAP1 (Y) (**Figure 5B**) <sup>32,46</sup>. The class I/ASCL2+ (HC5) tumor group shares transcriptome similarity with SCLC-P (**Figure 5B**), which is consistent with the co-expression pattern of ASCL2 and POU2F3 observed in multiple analyses (**Figure 3C and 4D**). Likewise, and concordant, the Class II/ASCL1+ (HC6) tumor group is transcriptionally aligned to SCLC-A (**Figure 5B**).

To investigate whether the ASCL1 and ASCL2 sub-classes from PARCB temporal study recapitulate patterns observed in clinical samples of prostate cancer, we compared *ASCL1* and *ASCL2* expression in PARCB temporal samples versus numerous clinical profiling datasets <sup>10,33-36</sup>. The results demonstrate that the expression levels of *ASCL1* and *ASCL2* are comparable between the PARCB model and clinical samples, and the transcriptional patterns of HC1 to HC6 generally corresponded with the transition from PRAD/CRPC-PRAD to SCNPC (**Figure 5C**). We further confirmed the general mutual exclusivity and low double positivity of *ASCL1/2* expression using an RNA *in situ* hybridization assay on both CRPC-PRAD and SCNPC clinical samples and CRPC PDX models (**Figure 5D and Figure S5A-B**).

By comparing the expression levels of *ASCL1* and *ASCL2* across a broad panel of pan-cancer cell lines, we found that almost all cancers, apart from lung cancers, can be divided into three categories (i) demonstrating expression of *ASCL1* (neuroblastoma), (ii) of *ASCL2* (colorectal and breast cancers), and (iii) double negative (other cancers) (**Figure 5E**). Only SCLC and other lung cancer cell lines have mixed levels of *ASCL1* and *ASCL2*. Combined with our results, this suggests a potential role for ASCL2 and POU2F3 in specifying intermediate, and/or heterogenous states in (small cell) lung cancer (**Figure 5E**). Protein expression analysis in lung squamous carcinoma (NCI-H1385), SCLC-A (NCI-H1385, NCI-H146 and DMS79), SCLC-P (NCI-H526 and COR-L311) and SCNPC (NCI-H660) cell lines further highlighted a mutually exclusive pattern of



ASCL1 and ASCL2 (**Figure S5C**). SCLC-N (NCI-H1694) is double negative for ASCL1 and ASCL2 and positive for NEUROD1 as expected (**Figure S5C**). Last but not the least, in patient tumor pan-cancer data, the exclusive expression of either *ASCL1* or *ASCL2* is again observed, highlighting that binary distinctions defined by ASCL1 and ASCL2 occur across multiple tissue types (**Figure 5F**). In sum, an inverse and generally mutually exclusive relationship between ASCL1 and ASCL2 is observed in multiple and pan-cancer contexts, and mutual exclusivity is strongly observed at the single cell level.

### **Alternating ASCL1 and ASCL2 expression through reciprocal interaction and TFAP4 epigenetic regulation**

With the evidence that *ASCL1* or *ASCL2* expression levels are mutually exclusive in single cells during SCNPC trans-differentiation, we explored two hypotheses: 1) These two factors mutually regulate each other's expression, or 2) they share a common upstream transcription factor that alternates their transcription through regulated differential binding to respective gene regulatory elements. To test the first hypothesis, we expressed V5-tagged ASCL2 in multiple PARCB tumor derived cell lines (lung and prostate) and observed that ASCL1 protein expression was significantly suppressed in these cells (**Figure 6A**). In contrast, expression of V5-tagged ASCL1 increased ASCL2 expressions both at protein and mRNA levels (**Figure 6A and Figure S6A**). Thus in our model cells, ASCL1 and ASCL2 mutually regulate each other at the protein level, but each in the opposite manner.

To test the second hypothesis of a common regulator, known promoter and enhancer regions of *ASCL1* and *ASCL2* were first annotated in the PARCB time course ATAC-sequencing data (**Figure 6B**). An opposing pattern of open and closed chromatin formation is found on both the *ASCL1* promoter and the *ASCL2* enhancer regions (**Figure 6B**). A rank list of transcription factors

that have matching motifs in the regions was generated to determine potential shared regulators<sup>58</sup> (**Figure 6C and Table S1H**). An extensive literature search of all the factors whose motifs were found in both *ASCL1* and *ASCL2* regulatory regions revealed that TFAP4 was reported to form different transcription complex to either activate or repress target genes, including facilitating epithelial-to-mesenchymal transition in colorectal cancer and repressing neuronal programs in non-neuronal cells<sup>59,60</sup>. The TFAP4 motif was shared in both the *ASCL1* promoter (ranked 2<sup>nd</sup>) and the *ASCL2* enhancer region (ranked 6<sup>th</sup>) in the top 8 list of shared transcription factor motifs (**Figure 6C**), and is expressed across all the SCLC, SCNPC and PARCB tumor derived cell lines tested (**Figure S5C and S6B**). Interestingly, NCI-H1385, a lung squamous carcinoma (non-small cell) cell line, has lower TFAP4 expression compared to other small cell neuroendocrine cell lines (**Figure S5C**).

The direct differential binding of TFAP4 to the *ASCL1* promoter and the *ASCL2* enhancer region was confirmed by the CUT&RUN technique<sup>61</sup>, a chromatin immunoprecipitation experiment using TFAP4 antibody in both *ASCL1*+ and *ASCL2*+ PARCB tumor derived cell lines. Despite cell lines having various degrees of TFAP4 binding signals due to potential mixed cell clones within the cell lines, TFAP4 was found to have higher binding affinity near the *ASCL1* promoter in *ASCL1*+ cell lines (P7-TP6) than *ASCL2*+ cell lines (P2-TP6 and T3-TP5) (**Figure S6C**). In contrast, TFAP4 consistently bound to *ASCL2* enhancer regions in *ASCL2*+ cell lines compared to *ASCL1*+ cell line (**Figure S6C**). This result supports that TFAP4 potentially regulates transcription of *ASCL1* and *ASCL2* in a context-specific manner.

To determine whether TFAP4 directly regulates the expression of *ASCL1* and *ASCL2*, we introduced a doxycycline-inducible CRISPR sgRNA targeting *TFAP4* in multiple *ASCL1*+ and *ASCL2*+ cell lines, including PARCB tumor-derived cell lines and the patient-derived cell line NCI-H660. Both *ASCL1* and *ASCL2* expression decreased, with various strength, after TFAP4 knockout was induced by the addition of doxycycline in the respective cell lines (**Figure 6F and**

**Figure S6D**). However, other lineage associated proteins did not change (**Figure 6F and Figure S6D**). Cell growth assays showed a mild decrease in P7-TP6 (ASCL1+) cell growth, and in contrast a drastic increase in P3-TP5 (ASCL2+) growth upon the knockout of TFAP4 (**Figure 6E**). To explore the clinical relevance of TFAP4 in cancer and SCNPC, we surveyed the expression of *TFAP4* across subtypes of cancers compared to normal tissue. There is a substantial increase in *TFAP4* expression in small cell cancers compared to adenocarcinoma, and compared to normal tissue, in both prostate and lung cancer indications (**Figure 6F**), as well as in pan cancer tumors (TCGA) vs. normal tissue (GTEx) (**Figure S6E**).

Thus in our transcriptional regulatory circuit studies, we found a reciprocal, non-symmetric regulatory relationship between ASCL1 and ASCL2; and that within this circuit, ASCL1 and ASCL2 have a shared positive regulatory factor, TFAP4. In the sum of our studies, the PARCB model provided a blueprint of SCNPC trans-differentiation as specified by temporal transcription factors (**Figure 6G**). In particular, ASCL1 and ASCL2 define distinct bifurcated sub-lineage trans-differentiation trajectories in small cell cancers, and binary transcriptional profiles in a pan-cancer context.

## DISCUSSION

SCNPC has a rare *de novo* presentation, however, trans-differentiation from prostate adenocarcinoma to SCN cancer is a frequent adverse consequence of cancer cells acquiring resistance to therapeutics repressing AR signaling<sup>8,9</sup>. In a pan-cancer context, therapy-induced trans-differentiation from adenocarcinoma to SCN cancer is a growing clinical challenge in lung cancer with the expansion of effective targeted therapies, such as EGFR, ALK, BRAF, KRAS inhibitors<sup>62</sup>. Genetically engineered mouse models of SCNPC and SCLC have been generated to provide insight into the tumorigenesis of SCN cancers<sup>12,18,31,43,63,64</sup>, with some models demonstrating evidence of the adenocarcinoma to SCN cancer transition<sup>13,31,65,66</sup>. Patient tumor-derived organoids and circulating tumor cells have also provided models for monitoring differentiation state transitions<sup>50,67</sup>, including reversion to non-SCN states via specific signaling inhibition<sup>50</sup>. Our PARCB forward genetics *in vivo* temporal transformation model further adds to these resources by being human cell-based, recapitulating the adenocarcinoma to SCN phenotype trans-differentiation at both the histological and molecular signature levels, and providing the temporal resolution to reveal an arc-like plasticity trajectory and associated stem cell-like (reprogrammed) intermediate states. A limitation of the PARCB model is that inhibition of the AR axis is not an initiating component of the trans-differentiation process.

Such an arc-like trajectory is commonly observed in unbiased profiling of development and differentiation processes, including in cancer contexts<sup>39,68-74</sup>. The pattern is reminiscent of temporal regulation in development, with the differentiation transition stage promoted by temporally regulated epigenetic and transcriptomic plasticity programs<sup>75-77</sup>.

The transcription profiles of the transition stage from adenocarcinoma to SCNPC provide evidence for an initial de-differentiation or reprogramming step when cells enter the trans-differentiation process, with enrichment of stem cell and iPSC programs. Furthermore, we find samples in the transitional state have a higher degree of entropy at both the epigenetic and gene

expression level. Our findings are in concordance with a recent study in an adenocarcinoma lung cancer mouse model where a highly plastic intermediate state was seen as cells transitioned from lung hyperplasia to adenocarcinoma <sup>19</sup>, and with past observations of increased entropy proceeding differentiation processes <sup>39</sup>. Together these findings support the idea that de-differentiation, and epigenetic loosening and/or cellular heterogeneity are prerequisites for further lineage trans-differentiation during cancer evolution.

At the end-stages, the trans-differentiation trajectory demonstrates a bifurcation, resulting in two neuroendocrine states, one characterized by ASCL2 and POU2F3 expression (Class I tumors), the other by ASCL1 expression (class II tumors). Throughout the trans-differentiation trajectory, individual cells demonstrate mutually exclusive expression of either ASCL1 or ASCL2, with emergence of ASCL2 generally earlier and more prominent than ASCL1. Thus, the ASCL2 state and double positive state may reflect a semi-stable and transitional state. The molecular switch from ASCL2 to ASCL1 demonstrates the dynamic transcriptional control in SCNPC. An analogous temporal shift from FOXA1 to FOXA2 orchestrated transcriptional programs was observed in an independent SCNPC temporal GEMM model <sup>43</sup>, and the FOXA1 to FOXA2 transition is reflected in the PARCB model (Figure S2D).

SCLC tumor subtypes are canonically defined by the predominant expression of one of four master regulators (ASCL1, NEUROD1, POU2F3, and YAP1) <sup>46</sup>, and tumors expressing ASCL1 have been reported in therapy induced SCNPC <sup>5,51</sup>. Nevertheless, single cell data from mouse models of SCNPC have identified both a distinct cell subpopulation with co-expression and open chromatin accessibility of *ASCL2* and *POU2F3* motifs <sup>31</sup>, and a *POU2F3* expression-dominant cell subpopulation <sup>50</sup>. Upon close examination of clinical prostate cancer expression datasets <sup>31,49-51</sup>, and upon performing RNA hybridization studies of prostate tumor histology sections, we found that ASCL2+ cells are common in castration-resistant and therapy-exposed prostate cancers. Thus, the previous reports combined with our findings support a potential cancer physiology role

for the ASCL2/POU2F3 subtype in prostate cancer trans-differentiation. In parallel, NEUROD1, a marker of a previously defined prostate (and SCLC) cancer subtype<sup>5,46</sup> has relatively low expression in the PARCB temporal study. However, a *NEUROD1*-expressing cell cluster is situated between the *ASCL1* and *ASCL2* cell clusters in the lineage analysis, suggesting a potential facilitating role in lineage bifurcation and trans-differentiation.

Prior links between master regulators POU2F3 and ASCL2 have previously been reported, such as a unique dependency on ASCL2 in the POU2F3 subtype of SCLC cell lines<sup>78</sup>. Whether ASCL2 and POU2F3 regulate highly overlapping transcriptional targets remains to be determined. One potential mechanism is through the co-activation of E-box and octamer DNA binding by ASCL2 and POU2F3, respectively. This interaction mechanism was observed previously between ASCL1 and POU3F2 (BRN2) in neurogenesis<sup>79</sup>. Further work will help answer if ASCL2 facilitates the transitional stage and/or is a more default program during the de-differentiated transition stage.

Despite sharing similar nomenclature and pro-neuronal properties in the literature<sup>20</sup>, ASCL1 and ASCL2 are known to play different roles in stem cell, lineage, and cancer biology<sup>22,29</sup>. ASCL1 is a prominent driver for neuroendocrine differentiation in normal cells<sup>22</sup>. However, recent cancer studies have shown that ASCL1 contributes to high lineage plasticity, resulting in subtype changes via remodeling of the global epigenetic state<sup>18,24</sup>. The role of ASCL2 requires further investigation to determine its balance of compensatory and competitive characteristics in regard to ASCL1 function in small cell neuroendocrine cancers. In our mechanistic studies, we found that increased ASCL1 leads to increased ASCL2 expression, whereas ASCL2 suppresses ASCL1 expression using PARCB tumor-derived cell lines from multiple tissues of origin (prostate and lung). This leads to a future testable hypothesis on whether existence or absence of ASCL2 is required to arrive at an ASCL1-positive neuroendocrine state via trans-differentiation.

A dynamic lineage plasticity among subtypes of SCLC has been reported<sup>18</sup>. However, the triggers and mechanisms underlying cancer cells switching to different lineages remain elusive. In SCNPC,

beyond our discovery of the reciprocal regulation between *ASCL1* and *ASCL2*, our results identified TFAP4 as an additional candidate member of this transcriptional circuitry. In particular, TFAP4 can alternate the expression of *ASCL1* and *ASCL2* by differential binding to *cis* regulatory elements on both genes. TFAP4 has been shown to have both activating and repressing properties in gene regulation through interactions with distinct transcription factors<sup>59,60</sup>. TFAP4 demonstrates substantial increased expression in small cell vs. non-small cell cancers and is elevated in cancers compared to normal tissue. Future mechanistic and functional studies on TFAP4 will help clarify its master regulator role in lineage trans-differentiation in SCNPC and SCLC.

In clinical therapy, different forms of tumor plasticity define the battle grounds for acquired resistance. In the primary prostate cancer setting, the vast majority of prostate cancers are adenocarcinomas while all other histologic types are rare. In the castration-resistant setting, especially with the clinical introduction of next-generation anti-AR therapies, many different variant histology has been observed, including rare cases of squamous carcinoma<sup>80</sup>. In this combat, trans-differentiation to a small cell neuroendocrine state in response to otherwise effective molecular therapies is an emerging challenge across multiple cancer types. The temporal profiling of SCNPC development in the human cell based PARCB model revealed that trans-differentiation from an adenocarcinoma to neuroendocrine state is a temporally complicated, yet systematically coordinated process. The combination of bulk and single cell profiling approaches allowed for the identification of an arc-like trajectory and a transitory period characterized by epigenetic loosening, which are shared in general by other differentiation and development processes. Consistent with genetically engineered mouse SCNPC models, and with the multiple subtypes of SCLC, we find a role for both *ASCL1* and *ASCL2/POU2F3* in trans-differentiation to SCNPC. The results from our model have provided insight into the regulatory crosstalk between different neuroendocrine master regulators and provide a resource for

identifying candidate approaches for blocking this clinically challenging case of trans-differentiation.

## **DECLARATION OF INTERESTS**

E.C. served as a paid consultant to DotQuant and received Institutional sponsored research funding unrelated to this work from AbbVie, Gilead, Sanofi, Zenith Epigenetics, Bayer Pharmaceuticals, Forma Therapeutics, Genentech, GSK, Janssen Research, Kronos Bio, Foghorn Therapeutics, and MacroGenics. P.S.N. has served as a paid consultant for Janssen, Merck, Bristol Myers Squibb and received research funding from Janssen for work unrelated to the present study. O.N.W. currently has consulting, equity, and/or board relationships with Trethera Corporation, Kronos Biosciences, Sofie Biosciences, Breakthrough Properties, Vida Ventures, Nammi Therapeutics, Two River, Iconovir, Appia BioSciences, Neogene Therapeutics, 76Bio, and Allogene Therapeutics. None of these companies contributed to or directed any of the research reported in this article. T.G.G. reports receiving an honorarium from Amgen, having consulting and equity agreements with Auron Therapeutics, Boundless Bio, Coherus BioSciences and Trethera Corporation. The lab of T.G.G. has completed a research agreement with ImmunoActiva. A provisional patent application related to this study was submitted.

## **INCLUSION AND DIVERSITY**

One or more of the authors of this paper self-identifies as a gender minority in their field of research. One or more of the authors of this paper self-identifies as a member of the LGBTQIA+ community.



## **ACKNOWLEDGEMENTS**

We thank the University of California, Los Angeles (UCLA) Tissue Procurement Core Laboratories for prostate tissue preparation and histological staining, and the UCLA Technology Center for Genomics and Bioinformatics for RNA sequencing, ATAC sequencing, CUT&RUN sequencing and single cell RNA sequencing. We thank the patients and their families, Bruce Montgomery, Celestia Higano, Evan Yu, Heather Cheng, Mike Schweizer, Andrew Hsieh, Lawrence True, Funda Vakar-Lopez, Martine Roudier and the rapid autopsy teams in the Urology and Laboratory Medicine & Pathology Departments at the University of Washington. Funding: This project is supported by an NIH UCLA SPORE in Prostate Cancer Grant P50CA092131 (O.N.W. and T.G.G.), the Department of Defense Prostate Cancer Research Program Idea Development Award W81XWH2110806 (O.N.W. and J.W.P.), NIH R01 Grant R01CA222877 (O.N.W. and T.G.G.), W.M. Keck Foundation Award 20182490 (O.N.W. and T.G.G.), UCLA Eli and Edythe Broad Center of Regenerative Medicine and Stem Cell Research Hal Gaba Director's Fund for Cancer Stem Cell Research (O.N.W. and T.G.G.), Parker Institute for Cancer Immunotherapy (O.N.W.), Pacific Northwest Prostate Cancer SPORE Grant P50CA97186 (C.M., E.C. and P.S.N), NIH R01 Grant R01CA234715 (P.S.N), NIH P01 Grant PO1CA163227 (C.M., E.C. and P.S.N) and the Institute for Prostate Cancer Research (C.M., E.C. and P.S.N). C.C. is supported by the UCLA Eli and Edythe Broad Center of Regenerative Medicine and Stem Cell Research predoctoral fellowship and UCLA Dissertation Year Fellowship. K.M.S. is supported by the UCLA Medical Scientist Training Program (NIH NIGMS T32 GM008042). G.V. is supported by UCLA Tumor Cell Biology Training Program (USHHS Ruth L. Kirschstein Institutional National Research Service Award T32 CA009056).

## **AUTHOR CONTRIBUTION**

Conceptualization, C.C., J.W.P., T.G.G., O.N.W.; Methodology, C.C., L.W., J.W.P., T.G.G., O.N.W. Investigation, C.C., T.S., L.W., L.T., G.V., N.J.B., Z.M., K.S., W.T., M.B.O., K.M.S., D.C., A.H., R.X., Y.Z., M.N.; Resources, C.M., E.C., P.S.N., Y.Z., J.H.; Writing, C.C., T.G.G., O.N.W.; Data Curation, W.T., Y.Z., T.G.G.; Supervision, T.G.G. and O.N.W.

## MAIN FIGURE LEGENDS

**Figure 1. Temporal gene expression programs of the PARCB transformation model reveal SCNPC trans-differentiation pathways.** (A) Schematic summary of PARCB time course study and representative Hematoxylin and eosin (H&E) staining and immunohistochemistry (IHC) staining of neuroendocrine markers (SYP and NCAM1) on sequential tumors from the tissue microarray. Time point (TP1-6) samples were sequenced using bulk RNA sequencing (green circle), bulk ATAC-sequencing (red circle) and/or single cell RNA sequencing (blue circle, tumors only). (B) Projection of the PARCB time course samples onto the PCA framework defined by pan-cancer clinical tumor datasets <sup>4,10,32-36</sup>. LUAD: Lung adenocarcinoma. LUAD norm: lung adenocarcinoma adjacent normal tissue. SCLC: small cell lung cancer. PRAD: prostate adenocarcinoma. PRAD norm: prostate adenocarcinoma adjacent normal tissue. CRPC: castration resistant prostate cancer. SCNPC: small cell neuroendocrine prostate cancer. (C) Average gene expression of selected SCNPC-associated proteins and markers. (D) Heatmap of hierarchical clusters (HC) of samples (columns) and corresponding differentially upregulated gene modules (rows). Differential expression defined by one HC vs all other HCs). (E) PCA of the PARCB time course samples and trans-differentiation trajectories including primary arc and secondary bifurcation. A 3-dimensional rotatable version of this figure is available on the PARCB Multi-omics Explorer website. [For review, a 3D rotatable version is included as Data S1.] (F) Selected enriched GO terms across HC. See also Figure S1.

**Figure 2. Sequential transcription regulators modulate reprogramming and neuroendocrine programs through a highly entropic and accessible chromatin state.** (A) Overall differential chromatin accessibility across HC. (B) PCA of chromatin accessibility of PARCB time course samples with entropy analysis using ATAC sequencing. (C) Overall mean accessible peaks near TSS of each HC in PARCB time course study. (D) Enriched motifs from

suites of transcription factors in each HC using ATAC-sequencing. Top 5 motif suites for each comparison are shown, with additional analysis in Figure S2B, and full results in Table S1D. (E) Top ranked transcription factors and known neuroendocrine transcription factors across PARCB time course using bulk RNA sequencing. HOXC TFs avg: Average expression of HOXC4, HOXC5, HOXC6, HOXC8, HOXC9, HOXC10, HOXC11, HOXC12 and HOXC13. (F) Expression of ASCL1, ASCL2, NEURD1 and POU2F3 in each HC. See also Figure S2.

**Figure 3. Transcription factor-defined cell populations contribute to lineage divergence and tumor heterogeneity.** (A) Dimension reduction UMAP analysis of four patient series (P2, P5, P6 and P7) over time (TP3-6) using single cell RNA sequencing. (B) Temporal UMAP analysis of all the samples. (C) Expression of selected markers and transcription factors. KRT5 marks basal cells. KRT15 marks luminal cells. The expression is presented in log normalized counts. (D) Top enriched inferred cell types from the Human Cell Type Database using SingleR<sup>48</sup>. (E) Projection of single cell RNA-sequencing samples on PCA framework by bulk RNA-sequencing samples (top panel) and the expression of selected markers and transcription factors (bottom panel). Each data point is a single cell colored by their corresponding HC. (F) Expression of ASCL1 (top) and ASCL2 (middle) and percentage of ASCL1/2 positive cells (cells with expression value >0) (bottom) in human biopsy and GEMM model tumors from five single cell RNA-sequencing datasets<sup>31,49-51</sup>. Other: prostatic intraepithelial neoplasia. NMYC\_RB\_M: *Pten*<sup>ff</sup>; *Rb1*<sup>ff</sup>; *MYCN*+ (PRN) and RB\_M: *Pten*<sup>ff</sup>; *Rb1*<sup>ff</sup> (PR) mouse model in Brady et al<sup>31</sup>. See also Figure S3.

**Figure 4. ASCL1 and ASCL2 specify independent transcriptional programs and sub-lineages in SCNPC.** (A) Inferred clonal tracing analysis of the PARCB time course samples using

Monocle 2<sup>52</sup>. **(B)** Relative expression of KRT5, ASCL1 and ASCL2 in the inferred clonal tracing analysis (pseudo-time). **(C)** Percentages of ASCL1 or ASCL2 positive, double positive and double negative cell populations over time. **(D)** Volcano plot of differential gene expression in high ASCL1+ vs high ASCL2+ cell populations. **(E)** Representative genes from the predicted transcriptional programs of ASCL1 and ASCL2 trained on data from patient and model prostate cancer tumors<sup>(6,10,33)</sup> including TCGA), as determined by the ARACNE algorithm<sup>81</sup>. **(F)** Western blot of panel of genes in the PARCB tumor derived cell lines from different tissue of origin (prostate, bladder and lung)<sup>6,7</sup>. **(G)** Representative images of *in situ* hybridization of ASCL1 and ASCL2 mRNA analysis on transitional tumors (P7-TP5 and P9-TP4). See also Figure S4.

**Figure 5. ASCL1 and ASCL2 as pan-cancer classifiers.** See also Figure S5. **(A)** Projection of the PARCB time course samples on the PCA framework defined by the CRPC subtypes using RNA sequencing (left) and ATAC-sequencing (right)<sup>57</sup>. SCL: stem-cell like. NEPC: Neuroendocrine prostate cancer. 3-dimensional rotatable versions of these figures are available on the PARCB Multi-omics Explorer website. [For review, 3D rotatable versions are included as Data S2 and Data S3.] **(B)** Projection of the PARCB time course samples on the PCA framework defined by the SCLC subtypes<sup>32,46</sup>. **(C)** mRNA expression of ASCL1 and ASCL2 in the PARCB time course samples and multiple sets of clinical CRPC-PRAD and SCNPC samples including TCGA and different research groups<sup>10,33-36</sup>. **(D)** Representative images of *in situ* RNA hybridization of ASCL1 and ASCL2 in clinical SCNPC tissues. **(E)** mRNA expression of ASCL1 and ASCL2 in pan cancer cell lines (CCLE). **(F)** mRNA expression of ASCL1 and ASCL2 in pan cancer tumors from TCGA.

**Figure 6. Alternating ASCL1 and ASCL2 expression through reciprocal interaction and TFAP4 epigenetic regulation.** See also Figure S6. **(A)** Western blot analysis of exogenously expressing either V5 tagged ASCL2 in ASCL1+ cell lines <sup>6</sup> (left) or V5-tagged ASCL1 in ASCL2+ cell lines (right). **(B)** Schematic of putative cis regulatory elements (CREs) of ASCL1 and ASCL2 (top) and the heatmap of open chromatin accessibility across CREs of ASCL1 and ASCL2 using the PARCB time course ATAC-sequencing (bottom). Red box: CREs containing predicted TFAP4 binding sites by HOMER motif enrichment analysis <sup>58</sup>. **(C)** Top 8 ranked transcription factor motifs in ASCL1 promoter and ASCL2 enhancer regions, ranked by p-values. **(D)** Western blot analysis of doxycycline-inducible knockout of TFAP4 and proteins of interest in P7-TP6 (ASCL1+) and P3-TP5 (ASCL2+) cell lines. DOX: doxycycline. **(E)** Cell proliferation analysis of P7-TP6 (ASCL1+) and P3-TP5 (ASCL2+) cell lines with doxycycline-inducible knockout of TFAP4. Ctrl: no addition of doxycycline. TFAP4: with addition of doxycycline. **(G)** Schematic summary of the PARCB time course study.

## MATERIAL AND METHOD DETAIL

### ***PARCB transformation temporal model***

Prostate tissues from donors were provided in a de-identified manner and therefore exempt from Institutional Review Board (IRB) approval. Processing of human tissue, isolation of basal cells, organoid transformation, and xenograft assay were described in detail previously<sup>6</sup>. 20,000 cells FACS-sorted cells per organoid were plated in 18-20ul of growth factor-reduced Matrigel (Cat# 356234, Corning) with PARCB lentiviruses (MOI=50/lentivirus). Organoids were cultured in the prostate organoid media<sup>82</sup> for about 10-14 days. Transduced organoids were harvested by dissociation of Matrigel with 1mg/mL Dispase (Cat# 17105041, Thermo Fisher Scientific). The organoids were washed three times with 1xPBS to remove Dispase and re-suspended in 10µl of growth factor reduced Matrigel and 10ul Matrigel with High Concentration (Cat# 354248, Corning). The organoid-Matrigel mixture was implanted subcutaneously in immunodeficient NOD.Cg-Prkdcscid Il2rgtm1Wjl/SzJ (NSG) mice<sup>83</sup>. Tumors were extracted in every two-week window, with the last tumor collection of the time course series determined by either reaching around 1cm in diameter in tumor size or ulceration, whichever came first. NSG mice had been transferred from the Jackson Laboratories and housed and bred under the care of the Division of Laboratory Animal Medicine at the University of California, Los Angeles (UCLA). All animal handling and subcutaneous injections were performed following the protocols approved by UCLA's Animal Research Committee.

### ***Cell lines***

NCI-H1385 (Cat# CRL-5867), NCI-H1930 (Cat# CRL-5906), NCI-H1694 (Cat# CRL-5888), NCI-H146 (Cat# HTB-173), DMS79 (Cat# CRL-2049), NCI-H526 (Cat# CRL-5811), and NCI-H660 (Cat# CRL-5813) were purchased from American Type Culture Collection (ATCC). COR-L311 was obtained from Sigma Aldrich (Cat# 96020721). All commercially available cell lines were cultured and maintained based on the instruction from the vendors. PARCB tumor derived cell

lines were generated using the previous method <sup>6</sup>. All the cell lines in the study are free of Mycoplasma using a MycoAlert™ PLUS Mycoplasma Detection Kit (Cat# LT07-703, Lonza).

### ***Lentiviral vectors and lentiviruses***

The myristoylated AKT1 vector (FU-myrAKT1-CGW), exogenous expression of cMYC and BCL2 (FU-cMYC-P2A-BCL2-CRW), dominant TP53 mutant (R175H) and shRNA targeting RB1 vector (FU-shRB1-TP53DN-CYW) have been described previously <sup>6</sup>. Exogenous expression of V5 tagged ASCL1 (pLENTI6.3-V5-ASCL1) is obtained from DNASU (Cat#: HsCD00852286) <sup>84</sup>. For making exogenous expression of ASCL2 containing vector (pLENTI6.3-V5-ASCL2), Gateway cloning (Cat# 11791020, Thermo Fisher) was performed using pLenti6/V5-DEST Gateway Vector (Cat# V49610, Thermo Fisher) and the entry plasmid (pDONR221-ASCL2) was obtained from DNASU (Cat# HsCD00829357) <sup>84</sup>. For making doxycycline- inducible sgTFAP4 (TLCv2-Cas9-BFP-sgTFAP4), TLCv2 (Cat# 87360, Addgene) was first digested with BamHI-HF (Cat# R3136, New England Biolabs) and NheI-HF (Cat# 3131, New England Biolabs) at 37°C for 1 hour and inserted with a synthesized fragment containing T2A-Hpal-BFP sequence (gBlock service provided by IDT) using Gibson Assembly (Cat# E5510, New England Biolabs). sgTFAP4 sequence was cloned into the previously described TLCv2-BFP vector using an established protocol <sup>85</sup>. sgTFAP4-primers are listed in the key resources table. Lentiviruses were produced and purified by a previously established method <sup>86</sup>.

### ***Tissue section, histology, and immunohistochemistry (IHC)***

PARCB model tumor tissues were fixed in 10% buffered formaldehyde overnight at 4°C and followed by 70% ethanol solution. Tissue microarray construction and hematoxylin and eosin (H&E) staining were performed by Translation Pathology Core Laboratory (TPCL) in UCLA using standard protocol. TPCL is a CAP/CLIA certified research facility in the UCLA Department



of Pathology and Laboratory Medicine and a UCLA Jonsson Comprehensive Cancer Center Shared Facility. For immunohistochemistry staining, formalin-fixed, paraffin-embedded (FFPE) sections were deparaffinized and rehydrated with a washing sequence of xylene and different concentration of ethanol. Citrate buffer (pH6.0) was used to retrieve antigens. The sections were incubated in citrate buffer and heated in a pressure cooker. 3% of H<sub>2</sub>O<sub>2</sub> in methanol was used to block endogenous peroxidase activity for 10 mins at room temperature. The sections were blocked then incubated with primary antibodies overnight at 4°C. Anti-mouse/rabbit secondary antibodies were used to detect proteins of interest and DAB EqV substrate was used to visualize the staining. All components were included in the ImmPRESS Kit (MP-7801-15 and MP-7802-15, Vector Laboratories) The slides were then dehydrated and mounted with Xylene-based drying medium (Cat# 22-050-262, Fisher Scientific).

### ***Western blot***

Cells were lysed on ice using UREA lysis buffer (8M UREA, 4% CHAPS, 2x protease inhibitor cocktail (Cat# 11697498001, Millipore Sigma)). Genomic DNA was removed by ultracentrifuge (Beckman Optima MAX-XP, rotor TLA-120.1, 48,000 rpm for 90 min). Protein concentrations were measured using the Pierce BCA Protein Assay Kit (Cat#: 23227, Thermo Scientific). Samples were electrophoresed on polyacrylamide gels (Cat# NW04120BOX, Thermo Fisher), transferred to nitrocellulose membranes (Cat# 88018, Thermo Fisher). Western blots were visualized using iBright CL1500 Imaging system (Cat#44114, Thermo Fisher).

### ***RT-qPCR***

Total RNA was isolated from cells using miRNeasy Mini Kit (Cat# 217004, Qiagen). cDNA was synthesized from 2 ug of total RNA using the SuperScript IV First-Strand Synthesis System (Cat# 18091050, Thermo Fisher). RT-qPCR was performed using SYBR Green PCR Master Mix (Cat# 4309155, Thermo Fisher). Amplification was carried out using the StepOne Real-Time PCR System (Cat# 4376357, Thermo Fisher) and analysis was performed using the

StepOne Software v2.3. with the following primers were used at a concentration of 250  $\mu$ M:

Relative quantification was determined using the Delta-Delta Ct Method. Primer sequences are listed in the key resources table.

### ***In situ RNA hybridization assay and image analysis***

The RNAscope Multiplex Fluorescent V2 kit was used to perform in situ hybridization on FFPE tissue microarray slides following the manufacturer's protocol (Cat# 323270, ACDBio). The Institutional Review Board of the University of Washington approved this study (protocol no. 2341). All rapid autopsy tissues were collected from patients who signed written informed consent under the aegis of the Prostate Cancer Donor Program at the University of Washington. The establishment of the patient-derived xenografts was approved by the University of Washington Institutional Animal Care and Use Committee (protocol no. 3202-01). For multiplex hybridization, the Double Z probes targeting ASCL1 (Cat# 459721-C2, ACDBio) and ASCL2 (Cat# 323100, ACDBio) were hybridized to the samples for 2 hours at 40°C. ASCL1 signal was visualized using Opal dye 520 (Cat# FP1487001KT, Akoya Biosciences) and ASCL2 signal was visualized using Opal dye 570 (Cat# FP1488001KT, Akoya Biosciences). DAPI (Cat# D3571, Thermo Fisher) was used to visualize nuclei. Confocal fluorescence images were acquired using an inverted Zeiss LSM 880 confocal microscope. All images were processed using Fiji (<https://imagej.net/software/fiji/>).

### ***Cell proliferation assay***

3000 cells per cell line in five replicates were seeded on 96-well plates on Day 0. Cell viability was measured on Day 1, 3, 4, 5 and 6. using Cell Titer-Glo Luminescent Cell Viability Assay (Cat# G7570, Promega). Luminescence was measured at an integration time of 0.5 second per well.

### ***Bulk RNA sequencing and dataset collection***

Tumors were dissociated into single cells, followed by cell sorting of triple colors (RFP, GFP and YFP) by flow cytometry. Total RNA was extracted from the cell lysates using miRNeasy mini kit (Cat# 217084, Qiagen). Libraries for RNA-sequencing of PARCB time course samples were prepared with KAPA Stranded mRNA-Seq Kit (Cat# KK8420, Roche). The workflow consists of mRNA enrichment and fragmentation. Sequencing was performed on Illumina HiSeq 3000 or NovaSeq 6000 for PE 2x150 run. Data quality check was done on Illumina SAV. Demultiplexing was performed with Illumina Bcl2fastq v2.19.1.403 software. Raw sequencing reads were processed through the UCSC TOIL RNA Sequencing pipeline<sup>1</sup> for quality control, adapter trimming, sequence alignment, and expression quantification. Briefly, sequence adapters were trimmed using CutAdapt v1.9, sequences were then aligned to human reference genome GRCh38 using STAR v2.4.2a and gene expression quantification was performed using RSEM v1.2.25 with transcript annotations from GENCODE v23<sup>87</sup>.

The FASTQ files of the Park dataset<sup>6</sup>, Beltran dataset<sup>33</sup>, George dataset<sup>32</sup> and Tang dataset<sup>57</sup> were all processed through the TOIL pipeline with the same parameters to get RSEM expected counts. The TOIL-RSEM expected counts of TCGA pan cancer samples were obtained directly from UCSC Xena browser (<https://xenabrowser.net/datapages>) and gene expression ( $\log_2(\text{TPM} + 1)$ ) of pan-cancer cell lines from the Cancer Cell Line Encyclopedia (CCLE) were downloaded from DepMap Portal (DepMap Public 22Q1) (<https://depmap.org/portal/download/all/>). The RSEM counts of all combined datasets were upper quartile normalized,  $\log_2(x+1)$  transformed (referred to as  $\log_2(\text{UQN}+1)$  counts) and filtered down to HUGO protein coding genes (<http://www.genenames.org/>) for the downstream analyses. SCLC subtypes<sup>46</sup> and CRPC subtypes<sup>57</sup> were previously defined. The details of the bulk RNA-sequencing of PARCB time course are described in Table S11.

### ***Differential gene expression analysis and hierarchical clustering***

PARCB time course samples were grouped into 6 hierarchical clusters (HC) by performing Ward's hierarchical clustering (k=6) on  $\log_2(\text{UQN} + 1)$  counts using the `hclust` function from the base R package, `Stats` (<https://stat.ethz.ch/R-manual/R-devel/library/stats/html/00Index.html>). Differential gene expression analysis was then performed on each HC in a “one vs. rest” fashion, i.e., between one cluster vs. the remaining five clusters, using DESeq2 with the following parameters: `independentFiltering=F`, `cooksCutoff=FALSE`, `alpha=0.1`<sup>88</sup>. For each HC vs. rest comparison, genes with a  $\log_2\text{FC} > 2$  and p-adjusted value  $< 0.05$  were considered upregulated for that HC gene module. However, four genes (IL1RL1, KRT36, PIK3CG, NPY) were upregulated among multiple HC vs. rest comparisons. As a result, these genes were assigned to the HC gene module with the smaller p-adjusted value for that gene. Z-scores for upregulated genes in each cluster were then plotted in a heatmap using `pheatmap` function. PARCB time course samples were subsequently categorized by this HC definition in downstream analyses.

### ***GO enrichment analysis***

Enrichment analysis was performed using the “GO\_Biological\_Process\_2021” database and the `enrichr` function from the R package, `enrichR`, using upregulated genes for each HC<sup>89</sup>. Pathways were selected based on their adjusted p-value for each HC. The results were plotted using `ggplot()`.

### ***Bulk ATAC sequencing and dataset collection***

Tumors were dissociated into single cells, followed by cell sorting of triple colors (RFP, GFP and YFP) by flow cytometry. ATAC-sequencing samples were prepared following the previously published protocol<sup>38</sup>. Bulk ATAC sequencing was performed in the Technology Center for Genomics & Bioinformatics Core in UCLA. Sequencing was performed on Illumina NovaSeq 6000 for PE 2x50 run. Data quality check was done on Illumina SAV. Demultiplexing was performed

with Illumina Bcl2fastq v2.19.1.403 software. The raw FASTQ files were processed using the published ENCODE ATAC-Seq Pipeline (<https://github.com/ENCODE-DCC/atac-seq-pipeline>). The reads were trimmed and aligned to hg38 using bowtie2. Picard was used to de-duplicate reads, which were then filtered for high-quality paired reads using SAMtools. All peak calling was performed using MACS2. The optimal irreproducible discovery rate (IDR) thresholded peak output was used for all downstream analyses, with a threshold P value of 0.05. Other ENCODE3 parameters were enforced with the flag-encode3. Reads that mapped to mitochondrial genes or blacklisted regions, as defined by the ENCODE pipeline, were removed. The peak files were merged using bedtools merge to create a consensus set of peaks across all samples, and the number of reads in each peak was determined using bedtools multicov<sup>90</sup>. A variance stabilizing transformation was performed on peak counts using DESeq2<sup>88</sup> and batch effects were removed using removeBatchEffect() from limma<sup>91</sup>. All downstream ATAC-sequencing analysis was performed using this matrix (referred to as VST peak counts), unless otherwise specified. P1-TP1 was not collected for ATAC-sequencing due to insufficient cell number for sequencing. P7-TP2 was not included for the processing due to low read counts (total of 1536). P1-TP5, P2-TP6 and P10-TP2 were not included in PCA due to reaching within 95<sup>th</sup> percentile of calculated Shannon entropy for all ATAC-sequencing samples. The details of the bulk ATAC-sequencing processing of PARCB temporal samples are described in Table S1J

Raw FASTQ files of Tang ATAC-sequencing dataset were downloaded from GSE193917<sup>57</sup>. The raw FASTQ files were processed using the same ENCODE pipeline described above with the same parameters.

### ***Differential chromatin accessibility and Transcription start site (TSS) analysis***

Differential peak analysis was performed on each HC in a one vs. rest fashion, as described above in the bulk RNA-sequencing analysis. Peaks were called hyper- or hypo- accessible if the

log<sub>2</sub> fold change was greater than 2 or less than 2, respectively, and had an adjusted p-value of less than 0.05. The z-scores of the union of all differentially accessible peaks were used to plot the heatmap using VST peak counts, with the rows ordered by chromosomal location.

For mapping peaks near TSS sites, the bigwig files containing ATAC-seq readings were first converted into wig files. Wig files from samples within the same HC were then merged by calculating the mean across peak regions using wiggleTools<sup>92</sup>. The TSS analysis was performed using deepTools and computeMatrix in reference-point mode with parameters referencePoint=TSS, a=2000, b=2000 to compute the scores from merged bigwigs in regions 2 kbp flanking the region of interest. plotHeatmap was used with parameters zMin=0, zMax=5, binSize=10 was to plot the TSS figure from the score matrix<sup>93</sup>.

### ***PCA and projection analyses***

Unsupervised PCA of the PARCB time course samples using log<sub>2</sub>(UQN +1) counts was performed using the prcomp function from the stats package available on R (described above). PC2 and PC3 sample scores were then multiplied by a 30-degree clockwise rotation matrix. Ellipses were drawn around samples with 95% confidence based on real time labels using stat\_ellipse() from ggplot2. The PCA projection of PARCB time course samples onto the framework using pan small cell cancer combined gene expression datasets have been discussed previously<sup>4</sup>. In brief, the input matrix for this PCA was centered but not scaled. PARCB time course samples were then projected by multiplying the data matrix by the PCA loadings. For projection of PARCB time course samples onto the framework using gene expression data of CRPC subtypes<sup>57</sup> or SCLC subtypes<sup>46</sup>, the same methodology was applied.

For projection of PARCB time course samples onto the framework using ATAC-seq data of CRPC subtypes<sup>57</sup>, peak coverage of the Tang dataset was determined using the consensus set of peaks from the PARCB time course data with function bedtools multicov<sup>90</sup>. Tang dataset peak read counts were then variance stabilized transformed using DESeq2<sup>88</sup>. PCA was

performed on VST peak read counts of the Tang dataset using the `prcomp` function with the parameters `center = T`, `scale = F`. PARCB time course samples were then projected onto the framework by multiplying PARCB time course VST peak read counts by PCA loadings.

For projection of PARCB time course single cells onto the framework defined by the bulk RNA-sequencing data, the single cell data after integration by batch was down-sampled for 1000 cells within each patient series or cluster. The single cell and bulk RNA-sequencing data were centered separately prior to projection. The projection was carried out by multiplying the single cell data matrix by PCA loadings of PARCB bulk samples.

### ***Transcription factor analysis***

Top ranked transcription factors (TF) were selected using the gene loading scores derived from the unsupervised PCA of gene expression described above. PC2 and PC3 loading scores were rotated 30 degrees clockwise by multiplying a 30-degree clockwise rotation matrix to the gene loading scores (resulting components called PC2' and PC3', respectively). The loading scores were then filtered to include only transcription factors<sup>37</sup>. The center of the TF loading scores was determined by taking the average of PC1, PC2', and PC3'. The Euclidean distance from the center was calculated for each TF, and the top 60 TFs furthest from center were selected. Hierarchical clustering ( $k = 5$ ) was performed on the  $\log_2(\text{UQN} + 1)$  counts of the top 60 TFs. The z-scores for each TF were plotted using `heatmap`. Average z-score of HOXC genes was calculated from HOXC 4-13 (except for HOXC7) in each PARCB time course sample.

### ***Shannon Entropy analysis***

Shannon entropy for each PARCB time course sample was calculated on variance stabilized transformed (VST) ATAC-sequencing peak counts using the `Entropy()` function from the R

package DescTools (<https://cran.r-project.org/web/packages/DescTools/index.html>). PARCB samples falling within the 95th percentile of calculated Shannon entropy scores were included in the following PCA. PCA was performed on VST peak counts and was plotted using ggplot2 with samples colored by their Entropy scores and ellipses with 95% confidence were drawn around each time point group using stat\_ellipse().

### ***Prostate cancer gene regulatory network analysis***

The RNA-sequencing data of PARCB time course study, Park dataset <sup>6</sup>, Beltran dataset <sup>33</sup>, and TCGA PRAD/PRAD-norm dataset were included in this analysis. TCGA PRAD/PRAD-norm data was down sampled to match the sample size of other cohorts. Gene network was built on the combined datasets using ARACNe-AP <sup>81</sup>.

### ***Signature scores (adult stem cell, adenocarcinoma and SCNPC)***

SCNPC signature was derived using Beltran dataset <sup>33</sup>, following the methods described previously <sup>6</sup>. The adult stem cell (ASC) signature in our analysis is defined in literature <sup>42</sup>. For prostate adenocarcinoma signature, differential gene expression analysis was performed on TCGA PRAD samples vs CRPC-PRAD and SCNPC samples from the Beltran dataset <sup>10,33</sup> using DESeq2. The adenocarcinoma signature was defined by all the upregulated genes ( $\log_2\text{FoldChange} > 2$  and  $\text{padj} < 0.05$ ) from the differential gene expression analysis.

Adenocarcinoma and SCNPC signature scores of our PARCB time course samples were calculated using gsva with method="ssgsea".

### ***Motif analysis***

Hyper-accessible peaks in each HC from the differential peak analysis described previously were used for motif enrichment analysis using GimmeMotifs 41,90. Differential motif analysis was performed on hyper-accessible peaks for each HC against a hg38 whole-genome background



using the maelstrom function with default parameters. The top 5 enriched motifs and their aggregated z-scores for each HC are shown in the heatmap (each individual HC vs all others). Additionally, we performed differential peak analysis on HC5 vs HC1-HC4 and HC6 vs HC1-HC4 with the same parameters as described previously using DESeq2. Likewise, hyper-accessible peaks for HC5 and HC6 in these comparisons were defined by a threshold of  $\log_2\text{FoldChange} > 2$  and  $\text{padj} < 0.05$ . Differential motif analysis was performed on the set of hyper-accessible peaks from HC5 vs HC1-4 and HC6 vs HC1-4 using the maelstrom function as described above. Note that in the GimmeMotif enrichment analysis, transcription factors are culled to minimize redundancy, and this step is impacted by the exact input data and sample group comparison indicated. Thus, each motif suite may contain slightly different enriched transcription factors. However, the transcription factor sets remain highly consistent between each case.

For identifying transcription factors that recognize ASCL1 and ASCL2 regulatory sequences, ASCL1 and ASCL2 promoter and enhancer regions were mapped using UCSC Genome Browser Gateway (<https://genome.ucsc.edu/cgi-bin/hgGateway>). Motif analysis was then performed on each ASCL1 and ASCL2 promoter and enhancer region using the findMotifGenome function from HOMER with the parameters -size 200 and -mask<sup>58</sup>. Resulting motifs were then ranked by their p-value. Additionally, ASCL1 and ASCL2 enhancer and promoter regions were mapped to accessible peaks from ATAC-sequencing data of the PARCB time course to identify chromatin changes of ASCL1 and ASCL2 cis-regulatory sequences. Peak regions from the PARCB consensus peak set overlapping with the ASCL1 and ASCL2 enhancer and promoter regions were then plotted in a heatmap using VST peak counts and scaled per sample.

### ***Single-cell RNA sequencing***

PARCB time course samples were sequenced in two batches: P2/P5 and P6/P7 series. Single cell gene expression libraries were created using Chromium Next GEM Single Cell 3' (v3.1

Chemistry) (Cat# PN1000123, 10x Genomics), Chromium Next GEM Chip G Single Cell Kit (Cat# PN1000120, 10x Genomics), and Single Index Kit T Set A (Cat# PN1000213, 10x Genomics) according to the manufacturer's instructions. Briefly, cells were loaded to target 10,000 cells to form GEMs and barcode individual cells. GEMs were then cleaned cDNA and libraries were also created according to manufacturer's instructions. Library quality was assessed using 4200 TapeStation System (Cat# G2991BA, Agilent) and D1000 ScreenTape (Cat# 5067-5582, Agilent) and Qubit 2.0 (Cat# Q32866, Invitrogen) for concentration and size distribution. Samples were sequenced using Novaseq 6000 sequencer (Cat# A00454, Illumina) using 100 cycles (28+8+91). The illumina base calling files were converted to FASTQ using the mkfastq function in Cell Ranger suite (<https://support.10xgenomics.com/single-cell-gene-expression/>). The reads were then aligned to GRCh38 for UMI counting with cellranger count function. The details of the single cell-seq of PARCB time course are described in Table S1K.

### ***UMAP analysis***

The downstream quality control, statistics and visualization of PARCB single cell RNAseq data were performed mainly using the Seurat (v3.2.3) R package<sup>94</sup>. Briefly, the data from all four patient series was first filtered for cells with total number of unique features above 500 and below 10000 as well as mitochondria feature counts below 10%. The mitochondrial genes and ribosomal genes were then removed from the count matrix for the downstream analysis. To overcome batch effect, we performed Seurat integration between batch 1 (Series P2 and P5) and 2 (Series P6 and P7). Briefly, for each batch, the two corresponding matrices were combined first, and log transformation and library size normalization were performed with NormalizeData function. Then the 2500 most variable genes were selected as anchor features to integrate for all coding genes. After integration, the top 30 principal components were used to perform UMAP analysis.

Processed single cell RNA-sequencing data of advanced prostate cancers were downloaded from the Single Cell Portal hosted by Broad Institute ([https://singlecell.broadinstitute.org/single\\_cell/study/SCP1244/transcriptional-mediators-of-treatment-resistance-in-lethal-prostate-cancer](https://singlecell.broadinstitute.org/single_cell/study/SCP1244/transcriptional-mediators-of-treatment-resistance-in-lethal-prostate-cancer))<sup>49</sup>. For this dataset, UMAP analysis was performed on TPM values of prostate cancer cells only as defined in the paper using the umap function in base R. For UMAP visualization of this dataset, TPM values were log2 transformed with a pseudo count of +1. Single cell RNA-sequencing data of N-myc GEMM tumors<sup>31</sup>, and human biopsy and GEMM tumors<sup>50</sup> were downloaded from the Gene Expression Omnibus (GEO) database with the accession numbers GSE151426 and GSE21035, respectively, and processed with cellranger count. In the Brady et al paper, single-cell data were first filtered for cells with total number of unique features > 200 and < 10000 as well as mitochondrial feature counts < 10%. We then performed Seurat SCTransform integration on each sample. Briefly, for each sample, the matrices were first combined and normalized using SCTransform function. Then the top 3000 most variable genes were selected as anchor features to integrate all genes. After integration, the top 15 principal components were used to perform UMAP analysis. In the Chan et al paper, GEMM single-cell data were filtered with the following thresholds nFeature\_RNA >200 & nFeature\_RNA < 8000 & percent.mt < 5 and human biopsy tissues single-cell data were filtered with nFeature\_RNA > 200 & nFeature\_RNA < 10000 & percent.mt < 5. Seurat integration of filtered cells for both datasets were then performed as described above. After integration, the top 50 principal components were used to perform UMAP analysis.

In the Dong et al analysis, the human biopsy scRNA-sequencing data was downloaded from GSE137829. We used the filtration parameters of the manuscript, total number of unique features > 500 and <7000, and mitochondrial feature counts < 10%. We filtered cells to only include epithelial (cancer) cells, as described by the CellType column in the annotation. Seurat

NormalizeData was used with the LogNormalize method and a scale factor of 10000. The top 30 principal components were used to perform UMAP analysis.

### ***Inferred cell type and cellular lineages analysis***

The cell type inferences of PARCB single cells were implemented using the singleR R package<sup>48</sup>. For scoring each cell for each general cell type, the Human Primary Cell Atlas data from LTLA/cellDex package that contains normalized expression values was used as the reference.

Single cell trajectory analysis of PARCB samples was performed using two different methods, expression-based method Monocle2<sup>52</sup> and RNA Velocity based method scVelo<sup>53</sup>. For Monocle2, the integrated Seurat object was used as the input for the program. DDRtree was used as the reduction method. Cells were ordered by the most variable 3000 genes in Seurat. For calculating pseudotime, the KRT5 population was selected as the root state. For RNA velocity, the spliced and unspliced counts were quantified by velocity accounting for repeat masking. The spliced counts were then normalized using Seurat sctransform method followed by integration by batch. The integrated data was used for UMAP visualization. In scVelo, the data was filtered for genes with a minimum of 5 shared counts. The top 3000 highly variable genes were extracted based on the dispersion. Velocities were estimated by dynamical model and then projected onto the UMAP embedding.

### ***Differential gene expression analysis in single cells***

FindMarkers function in Seurat R package (described above) was used to identify differential expressed genes between ASCL1+ and ASCL2+ single cell populations. Patient series was regressed out by including it as the covariate. ASCL1+ cells and ASCL2+ cells are defined as cells with log normalized expression counts > 0 for ASCL1 or ASCL2, respectively. Genes that

are differentially expressed in ASCL1+ population were defined by the difference of gene expression in ASCL1+ cells minus the one in ASCL2 expression (log and library size normalized) above 3. Genes that are differentially expressed in ASCL2+ cells were defined by such a difference below -1.

### ***CUT&RUN sequencing***

The CUT&RUN experiment was performed using previously established method<sup>61</sup> (Skene et al., 2018) and the manufacturer's protocol (Cat# 86652, Cell Signaling). 100k live cells were used per reaction. 50pg of Spike-In DNA (Cat# 12931, Cell Signaling) was added per reaction for downstream normalization. DNA was purified using MinElute PCR Purification Kit (Cat# 28004, Qiagen), followed by fragmentation by using sonicator (Cat# M202, Covaris). Dual size selection was applied using KAPA Pure beads (Cat# KR1245, Roche). DNA Libraries were prepared with the KAPA DNA HyperPrep kit (Cat# KK8504, Roche).

Sequencing was performed on Illumina HiSeq3000 for a SE 1x50 run. Data quality check was done on Illumina SAV. Demultiplexing was performed with Illumina Bcl2fastq v2.19.1.403 software. Raw FASTQ files were processed using the published ENCODE-TF CHIP Seq pipeline. Batch 1 samples (P3-TP5 and P7-TP6) were processed with the parameter "chip.paired\_end" : false while Batch 2 sample (P2-TP6) were processed with the parameter "chip.paired\_end" : true. (<https://github.com/ENCODE-DCC/chip-seq-pipeline2>). For all samples, the reads were trimmed and aligned to hg38 (target) and *S. cerevisiae* strain S288C (spike-in) reference genomes using bowtie2. After alignment, Picard was used to remove PCR duplicates reads and SAMtools was used to further filter high-quality paired reads (i.e., remove reads that were unmapped, not primary alignment, reads failing platform, and/or multi-mapped). Peak calling was performed using MACS2. Peaks overlapping with blacklisted regions were removed

(<https://www.encodeproject.org/files/ENCFF356LFX/>). Lastly, spike-in normalization factors were calculated following established protocol<sup>95</sup>. The details of the CUT&RUN sequencing of PARCB time course are described in Table S1L.

## **QUANTIFICATION AND STATISTICAL ANALYSIS**

All data were analyzed and processed using R v4.1.2, Python v3.11.5 and Excel. Error bars show mean  $\pm$  SD unless otherwise specified. Significance was determined by Student's two-tailed unpaired t tests or Wald test with 95% confidence intervals. P values  $<0.05$  is considered statistically significant. P values were adjusted based on various methods dependent on the analysis including Benjamin-Hochberg method (Figure 1D and Figure 1F) and Bonferroni correction (Figure 4D). No statistical methods were used to predetermine sample sizes. Other details such as sequencing processing can be found in Table S1. All statistical methods for the bioinformatic analyses are described in detail in the method section.

## **ADDITIONAL RESOURCES**

PARCB Multi-omics Explorer provides an interactive platform for visualization of gene expression using bulk RNA-sequencing and single cell RNA-sequencing of this time course study (<https://systems.crump.ucla.edu/transdiff/>).

**SUPPLEMENTAL TABLE** (Available on [Chen et al 2023](#))

**Table S1. Supplemental information of bioinformatic analyses, related to Figure 1, 2, 4**

**and 6. A)** Upregulated genes in each hierarchical clusters (HC); **B)** PCA scores of PARCB time course samples with HC and timepoint annotations; **C)** Enrichr GO Biological Processes 2021 results of upregulated genes per HC; **D)** Motif enrichment analysis per HC; **E)** List of weighted transcription factors for PCA loadings of PARCB time course data; **F)** Differential genes in ASCL1 vs ASCL2 cell populations; **G)** List of predicted gene network of ASCL1 and ASCL2; **H)** Ranked transcription factors motifs in ASCL1 and ASCL2 cis regulatory sequences; **I)** RNA-seq sequencing statistics; **J)** ATAC-seq sequencing statistics; **K)** Single Cell RNA sequencing statistics of PARCB time course sample; **L)** CUT&RUN sequencing statistics.

**SUPPLEMENTAL DATA** (Available on [PARCB Multi-omics Explorer](#))

**Data S1. PCA of PARCB time course as a 3D rotatable object, related to Figure 1E.**

**Data S2. Projection of RNA-seq as a 3D rotatable object, related to Figure 5A.**

**Data S3. Projection of ATAC-seq as a 3D rotatable object, related to Figure 5A**

Figure 1

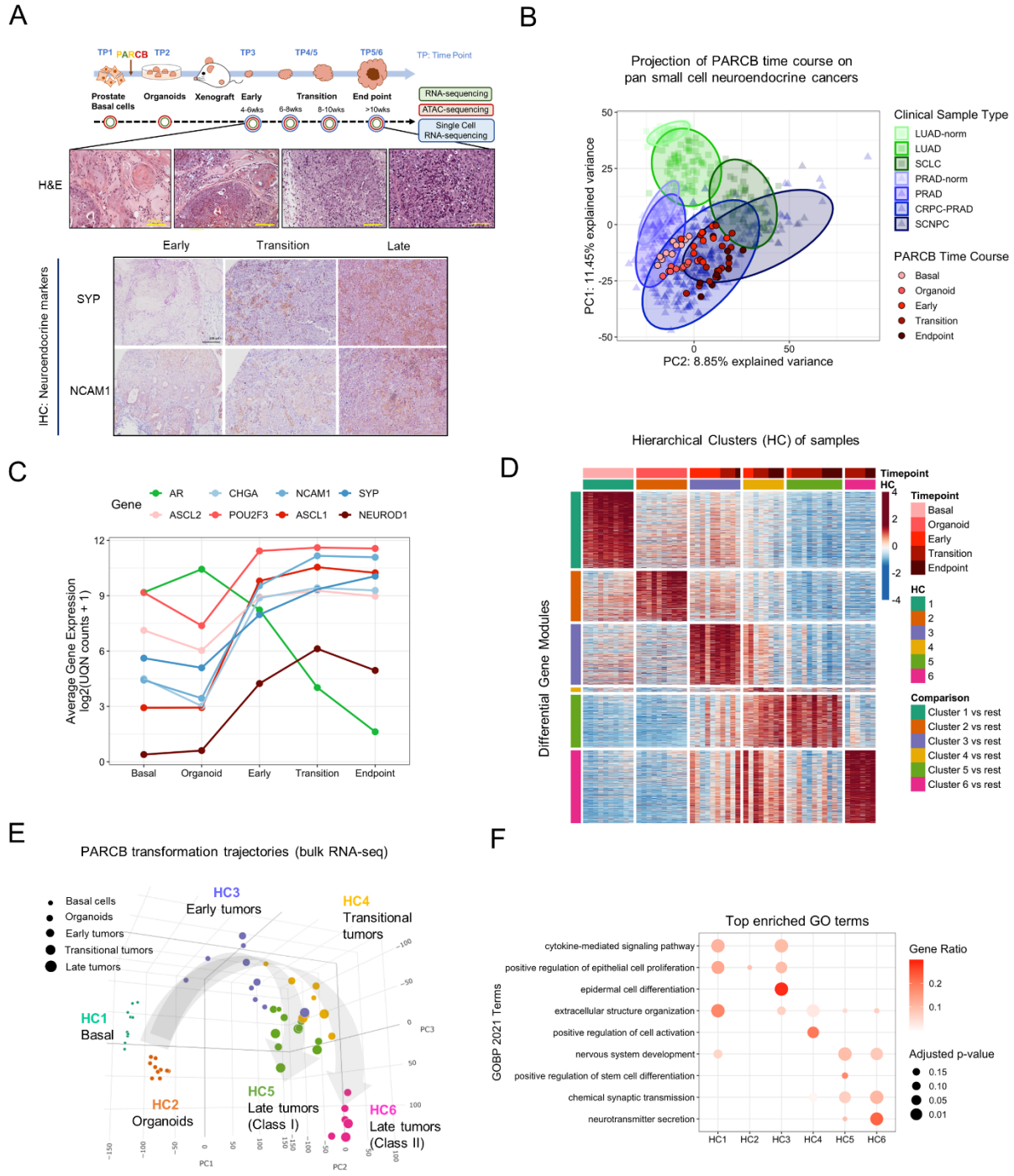




Figure 2

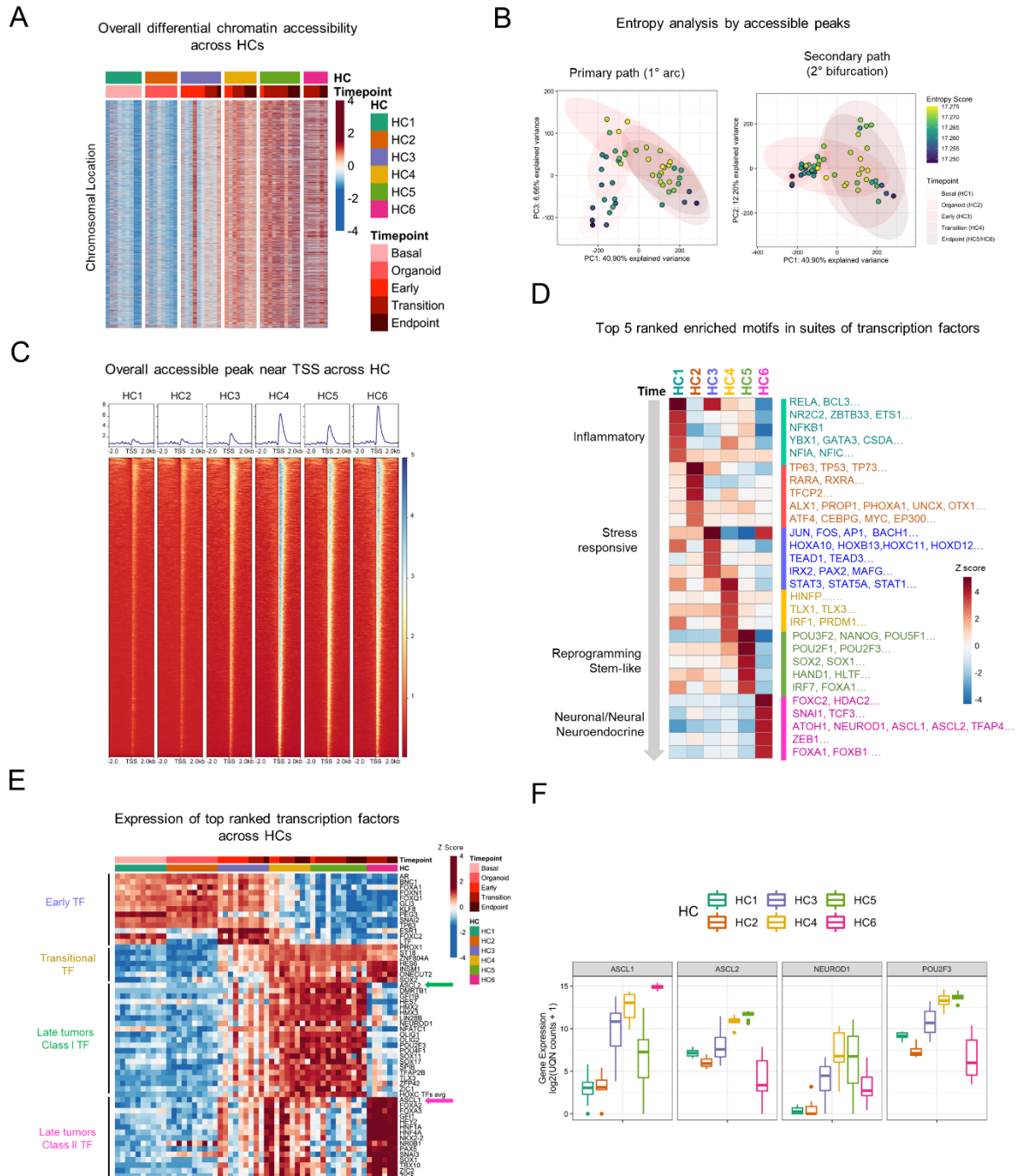


Figure 3

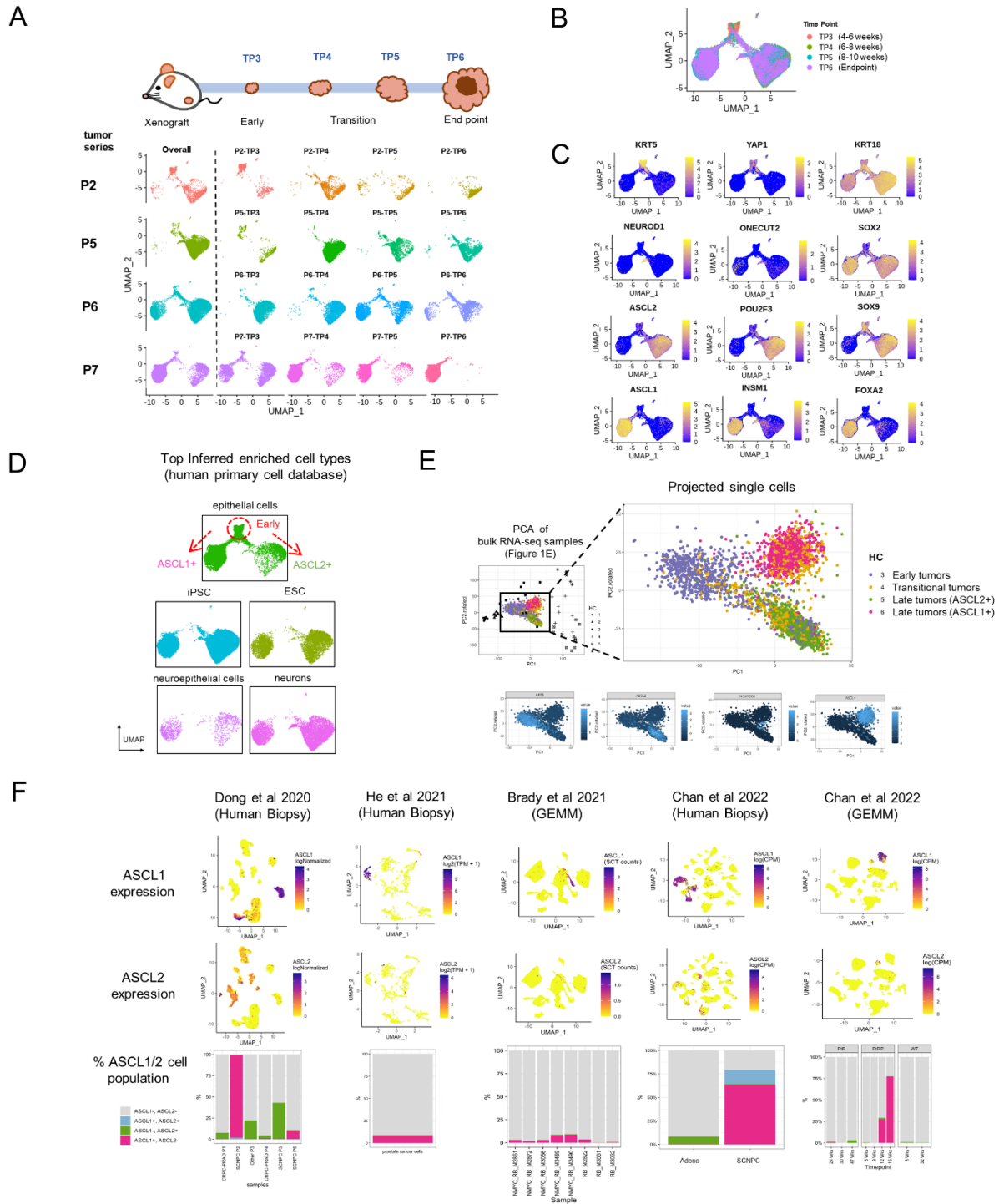


Figure 4

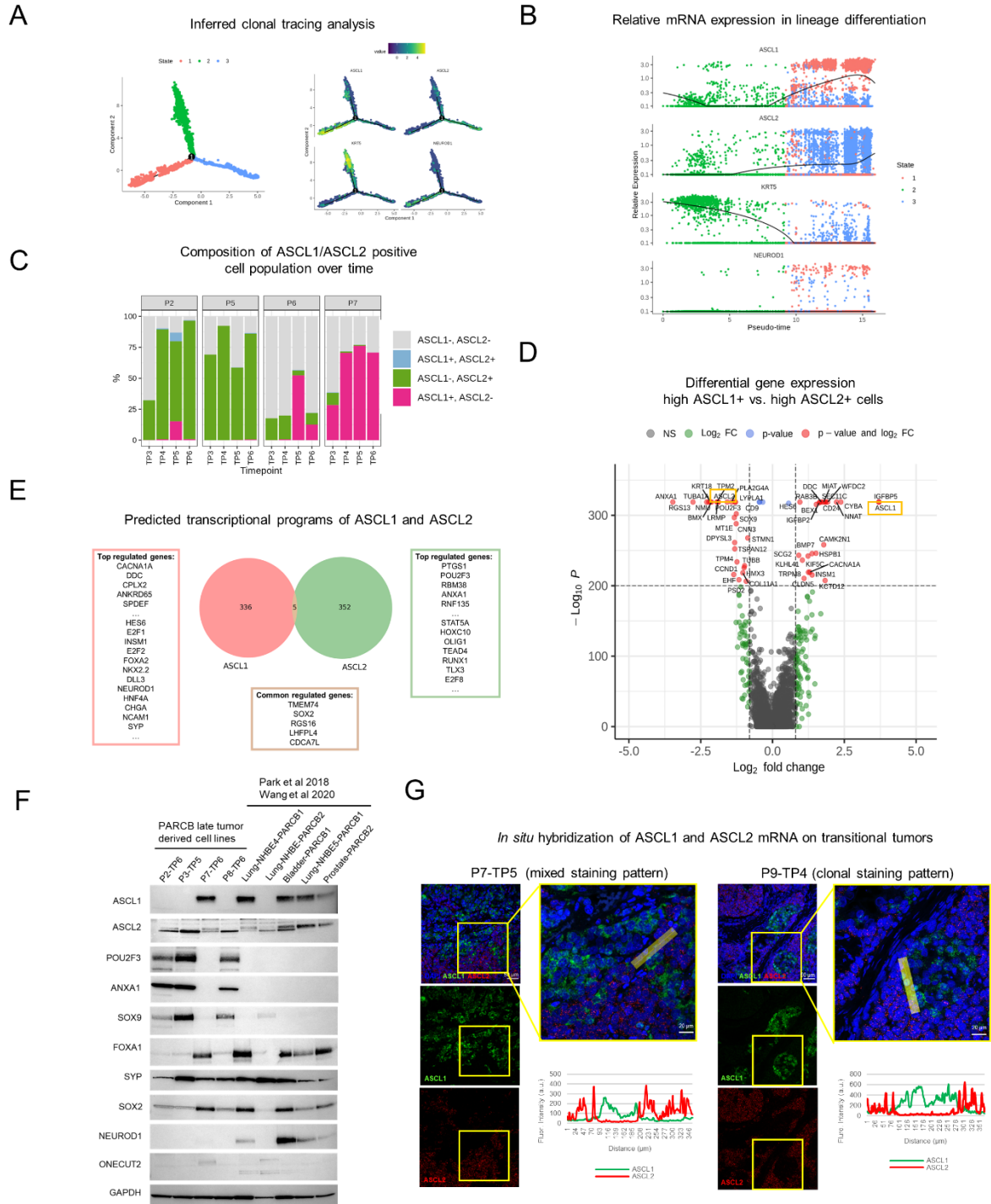




Figure 6

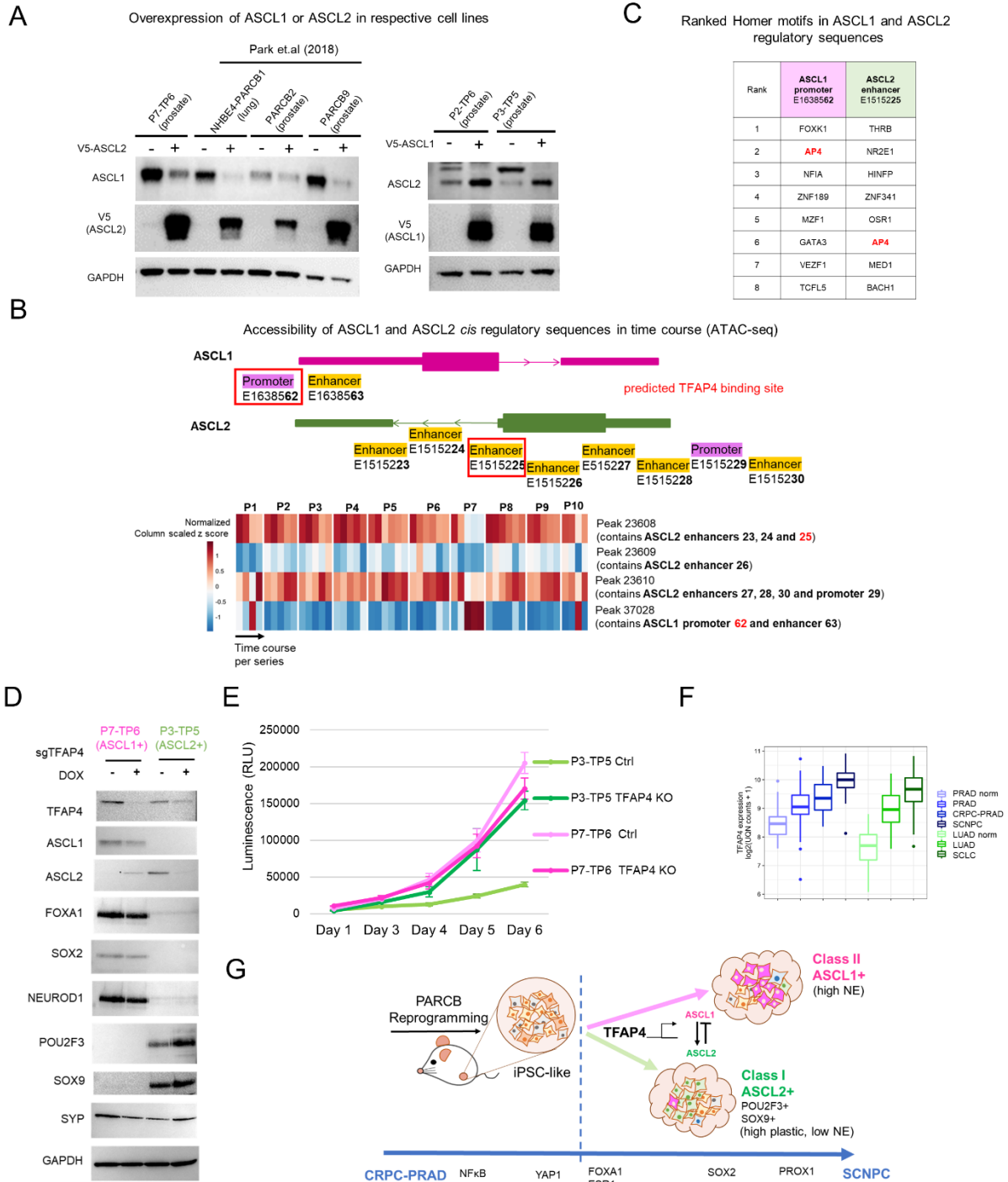


Figure S1

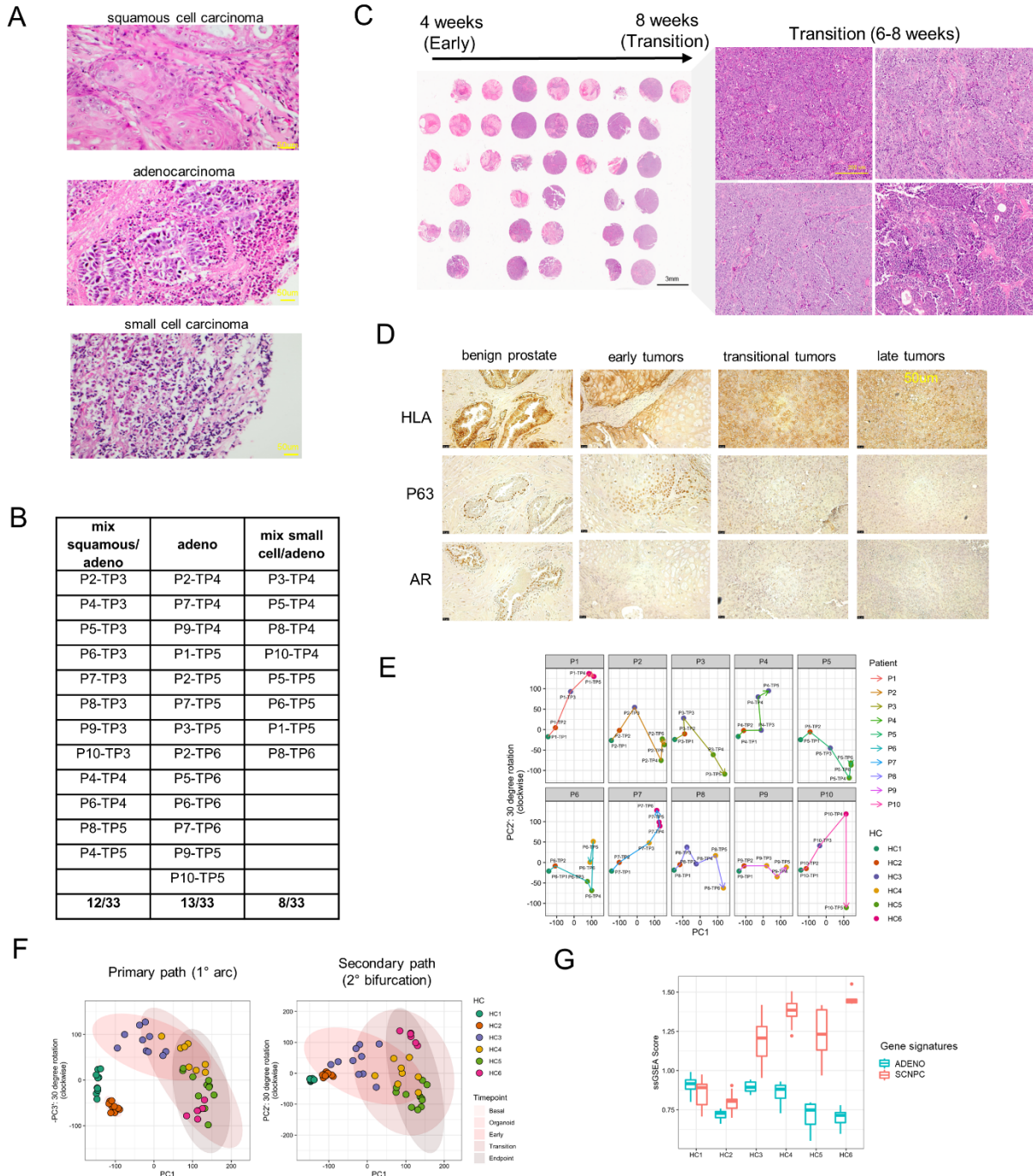


Figure S2

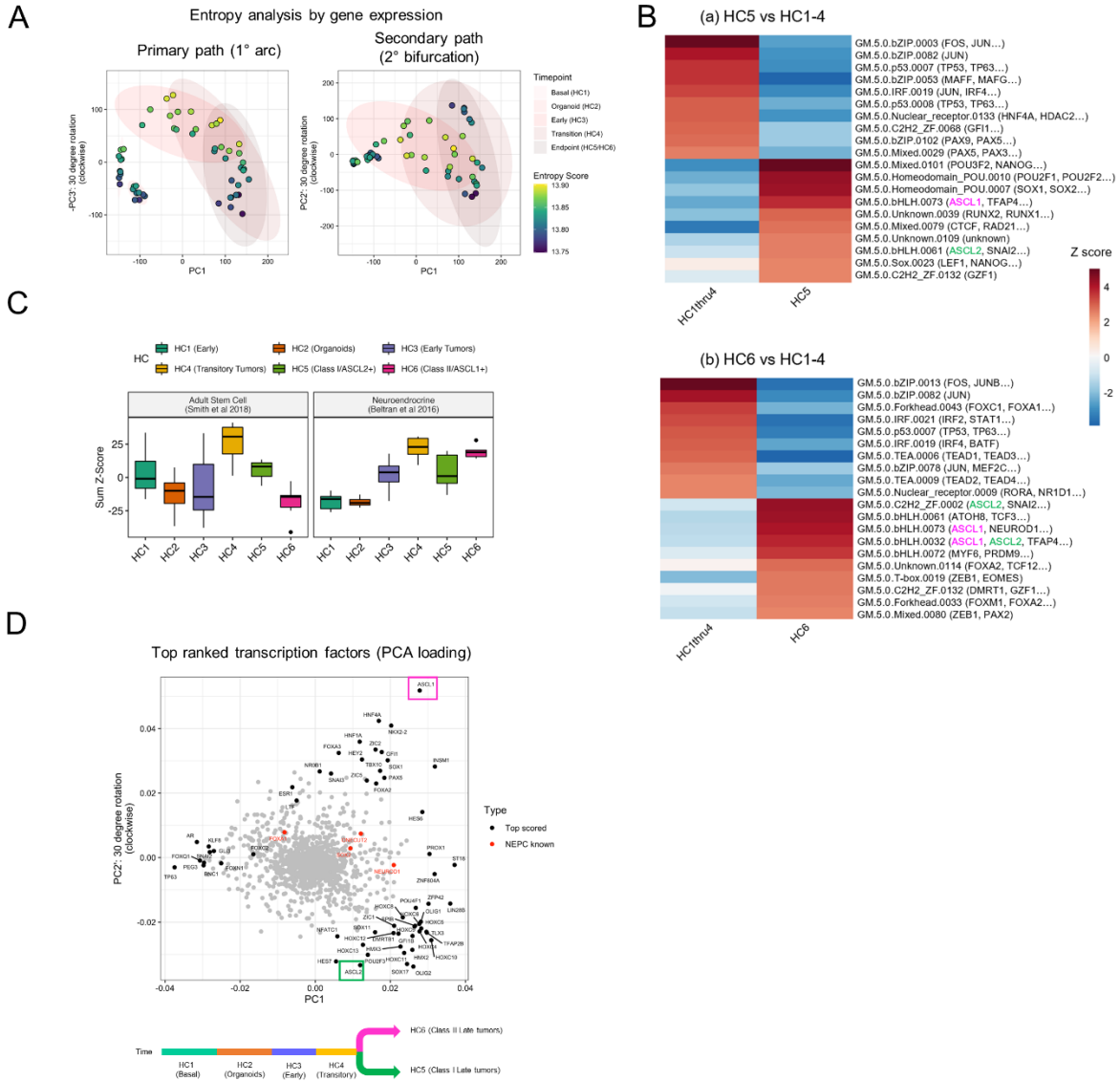


Figure S3

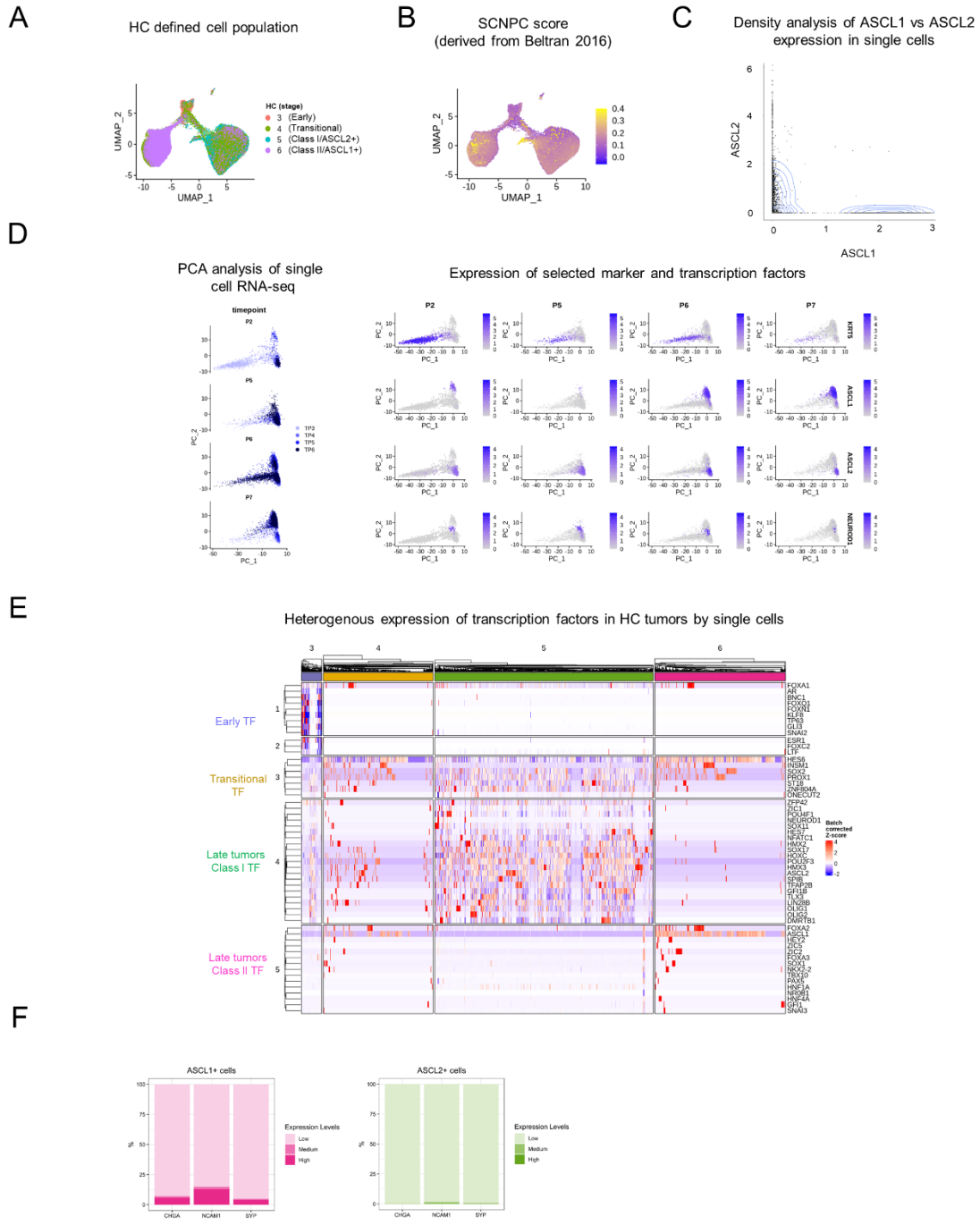
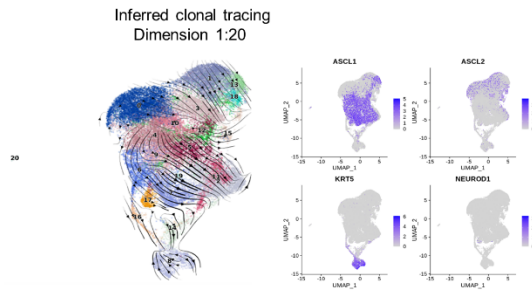




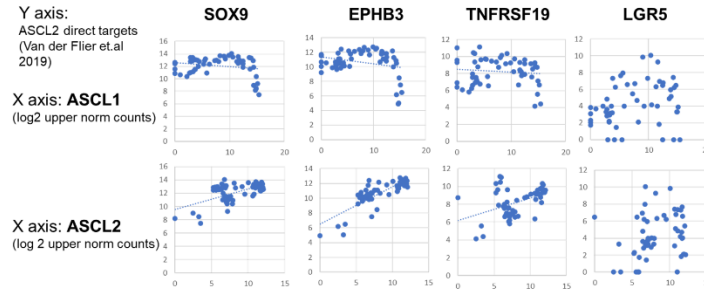
Figure S4

A



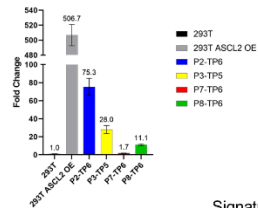
B

Expression of ASCL2 direct targets (Van der Flier et al 2019) vs ASCL1 or ASCL2 in PARCB time course study



C

RT-qPCR of ASCL2 in PARCB tumor derived cell lines



D

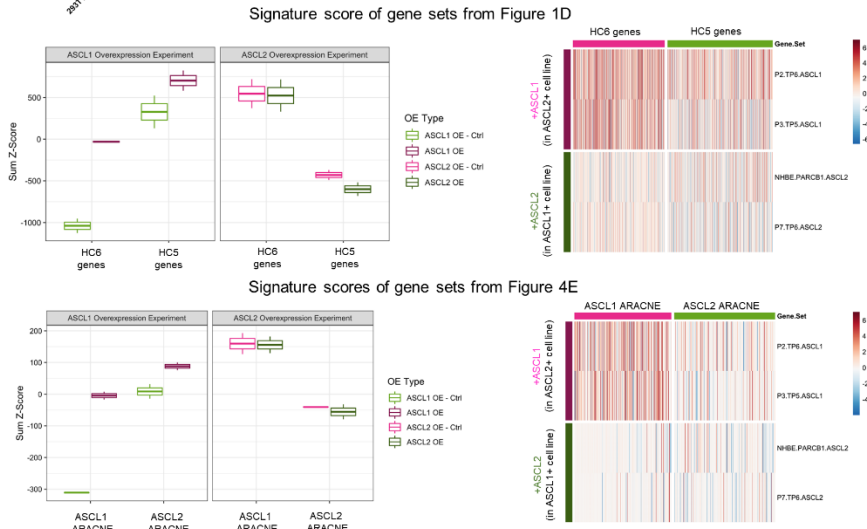
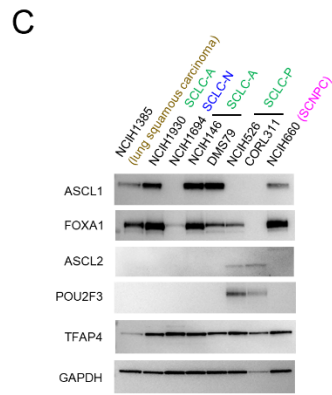
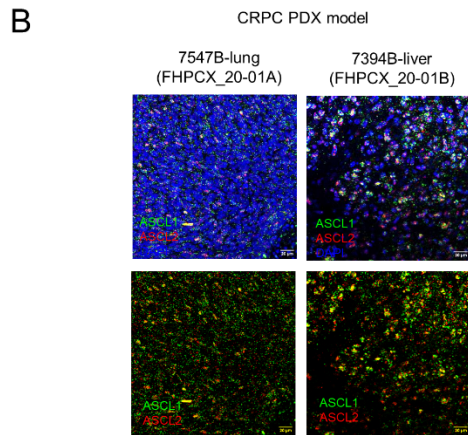
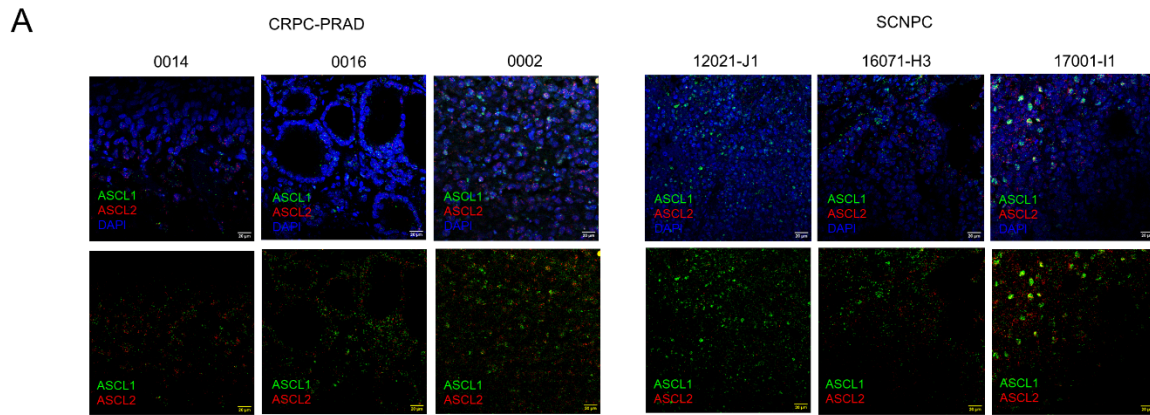


Figure S5





## Reference

1. Nadal, R., Schweizer, M., Kryvenko, O.N., Epstein, J.I., and Eisenberger, M.A. (2014). Small cell carcinoma of the prostate. *Nat Rev Urol* 11, 213-219. 10.1038/nrurol.2014.21.
2. Pietanza, M.C., Byers, L.A., Minna, J.D., and Rudin, C.M. (2015). Small cell lung cancer: will recent progress lead to improved outcomes? *Clin Cancer Res* 21, 2244-2255. 10.1158/1078-0432.CCR-14-2958.
3. Yamada, Y., and Beltran, H. (2021). Clinical and Biological Features of Neuroendocrine Prostate Cancer. *Curr Oncol Rep* 23, 15. 10.1007/s11912-020-01003-9.
4. Balanis, N.G., Sheu, K.M., Esedebe, F.N., Patel, S.J., Smith, B.A., Park, J.W., Alhani, S., Gomperts, B.N., Huang, J., Witte, O.N., and Graeber, T.G. (2019). Pan-cancer Convergence to a Small-Cell Neuroendocrine Phenotype that Shares Susceptibilities with Hematological Malignancies. *Cancer Cell* 36, 17-34 e17. 10.1016/j.ccell.2019.06.005.
5. Cejas, P., Xie, Y., Font-Tello, A., Lim, K., Syamala, S., Qiu, X., Tewari, A.K., Shah, N., Nguyen, H.M., Patel, R.A., et al. (2021). Subtype heterogeneity and epigenetic convergence in neuroendocrine prostate cancer. *Nat Commun* 12, 5775. 10.1038/s41467-021-26042-z.
6. Park, J.W., Lee, J.K., Sheu, K.M., Wang, L., Balanis, N.G., Nguyen, K., Smith, B.A., Cheng, C., Tsai, B.L., Cheng, D.H., et al. (2018). Reprogramming normal human epithelial tissues to a common, lethal neuroendocrine cancer lineage. *Science* 362, 91-95. 10.1126/science.aat5749.
7. Wang, L., Smith, B.A., Balanis, N.G., Tsai, B.L., Nguyen, K., Cheng, M.W., Obusan, M.B., Esedebe, F.N., Patel, S.J., Zhang, H., et al. (2020). A genetically defined disease model reveals that urothelial cells can initiate divergent bladder cancer phenotypes. *Proc Natl Acad Sci U S A* 117, 563-572. 10.1073/pnas.1915770117.

8. Aggarwal, R., Huang, J., Alumkal, J.J., Zhang, L., Feng, F.Y., Thomas, G.V., Weinstein, A.S., Friedl, V., Zhang, C., Witte, O.N., et al. (2018). Clinical and Genomic Characterization of Treatment-Emergent Small-Cell Neuroendocrine Prostate Cancer: A Multi-institutional Prospective Study. *J Clin Oncol* 36, 2492-2503. 10.1200/JCO.2017.77.6880.
9. Dicken, H., Hensley, P.J., and Kyprianou, N. (2019). Prostate tumor neuroendocrine differentiation via EMT: The road less traveled. *Asian J Urol* 6, 82-90. 10.1016/j.ajur.2018.11.001.
10. Beltran, H., Hruszkewycz, A., Scher, H.I., Hildesheim, J., Isaacs, J., Yu, E.Y., Kelly, K., Lin, D., Dicker, A., Arnold, J., et al. (2019). The Role of Lineage Plasticity in Prostate Cancer Therapy Resistance. *Clin Cancer Res* 25, 6916-6924. 10.1158/1078-0432.CCR-19-1423.
11. Davies, A., Zoubeidi, A., and Selth, L.A. (2020). The epigenetic and transcriptional landscape of neuroendocrine prostate cancer. *Endocr Relat Cancer* 27, R35-R50. 10.1530/ERC-19-0420.
12. Ku, S.Y., Rosario, S., Wang, Y., Mu, P., Seshadri, M., Goodrich, Z.W., Goodrich, M.M., Labbe, D.P., Gomez, E.C., Wang, J., et al. (2017). Rb1 and Trp53 cooperate to suppress prostate cancer lineage plasticity, metastasis, and antiandrogen resistance. *Science* 355, 78-83. 10.1126/science.aah4199.
13. Mu, P., Zhang, Z., Benelli, M., Karthaus, W.R., Hoover, E., Chen, C.C., Wongvipat, J., Ku, S.Y., Gao, D., Cao, Z., et al. (2017). SOX2 promotes lineage plasticity and antiandrogen resistance in TP53- and RB1-deficient prostate cancer. *Science* 355, 84-88. 10.1126/science.aah4307.
14. Adams, E.J., Karthaus, W.R., Hoover, E., Liu, D., Gruet, A., Zhang, Z., Cho, H., DiLoreto, R., Chhangawala, S., Liu, Y., et al. (2019). FOXA1 mutations alter pioneering

- activity, differentiation and prostate cancer phenotypes. *Nature* 571, 408-412.  
10.1038/s41586-019-1318-9.
15. Parolia, A., Cieslik, M., Chu, S.C., Xiao, L., Ouchi, T., Zhang, Y., Wang, X., Vats, P., Cao, X., Pitchiaya, S., et al. (2019). Distinct structural classes of activating FOXA1 alterations in advanced prostate cancer. *Nature* 571, 413-418. 10.1038/s41586-019-1347-4.
  16. Guo, H., Ci, X., Ahmed, M., Hua, J.T., Soares, F., Lin, D., Puca, L., Vosoughi, A., Xue, H., Li, E., et al. (2019). ONECUT2 is a driver of neuroendocrine prostate cancer. *Nat Commun* 10, 278. 10.1038/s41467-018-08133-6.
  17. Rotinen, M., You, S., Yang, J., Coetzee, S.G., Reis-Sobreiro, M., Huang, W.C., Huang, F., Pan, X., Yanez, A., Hazelett, D.J., et al. (2018). ONECUT2 is a targetable master regulator of lethal prostate cancer that suppresses the androgen axis. *Nat Med* 24, 1887-1898. 10.1038/s41591-018-0241-1.
  18. Ireland, A.S., Micinski, A.M., Kastner, D.W., Guo, B., Wait, S.J., Spainhower, K.B., Conley, C.C., Chen, O.S., Guthrie, M.R., Soltero, D., et al. (2020). MYC Drives Temporal Evolution of Small Cell Lung Cancer Subtypes by Reprogramming Neuroendocrine Fate. *Cancer Cell* 38, 60-78 e12. 10.1016/j.ccell.2020.05.001.
  19. Marjanovic, N.D., Hofree, M., Chan, J.E., Canner, D., Wu, K., Trakala, M., Hartmann, G.G., Smith, O.C., Kim, J.Y., Evans, K.V., et al. (2020). Emergence of a High-Plasticity Cell State during Lung Cancer Evolution. *Cancer Cell* 38, 229-246 e213. 10.1016/j.ccell.2020.06.012.
  20. Garcia-Bellido, A., and Santamaria, P. (1978). Developmental Analysis of the Achaete-Scute System of *DROSOPHILA MELANOGASTER*. *Genetics* 88, 469-486. 10.1093/genetics/88.3.469.

21. Garcia-Bellido, A., and de Celis, J.F. (2009). The complex tale of the achaete-scute complex: a paradigmatic case in the analysis of gene organization and function during development. *Genetics* 182, 631-639. 10.1534/genetics.109.104083.
22. Borges, M., Linnoila, R.I., van de Velde, H.J., Chen, H., Nelkin, B.D., Mabry, M., Baylin, S.B., and Ball, D.W. (1997). An achaete-scute homologue essential for neuroendocrine differentiation in the lung. *Nature* 386, 852-855. 10.1038/386852a0.
23. Borromeo, M.D., Savage, T.K., Kollipara, R.K., He, M., Augustyn, A., Osborne, J.K., Girard, L., Minna, J.D., Gazdar, A.F., Cobb, M.H., and Johnson, J.E. (2016). ASCL1 and NEUROD1 Reveal Heterogeneity in Pulmonary Neuroendocrine Tumors and Regulate Distinct Genetic Programs. *Cell Rep* 16, 1259-1272. 10.1016/j.celrep.2016.06.081.
24. Nouruzi, S., Ganguli, D., Tabrizian, N., Kobelev, M., Sivak, O., Namekawa, T., Thaper, D., Baca, S.C., Freedman, M.L., Aguda, A., et al. (2022). ASCL1 activates neuronal stem cell-like lineage programming through remodeling of the chromatin landscape in prostate cancer. *Nat Commun* 13, 2282. 10.1038/s41467-022-29963-5.
25. Guillemot, F., Nagy, A., Auerbach, A., Rossant, J., and Joyner, A.L. (1994). Essential role of Mash-2 in extraembryonic development. *Nature* 371, 333-336. 10.1038/371333a0.
26. Kinoshita, M., Li, M.A., Barber, M., Mansfield, W., Dietmann, S., and Smith, A. (2021). Disabling de novo DNA methylation in embryonic stem cells allows an illegitimate fate trajectory. *Proc Natl Acad Sci U S A* 118. 10.1073/pnas.2109475118.
27. Murata, K., Jadhav, U., Madha, S., van Es, J., Dean, J., Cavazza, A., Wucherpennig, K., Michor, F., Clevers, H., and Shivdasani, R.A. (2020). Ascl2-Dependent Cell Dedifferentiation Drives Regeneration of Ablated Intestinal Stem Cells. *Cell Stem Cell* 26, 377-390 e376. 10.1016/j.stem.2019.12.011.
28. Stange, D.E., Engel, F., Longerich, T., Koo, B.K., Koch, M., Delhomme, N., Aigner, M., Toedt, G., Schirmacher, P., Lichter, P., et al. (2010). Expression of an ASCL2 related

- stem cell signature and IGF2 in colorectal cancer liver metastases with 11p15.5 gain. *Gut* 59, 1236-1244. 10.1136/gut.2009.195701.
29. van der Flier, L.G., van Gijn, M.E., Hatzis, P., Kujala, P., Haegebarth, A., Stange, D.E., Begthel, H., van den Born, M., Guryev, V., Oving, I., et al. (2009). Transcription factor achaete scute-like 2 controls intestinal stem cell fate. *Cell* 136, 903-912. 10.1016/j.cell.2009.01.031.
30. Zhu, R., Yang, Y., Tian, Y., Bai, J., Zhang, X., Li, X., Peng, Z., He, Y., Chen, L., Pan, Q., et al. (2012). Ascl2 knockdown results in tumor growth arrest by miRNA-302b-related inhibition of colon cancer progenitor cells. *PLoS One* 7, e32170. 10.1371/journal.pone.0032170.
31. Brady, N.J., Bagadion, A.M., Singh, R., Conteduca, V., Van Emmenis, L., Arceci, E., Pakula, H., Carelli, R., Khani, F., Bakht, M., et al. (2021). Temporal evolution of cellular heterogeneity during the progression to advanced AR-negative prostate cancer. *Nat Commun* 12, 3372. 10.1038/s41467-021-23780-y.
32. George, J., Lim, J.S., Jang, S.J., Cun, Y., Ozretic, L., Kong, G., Leenders, F., Lu, X., Fernandez-Cuesta, L., Bosco, G., et al. (2015). Comprehensive genomic profiles of small cell lung cancer. *Nature* 524, 47-53. 10.1038/nature14664.
33. Beltran, H., Prandi, D., Mosquera, J.M., Benelli, M., Puca, L., Cyrta, J., Marotz, C., Giannopoulou, E., Chakravarthi, B.V., Varambally, S., et al. (2016). Divergent clonal evolution of castration-resistant neuroendocrine prostate cancer. *Nat Med* 22, 298-305. 10.1038/nm.4045.
34. Abida, W., Cyrta, J., Heller, G., Prandi, D., Armenia, J., Coleman, I., Cieslik, M., Benelli, M., Robinson, D., Van Allen, E.M., et al. (2019). Genomic correlates of clinical outcome in advanced prostate cancer. *Proc Natl Acad Sci U S A* 116, 11428-11436. 10.1073/pnas.1902651116.



35. Labrecque, M.P., Coleman, I.M., Brown, L.G., True, L.D., Kollath, L., Lakely, B., Nguyen, H.M., Yang, Y.C., da Costa, R.M.G., Kaipainen, A., et al. (2019). Molecular profiling stratifies diverse phenotypes of treatment-refractory metastatic castration-resistant prostate cancer. *J Clin Invest* 129, 4492-4505. 10.1172/JCI128212.
36. Sharp, A., Welti, J.C., Lambros, M.B.K., Dolling, D., Rodrigues, D.N., Pope, L., Aversa, C., Figueiredo, I., Fraser, J., Ahmad, Z., et al. (2019). Clinical Utility of Circulating Tumour Cell Androgen Receptor Splice Variant-7 Status in Metastatic Castration-resistant Prostate Cancer. *Eur Urol* 76, 676-685. 10.1016/j.eururo.2019.04.006.
37. Lambert, S.A., Jolma, A., Campitelli, L.F., Das, P.K., Yin, Y., Albu, M., Chen, X., Taipale, J., Hughes, T.R., and Weirauch, M.T. (2018). The Human Transcription Factors. *Cell* 175, 598-599. 10.1016/j.cell.2018.09.045.
38. Buenrostro, J.D., Giresi, P.G., Zaba, L.C., Chang, H.Y., and Greenleaf, W.J. (2013). Transposition of native chromatin for fast and sensitive epigenomic profiling of open chromatin, DNA-binding proteins and nucleosome position. *Nat Methods* 10, 1213-1218. 10.1038/nmeth.2688.
39. Richard, A., Boullu, L., Herbach, U., Bonnafoux, A., Morin, V., Vallin, E., Guillemin, A., Papili Gao, N., Gunawan, R., Cosette, J., et al. (2016). Single-Cell-Based Analysis Highlights a Surge in Cell-to-Cell Molecular Variability Preceding Irreversible Commitment in a Differentiation Process. *PLoS Biol* 14, e1002585. 10.1371/journal.pbio.1002585.
40. Shannon, C.E. (1997). The mathematical theory of communication. 1963. *MD Comput* 14, 306-317.
41. van Heeringen, S.J., and Veenstra, G.J. (2011). GimmeMotifs: a de novo motif prediction pipeline for ChIP-sequencing experiments. *Bioinformatics* 27, 270-271. 10.1093/bioinformatics/btq636.

42. Smith, B.A., Balanis, N.G., Nanjundiah, A., Sheu, K.M., Tsai, B.L., Zhang, Q., Park, J.W., Thompson, M., Huang, J., Witte, O.N., and Graeber, T.G. (2018). A Human Adult Stem Cell Signature Marks Aggressive Variants across Epithelial Cancers. *Cell Rep* 24, 3353-3366 e3355. 10.1016/j.celrep.2018.08.062.
43. Han, M., Li, F., Zhang, Y., Dai, P., He, J., Li, Y., Zhu, Y., Zheng, J., Huang, H., Bai, F., and Gao, D. (2022). FOXA2 drives lineage plasticity and KIT pathway activation in neuroendocrine prostate cancer. *Cancer Cell* 40, 1306-1323 e1308. 10.1016/j.ccell.2022.10.011.
44. Park, J.W., Lee, J.K., Witte, O.N., and Huang, J. (2017). FOXA2 is a sensitive and specific marker for small cell neuroendocrine carcinoma of the prostate. *Mod Pathol* 30, 1262-1272. 10.1038/modpathol.2017.44.
45. Sreekumar, A., and Saini, S. (2023). Role of transcription factors and chromatin modifiers in driving lineage reprogramming in treatment-induced neuroendocrine prostate cancer. *Front Cell Dev Biol* 11, 1075707. 10.3389/fcell.2023.1075707.
46. Rudin, C.M., Poirier, J.T., Byers, L.A., Dive, C., Dowlati, A., George, J., Heymach, J.V., Johnson, J.E., Lehman, J.M., MacPherson, D., et al. (2019). Molecular subtypes of small cell lung cancer: a synthesis of human and mouse model data. *Nat Rev Cancer* 19, 289-297. 10.1038/s41568-019-0133-9.
47. Cheng, S., Prieto-Dominguez, N., Yang, S., Connelly, Z.M., StPierre, S., Rushing, B., Watkins, A., Shi, L., Lakey, M., Baiamonte, L.B., et al. (2020). The expression of YAP1 is increased in high-grade prostatic adenocarcinoma but is reduced in neuroendocrine prostate cancer. *Prostate Cancer Prostatic Dis* 23, 661-669. 10.1038/s41391-020-0229-z.
48. Aran, D., Looney, A.P., Liu, L., Wu, E., Fong, V., Hsu, A., Chak, S., Naikawadi, R.P., Wolters, P.J., Abate, A.R., et al. (2019). Reference-based analysis of lung single-cell

- sequencing reveals a transitional profibrotic macrophage. *Nat Immunol* 20, 163-172.  
10.1038/s41590-018-0276-y.
49. He, M.X., Cuoco, M.S., Crowdis, J., Bosma-Moody, A., Zhang, Z., Bi, K., Kanodia, A., Su, M.J., Ku, S.Y., Garcia, M.M., et al. (2021). Transcriptional mediators of treatment resistance in lethal prostate cancer. *Nat Med* 27, 426-433. 10.1038/s41591-021-01244-6.
  50. Chan, J.M., Zaidi, S., Love, J.R., Zhao, J.L., Setty, M., Wadosky, K.M., Gopalan, A., Choo, Z.N., Persad, S., Choi, J., et al. (2022). Lineage plasticity in prostate cancer depends on JAK/STAT inflammatory signaling. *Science* 377, 1180-1191.  
10.1126/science.abn0478.
  51. Dong, B., Miao, J., Wang, Y., Luo, W., Ji, Z., Lai, H., Zhang, M., Cheng, X., Wang, J., Fang, Y., et al. (2020). Single-cell analysis supports a luminal-neuroendocrine transdifferentiation in human prostate cancer. *Commun Biol* 3, 778. 10.1038/s42003-020-01476-1.
  52. Qiu, X., Mao, Q., Tang, Y., Wang, L., Chawla, R., Pliner, H.A., and Trapnell, C. (2017). Reversed graph embedding resolves complex single-cell trajectories. *Nat Methods* 14, 979-982. 10.1038/nmeth.4402.
  53. Bergen, V., Lange, M., Peidli, S., Wolf, F.A., and Theis, F.J. (2020). Generalizing RNA velocity to transient cell states through dynamical modeling. *Nat Biotechnol* 38, 1408-1414. 10.1038/s41587-020-0591-3.
  54. Barker, N., van Es, J.H., Kuipers, J., Kujala, P., van den Born, M., Cozijnsen, M., Haegebarth, A., Korving, J., Begthel, H., Peters, P.J., and Clevers, H. (2007). Identification of stem cells in small intestine and colon by marker gene *Lgr5*. *Nature* 449, 1003-1007. 10.1038/nature06196.
  55. Margolin, A.A., Nemenman, I., Basso, K., Wiggins, C., Stolovitzky, G., Dalla Favera, R., and Califano, A. (2006). ARACNE: an algorithm for the reconstruction of gene regulatory

- networks in a mammalian cellular context. *BMC Bioinformatics* 7 *Suppl 1*, S7.  
10.1186/1471-2105-7-S1-S7.
56. Gay, C.M., Stewart, C.A., Park, E.M., Diao, L., Groves, S.M., Heeke, S., Nabet, B.Y., Fujimoto, J., Solis, L.M., Lu, W., et al. (2021). Patterns of transcription factor programs and immune pathway activation define four major subtypes of SCLC with distinct therapeutic vulnerabilities. *Cancer Cell* 39, 346-360 e347. 10.1016/j.ccell.2020.12.014.
57. Tang, F., Xu, D., Wang, S., Wong, C.K., Martinez-Fundichely, A., Lee, C.J., Cohen, S., Park, J., Hill, C.E., Eng, K., et al. (2022). Chromatin profiles classify castration-resistant prostate cancers suggesting therapeutic targets. *Science* 376, eabe1505.  
10.1126/science.abe1505.
58. Heinz, S., Benner, C., Spann, N., Bertolino, E., Lin, Y.C., Laslo, P., Cheng, J.X., Murre, C., Singh, H., and Glass, C.K. (2010). Simple combinations of lineage-determining transcription factors prime cis-regulatory elements required for macrophage and B cell identities. *Mol Cell* 38, 576-589. 10.1016/j.molcel.2010.05.004.
59. Jackstadt, R., Roh, S., Neumann, J., Jung, P., Hoffmann, R., Horst, D., Berens, C., Bornkamm, G.W., Kirchner, T., Menssen, A., and Hermeking, H. (2013). AP4 is a mediator of epithelial-mesenchymal transition and metastasis in colorectal cancer. *J Exp Med* 210, 1331-1350. 10.1084/jem.20120812.
60. Kim, M.Y., Jeong, B.C., Lee, J.H., Kee, H.J., Kook, H., Kim, N.S., Kim, Y.H., Kim, J.K., Ahn, K.Y., and Kim, K.K. (2006). A repressor complex, AP4 transcription factor and geminin, negatively regulates expression of target genes in nonneuronal cells. *Proc Natl Acad Sci U S A* 103, 13074-13079. 10.1073/pnas.0601915103.
61. Skene, P.J., Henikoff, J.G., and Henikoff, S. (2018). Targeted in situ genome-wide profiling with high efficiency for low cell numbers. *Nat Protoc* 13, 1006-1019.  
10.1038/nprot.2018.015.

62. Rudin, C.M., Brambilla, E., Faivre-Finn, C., and Sage, J. (2021). Small-cell lung cancer. *Nat Rev Dis Primers* 7, 3. 10.1038/s41572-020-00235-0.
63. Schaffer, B.E., Park, K.S., Yiu, G., Conklin, J.F., Lin, C., Burkhart, D.L., Karnezis, A.N., Sweet-Cordero, E.A., and Sage, J. (2010). Loss of p130 accelerates tumor development in a mouse model for human small-cell lung carcinoma. *Cancer Res* 70, 3877-3883. 10.1158/0008-5472.CAN-09-4228.
64. Jia, D., Augert, A., Kim, D.W., Eastwood, E., Wu, N., Ibrahim, A.H., Kim, K.B., Dunn, C.T., Pillai, S.P.S., Gazdar, A.F., et al. (2018). Crebbp Loss Drives Small Cell Lung Cancer and Increases Sensitivity to HDAC Inhibition. *Cancer Discov* 8, 1422-1437. 10.1158/2159-8290.CD-18-0385.
65. Bishop, J.L., Thaper, D., Vahid, S., Davies, A., Ketola, K., Kuruma, H., Jama, R., Nip, K.M., Angeles, A., Johnson, F., et al. (2017). The Master Neural Transcription Factor BRN2 Is an Androgen Receptor-Suppressed Driver of Neuroendocrine Differentiation in Prostate Cancer. *Cancer Discov* 7, 54-71. 10.1158/2159-8290.CD-15-1263.
66. Zou, M., Toivanen, R., Mitrofanova, A., Floch, N., Hayati, S., Sun, Y., Le Magnen, C., Chester, D., Mostaghel, E.A., Califano, A., et al. (2017). Transdifferentiation as a Mechanism of Treatment Resistance in a Mouse Model of Castration-Resistant Prostate Cancer. *Cancer Discov* 7, 736-749. 10.1158/2159-8290.CD-16-1174.
67. Faugeroux, V., Pailler, E., Oulhen, M., Deas, O., Brulle-Soumare, L., Hervieu, C., Marty, V., Alexandrova, K., Andree, K.C., Stoecklein, N.H., et al. (2020). Genetic characterization of a unique neuroendocrine transdifferentiation prostate circulating tumor cell-derived eXplant model. *Nat Commun* 11, 1884. 10.1038/s41467-020-15426-2.
68. Tsoi, J., Robert, L., Paraiso, K., Galvan, C., Sheu, K.M., Lay, J., Wong, D.J.L., Atefi, M., Shirazi, R., Wang, X., et al. (2018). Multi-stage Differentiation Defines Melanoma Subtypes with Differential Vulnerability to Drug-Induced Iron-Dependent Oxidative Stress. *Cancer Cell* 33, 890-904 e895. 10.1016/j.ccell.2018.03.017.

69. Deng, Q., Ramskold, D., Reinius, B., and Sandberg, R. (2014). Single-cell RNA-seq reveals dynamic, random monoallelic gene expression in mammalian cells. *Science* *343*, 193-196. [10.1126/science.1245316](https://doi.org/10.1126/science.1245316).
70. Basili, D., Zhang, J.L., Herbert, J., Kroll, K., Denslow, N.D., Martyniuk, C.J., Falciani, F., and Antczak, P. (2018). In Silico Computational Transcriptomics Reveals Novel Endocrine Disruptors in Largemouth Bass (*Micropterus salmoides*). *Environ Sci Technol* *52*, 7553-7565. [10.1021/acs.est.8b02805](https://doi.org/10.1021/acs.est.8b02805).
71. Jiang, S., Williams, K., Kong, X., Zeng, W., Nguyen, N.V., Ma, X., Tawil, R., Yokomori, K., and Mortazavi, A. (2020). Single-nucleus RNA-seq identifies divergent populations of FSHD2 myotube nuclei. *PLoS Genet* *16*, e1008754. [10.1371/journal.pgen.1008754](https://doi.org/10.1371/journal.pgen.1008754).
72. Kassambara, A., Reme, T., Jourdan, M., Fest, T., Hose, D., Tarte, K., and Klein, B. (2015). GenomicScape: an easy-to-use web tool for gene expression data analysis. Application to investigate the molecular events in the differentiation of B cells into plasma cells. *PLoS Comput Biol* *11*, e1004077. [10.1371/journal.pcbi.1004077](https://doi.org/10.1371/journal.pcbi.1004077).
73. O'Meara, C.C., Wamstad, J.A., Gladstone, R.A., Fomovsky, G.M., Butty, V.L., Shrikumar, A., Gannon, J.B., Boyer, L.A., and Lee, R.T. (2015). Transcriptional reversion of cardiac myocyte fate during mammalian cardiac regeneration. *Circ Res* *116*, 804-815. [10.1161/CIRCRESAHA.116.304269](https://doi.org/10.1161/CIRCRESAHA.116.304269).
74. Yan, L., Yang, M., Guo, H., Yang, L., Wu, J., Li, R., Liu, P., Lian, Y., Zheng, X., Yan, J., et al. (2013). Single-cell RNA-Seq profiling of human preimplantation embryos and embryonic stem cells. *Nature Structural & Molecular Biology* *20*, 1131-1139. [10.1038/nsmb.2660](https://doi.org/10.1038/nsmb.2660).
75. Ebisuya, M., and Briscoe, J. (2018). What does time mean in development? *Development* *145*. [10.1242/dev.164368](https://doi.org/10.1242/dev.164368).

76. Ivakhnitskaia, E., Lin, R.W., Hamada, K., and Chang, C. (2018). Timing of neuronal plasticity in development and aging. *Wiley Interdiscip Rev Dev Biol* 7. 10.1002/wdev.305.
77. Montavon, T., and Soshnikova, N. (2014). Hox gene regulation and timing in embryogenesis. *Semin Cell Dev Biol* 34, 76-84. 10.1016/j.semcdb.2014.06.005.
78. Huang, Y.H., Klingbeil, O., He, X.Y., Wu, X.S., Arun, G., Lu, B., Somerville, T.D.D., Milazzo, J.P., Wilkinson, J.E., Demerdash, O.E., et al. (2018). POU2F3 is a master regulator of a tuft cell-like variant of small cell lung cancer. *Genes Dev* 32, 915-928. 10.1101/gad.314815.118.
79. Castro, D.S., Skowronska-Krawczyk, D., Armant, O., Donaldson, I.J., Parras, C., Hunt, C., Critchley, J.A., Nguyen, L., Gossler, A., Gottgens, B., et al. (2006). Proneural bHLH and Brn proteins coregulate a neurogenic program through cooperative binding to a conserved DNA motif. *Dev Cell* 11, 831-844. 10.1016/j.devcel.2006.10.006.
80. Weindorf, S.C., Taylor, A.S., Kumar-Sinha, C., Robinson, D., Wu, Y.M., Cao, X., Spratt, D.E., Kim, M.M., Lagstein, A., Chinnaiyan, A.M., and Mehra, R. (2019). Metastatic castration resistant prostate cancer with squamous cell, small cell, and sarcomatoid elements-a clinicopathologic and genomic sequencing-based discussion. *Med Oncol* 36, 27. 10.1007/s12032-019-1250-8.
81. Lachmann, A., Giorgi, F.M., Lopez, G., and Califano, A. (2016). ARACNe-AP: gene network reverse engineering through adaptive partitioning inference of mutual information. *Bioinformatics* 32, 2233-2235. 10.1093/bioinformatics/btw216.
82. Drost, J., Karthaus, W.R., Gao, D., Driehuis, E., Sawyers, C.L., Chen, Y., and Clevers, H. (2016). Organoid culture systems for prostate epithelial and cancer tissue. *Nat Protoc* 11, 347-358. 10.1038/nprot.2016.006.
83. Shultz, L.D., Ishikawa, F., and Greiner, D.L. (2007). Humanized mice in translational biomedical research. *Nat Rev Immunol* 7, 118-130. 10.1038/nri2017.

84. Seiler, C.Y., Park, J.G., Sharma, A., Hunter, P., Surapaneni, P., Sedillo, C., Field, J., Algar, R., Price, A., Steel, J., et al. (2014). DNASU plasmid and PSI:Biological-Materials repositories: resources to accelerate biological research. *Nucleic Acids Res* 42, D1253-1260. 10.1093/nar/gkt1060.
85. Joung, J., Konermann, S., Gootenberg, J.S., Abudayyeh, O.O., Platt, R.J., Brigham, M.D., Sanjana, N.E., and Zhang, F. (2017). Genome-scale CRISPR-Cas9 knockout and transcriptional activation screening. *Nat Protoc* 12, 828-863. 10.1038/nprot.2017.016.
86. Tiscornia, G., Singer, O., and Verma, I.M. (2006). Production and purification of lentiviral vectors. *Nat Protoc* 1, 241-245. 10.1038/nprot.2006.37.
87. Vivian, J., Rao, A.A., Nothhaft, F.A., Ketchum, C., Armstrong, J., Novak, A., Pfeil, J., Narkizian, J., Deran, A.D., Musselman-Brown, A., et al. (2017). Toil enables reproducible, open source, big biomedical data analyses. *Nat Biotechnol* 35, 314-316. 10.1038/nbt.3772.
88. Love, M.I., Huber, W., and Anders, S. (2014). Moderated estimation of fold change and dispersion for RNA-seq data with DESeq2. *Genome Biol* 15, 550. 10.1186/s13059-014-0550-8.
89. Kuleshov, M.V., Jones, M.R., Rouillard, A.D., Fernandez, N.F., Duan, Q., Wang, Z., Koplev, S., Jenkins, S.L., Jagodnik, K.M., Lachmann, A., et al. (2016). Enrichr: a comprehensive gene set enrichment analysis web server 2016 update. *Nucleic Acids Res* 44, W90-97. 10.1093/nar/gkw377.
90. Quinlan, A.R., and Hall, I.M. (2010). BEDTools: a flexible suite of utilities for comparing genomic features. *Bioinformatics* 26, 841-842. 10.1093/bioinformatics/btq033.
91. Ritchie, M.E., Phipson, B., Wu, D., Hu, Y., Law, C.W., Shi, W., and Smyth, G.K. (2015). limma powers differential expression analyses for RNA-sequencing and microarray studies. *Nucleic Acids Res* 43, e47. 10.1093/nar/gkv007.



92. Zerbino, D.R., Johnson, N., Juettemann, T., Wilder, S.P., and Flicek, P. (2014). WiggleTools: parallel processing of large collections of genome-wide datasets for visualization and statistical analysis. *Bioinformatics* 30, 1008-1009. 10.1093/bioinformatics/btt737.
93. Ramirez, F., Ryan, D.P., Gruning, B., Bhardwaj, V., Kilpert, F., Richter, A.S., Heyne, S., Dundar, F., and Manke, T. (2016). deepTools2: a next generation web server for deep-sequencing data analysis. *Nucleic Acids Res* 44, W160-165. 10.1093/nar/gkw257.
94. Stuart, T., Butler, A., Hoffman, P., Hafemeister, C., Papalexi, E., Mauck, W.M., 3rd, Hao, Y., Stoeckius, M., Smibert, P., and Satija, R. (2019). Comprehensive Integration of Single-Cell Data. *Cell* 177, 1888-1902 e1821. 10.1016/j.cell.2019.05.031.
95. Greulich, F., Mechtidou, A., Horn, T., and Uhlenhaut, N.H. (2021). Protocol for using heterologous spike-ins to normalize for technical variation in chromatin immunoprecipitation. *STAR Protoc* 2, 100609. 10.1016/j.xpro.2021.100609.
96. Chen, C.C., Tran, W., Song, K., Sugimoto, T., Obusan, M.B., Wang, L., Sheu, K.M., Cheng, D., Ta, L., Varuzhanyan, G., et al. (2023). Temporal evolution reveals bifurcated lineages in aggressive neuroendocrine small cell prostate cancer trans-differentiation. *Cancer Cell* 41, 2066-2082 e2069. 10.1016/j.ccell.2023.10.009.
97. Liu, Q., Zhang, J., Guo, C., Wang, M., Wang, C., Yan, Y., Sun, L., Wang, D., Zhang, L., Yu, H., et al. (2024). Proteogenomic characterization of small cell lung cancer identifies biological insights and subtype-specific therapeutic strategies. *Cell* 187, 184-203 e128. 10.1016/j.cell.2023.12.004.
98. de The, H. (2018). Differentiation therapy revisited. *Nat Rev Cancer* 18, 117-127. 10.1038/nrc.2017.103.
99. Chen, H., Gesumaria, L., Park, Y.K., Oliver, T.G., Singer, D.S., Ge, K., and Schrupp, D.S. (2023). BET Inhibitors Target the SCLC-N Subtype of Small-Cell Lung Cancer by

Blocking NEUROD1 Transactivation. *Mol Cancer Res* 21, 91-101. 10.1158/1541-7786.MCR-22-0594.

100. Xiao, L., Parolia, A., Qiao, Y., Bawa, P., Eyunni, S., Mannan, R., Carson, S.E., Chang, Y., Wang, X., Zhang, Y., et al. (2022). Targeting SWI/SNF ATPases in enhancer-addicted prostate cancer. *Nature* 601, 434-439. 10.1038/s41586-021-04246-z.

### **Chapter 3: Discussion and Closing Remarks**

Most trans-differentiation cases from adenocarcinoma to small cell neuroendocrine carcinoma result from acquired resistance against prior targeted treatments in both prostate and lung cancers. It becomes evident that though the underlying biology of trans-differentiation is complicated, it is systematically coordinated by distinct stages of transcriptional changes and master regulators.

This study provides a blueprint for the development of small cell neuroendocrine prostate cancer. With a multi-omics approach integrated with time, the study shows that there exists a bifurcation from a common neuroendocrine differentiation trajectory towards the end stage of the disease progression<sup>96</sup>. Continued work in identifying subtype-specific therapeutic vulnerability presents a potential avenue for precision medicine. Emerging evidence has also suggested that cross-functional profiling such as proteogenomics and spatial transcriptomic analysis could add more dimensions to deepening our understanding of this seemingly complex disease<sup>97</sup>.

Besides targeting the advanced small cell neuroendocrine stage of cancers, a prevention or redirection of the differentiation pathway during the disease course may suggest an alternative treatment option for poorly differentiated tumors. Our research opens such potentiality by delineating temporal transcriptional events and pinpointing the emergence of various transcription factors during SCNPC development. Differentiation therapy for solid tumors has been explored but not yet matured in clinical development. Several mechanisms adopted by differentiation therapy include reprogramming, elimination of cell renewal and induction of antitumor immune responses to achieve therapeutic outcomes<sup>98</sup>. Despite the technical challenges in the research and design of clinical trials, which may be difficult for differentiation therapy, identifying more targetable candidates and understanding their mechanisms will accelerate such developments.

Much appreciation and emphasis have been put on identifying transcriptional master regulators in neuroendocrine trans-differentiation. Although some transcription factors may not be directly druggable, targeting the transcriptional axis, such as trans-activator, may provide an alternative

approach. For example, the Chen group identified a BET inhibitor that disrupts the physical interaction between BET bromodomain proteins and NEUROD1, reducing SCLC-N subtype growth *in vitro* and *in vivo*<sup>99</sup>. Besides the extensive study on inhibitors of chromatin modifier EZH2, the other group has explored the possibility of targeting the nucleosome remodeling SWI/SNF complex with a proteolysis-targeting chimera degrader in CRPC<sup>100</sup>. Prospective development of such therapeutic approaches is anticipated in the next generation as more pre-clinical models in prostate cancer are established and our knowledge of pathogenesis is strengthened.

An increasing number of transcriptional parallels and similarities between SCNPC and SCLC have been identified. Outside of tissue-specific molecular events, SCNPC and SCLC share distinct transcriptional patterns from their adenocarcinoma counterparts. In this study, we have validated transcriptional events such as the mutual exclusivity and feedback loop between ASCL1 and ASCL2 expression and their associated transcriptional programs. More work in applying this knowledge to study the molecular mechanism and explore therapeutic opportunity is needed.

This dissertation unravels a timely coordination of transcription factors, suggesting that a combinatorial approach of targeting factors may be warranted. Decades of research has shown that a simple combination of lineage-determining transcription factors are essentially responsible for cell type differentiation<sup>58</sup>. The elimination of passenger events and identification of driver transcription factors is an important attribute for the combinatorial strategy. Our collaborators have made significant progress in determining the minimal number of critical factors that sufficiently transform prostate cancer *in vitro*, which will provide a powerful tool for future studies.

The main objective of the dissertation is to study transcriptional development of SCNPC through multi-omics profiling, however, we anticipate a broader application to pan small cell cancers including lung, bladder and ovarian. Future work is needed to identify the shared molecular mechanism and vulnerability.